REFERENCES

1. a. G.A. Somorjai, Chemistry in Two Dimensions: Surfaces, (Cornell University Press, Ithaca, 1981).

   b. A. Zangwill, Physics at Surfaces, (Cambridge University Press: New York, 1988).

2. a. G. Ertl and J. Küppers, Low Energy Electrons and Surface Chemistry, (VCH Verlagsgesellschaft, Weinheim, 1985).

   b. D.P. Woodruff and T.A. Delchar, Modern Techniques of Surface Science, (Cambridge University Press: New York, 1986).

3. M.R. Albert and J.T. Yates, The Surface Scientist's Guide to Organometallic Chemistry, (American Chemical Society, Washington, 1987).

4. D.R. Kahn, E.E. Petersen and G.A. Somorjai, J. Catal., 34 (1974) 294.

5. B.A. Sexton and G.A. Somorjai, J. Catal. 46 (1977) 167.

6. D.W. Goodman, R.D. Kelley, T.E. Madey and J.T. Yates, J. Catal., 63 (1980) 226.

7. H.P. Bonzel and H.J. Krebs, Surf. Sci., 91 (1980) 499.

8. C.T. Campbell and M.T. Paffett, Surf. Sci., 139 (1984) 396.

9. C.T. Campbell, Adv. in Catal., 36 (1989) 1.

10. C.N. Satterfield, Heterogeneous Catalysis in Practice, (McGraw-Hill, New York, 1980).

11. G.C. Bond, Heterogeneous Catalysis: Principles and Applications, (Oxford: New York, 1987).

12. F. Bozso, G. Ertl, M. Grunze and M. Weiss, J. Catal. 49 (1987).

13. F. Bozso, G. Ertl and M. Weiss, J. Catal. 50 (1977) 519.

14. F. Bozso, G. Ertl, M. Grunze and M. Weiss, Appl. Surf. Sci. 1 (1977) 103.

15. R. Imbihl, R. J. Behm, K. Christmann, G. Ertl and T. Matsushima, Surf. Sci. 117 (1982) 257.

16. M. Grunze, F. Bozso, G. Ertl and M. Weiss, Appl. Surf. Sci. 1 (1978) 241.

17. M. Weiss, G. Ertl and F. Nitschke, Appl. Surf. Sci. 2 (1979) 614.

18. G. Ertl, Cat. Rev. Sci. Eng. 21 (1980) 201.

19. P. Stoltze and J.K. Nørskov, J. Catal. 110 (1988) 1.

20. a. N.D. Spencer, R.C. Schoonmaker and G.A. Somorjai, J. Catal. 74 (1982) 129.

    b. S.R. Bare, D.R. Strongin and G.A. Somorjai, J. Phys. Chem. 90 (1986) 4726.

    c. D.R. Strongin and G.A. Somorjai, J. Catal. 109 (1988) 51.

21. D.R. Strongin, J. Carraza, S.R. Bare and G.A. Somorjai, J. Catal. 103 (1987) 213.

22. M. Asscher, J. Carraza, M.M. Khan, K.B. Lewis and G.A. Somorjai, J. Catal. 98 (1986) 277.

23. M. Vannice, Catal. Rev., 14 (1976) 153.

24. R.D. Kelley and D.W. goodman, in: The Chemical Physics of Solid Surfaces and Heterogeneous Catalysis, Vol. 4, Eds. D.A. King and D.P. Woodruff, (Elsevier, Amsterdam, 1982).

25. R.D. Kelley and D.W. Goodman, Surf. Sci. 123 (1982) L743.

26. M.A. Vannice, J. Catal., 44 (1976) 152.

27. D.W. Goodman, R.D. Kelley, T.E. Madey and J.M. White, J. Catal., 64 (1980) 479.

28. P.R. Wentrcek, B.J. Wood and H. Wise, J. Catal., 43 (1976) 363.

29. J.A. Rabo, A.P. Risch and M.L. Poutsma, J. Catal., 53 (1978) 295.

30. M. Araki and V. Ponec, J. Catal., 44 (1979) 439.

31. D.W. Goodman and J.T. Yates, J. Catal., 82 (1983) 255.

32. D.W. Goodman and J.M. White, Surf. Sci., 90 (1979) 201.

33. D.W. Goodman, T.E. Madey, M. Ono and J.T. Yates, J. Catal., 50 (1977) 279.

34. T.J. Udovic, R.D. Kelley and T.E. Madey, Surf. Sci., 150 (1985) L71.

35. A. Cichowlas, E.P. Yesodharam and A. Brenner, Appl. Catal., 11 (1984) 353.

36. D.G. Castner, R.L. Blackadar and G.A. Somorjai, J. Catal., 66 (1980) 257.

37. D.J. Dwyer, K. Yoshida and G.A. Somorjai, Adv. in Chemistry Series, American Chem. Soc., 178 (1979) 65.

38. M. Logan, A. Gellman and G.A. Somorjai, J. Catal., 94 (1985) 60.

39. M.A. Vannice, J. Catal., 37 (1975) 449.

40. a. J.C. Geerlings, M.C. Zonnevylle and C.P.M. De Groot, Catal. Lett. 5 (1990) 309.

b. J.C. Geerlings, M.C. Zonnevylle and C.P.M. De Groot, Surf. Sci. 241 (1991) 302, 315.

41. a. J.H. Sinfelt, Bimetallic Catalysts, (Wiley, New York, 1983).

b. J.A. Rodriguez and D.W. Goodman, J. Phys. Chem. 95 (1991) in press.

42. W.M.H. Sachtler, Faraday Discuss. Chem. Soc., 72 (1981) 7.

43. a. J.E. Houston, C.H.F. Peden, D.S. Blair and D.W. Goodman, Surf. Sci., 167 (1986) 427.

b. J.A. Rodriguez, R.A. Campbell and D.W. Goodman, J. Phys. Chem. 94 (1990) 6936; 95 (1991) in press.

44. J.E. Houston, C.H.F. Penden, P.J. Feibelman and D.R. Hamann, Phys. Rev. Lett., 56 (1986) 375.

45. C.H.F. Peden and D.W. Goodman, J. Catal., 104 (1987) 347.

46. C.H.F. Peden and D.W. Goodman, Ind. Eng. Chem. Fundam., 25 (1986) 58.

47. R.W. Judd, M.A. Reichelt and R.M. Lambert, Surf. Sci., 198 (1988) 26.

48. I. Hamedeh and R. Gomer, Surf. Sci., 154 (1985) 168.

49. a. P.J. Berlowitz and D.W. Goodman, Surf. Sci., 187 (1987) 463.

b. P.J. Berlowitz and D.W. Goodman, Langmuir, 4 (1988) 1901.

50. R.A. Campbell, J.A. Rodriguez and D.W. Goodman, Surf. Sci. 240 (1990) 71.

51. C.M. Greenlief, P.J. Berlowitz, D.W. Goodman and J.M. White, J. Phys. Chem., 91 (1987) 6669.

52. R.A. Campbell, J.A. Rodriguez and D.W. Goodman, Surf. Sci. in press.

53. J.W. He, W.L. Shea, X. Jiang and D.W. Goodman, J. Vac. Sci. Technol. A 8 (1990) 2435.

54. a. J.W. He and D.W. Goodman, J. Phys. Chem., 94 (1990) 1496.

b. J.A. Rodriguez, R.A. Campbell and D.W. Goodman, Surf. Sci. in press.

55. K. Christmann, O. Schober, G. Ertl and M. Neumann, J. Chem. Phys., 60 (1974) 4528.

56. K. Christmann, G. Ertl and H. Shimizu, J. Catal., 61 (1980) 397.

57. C. Park, E. Bauer and H. Poppa, Surf. Sci., 187 (1987) 86.

58. D.W. Goodman, in: Heterogeneous Catalysis (Proceedings of IUCCP Conference), Texas A&M University (1984).

59. B.G. Johnson, C.H. Bartholomew and D.W. Goodman, J. Catal., 128 (1991) 231.

60. B. Imelik, C. Naccache, G. Couduier, H. Praliud, P. Meriaudeau, P. Gallezot, G.A. Martin and J.C. Vedrine, Eds., Metal-Support and Metal-Additive Effects in Catalysts, (Elsevier, Amsterdam, 1982).

61. D.W. Goodman and M. Kiskinova, Surf. Sci., 105 (1981) L265.

62. M. Kiskinova and D.W. Goodman, Surf. Sci., 108 (1981) 64.

63. D.W. Goodman, Appl. Surf. Sci., 19 (1984) 1.

64. S. Johnson and R.J. Madix, Surf. Sci., 108 (1981) 77.

65. E.L. Hardegree, P. Ho and J.M. White, Surf. Sci., 165 (1988) 488.

66. C. Kittel, Introduction to Solid State Physics, 6th ed., (Wiley, New York, 1986) p. 76.

67. J.R. Rostrup-Nielsen and K. Pedersen, J. Catal., 59 (1979) 395.

68. C.H.F. Peden and D.W. Goodman, ACS Symposium Series, Proceedings of Sym. on the Surface Science of Catalysis, M.L. Devinny and J.L. Gland, Eds.; Philadelphia 1984.

69. P.D. Szuromi, R.D. Kelley and T.E. Madey, J. Phys. Chem., 90 (1986) 6499.

70. C.T. Campbell and D.W. Goodman, Surf. Sci., 123 (1982) 413.

71. G.A. Mills and F.W. Steffgen, Catal. Rev., 8 (1973) 159.

72. P. Schoubye, J. Catal., 14 (1969) 238.

73. G. Blyholder, J. Phys. Chem., 68 (1964) 2772.

74. G. Blyholder, J. Phys. Chem., 79 (1975) 756.

75. F.A. Cotton and G. Wilkinson, Advanced Inorganic Chemistry, 4th ed. (Wiley, New York, 1980) p. 82-86.

76. P.S. Bagus, K. Hermann and C.W. Bauschlicher, J. Chem. Phys., 81 (1984) 1966.

77. P.S. Bagus and K. Hermann, Phys. Rev. B, 33 (1986) 2987.

78. K. Hermann, P.S. Bagus and C.J. Nelin, Phys. Rev. B, 35 (1987) 9467.

79. J. Rogozik and V. Dose, Surf. Sci., 176 (1986) L847.

80. K.L. D'Amico, F.R. McFeely and E.I. Solomon, J. Amer. Chem. Soc., 105 (1983) 6380.

81. H. Ibach and D.L. Mills, Electron Energy Loss Spectroscopy and Surface Vibrations, (Academic Press, New York, 1982).

82. J.A. Rodriguez and C.T. Campbell, J. Phys. Chem., 91 (1987) 2161.

83. J. Benziger and R.J. Madix, Surf. Sci., 94 (1980) 119.

84. N.K. Ray and A.B. Anderson, Surf. Sci., 125 (1983) 803.

85. R.C. Baetzold, Phys. Rev. B, 30 (1984) 6870.

86. M.C. Zonnevylle and R. Hoffman, Langmuir, 3 (1987) 452.

87. A.J. Freeman, C. Fu and E. Wimmer, J. Vac. Sci. Technol. A, 4 (1986) 1265.

88. J.M. MacLaren, J.B. Pendry, R.W. Joyner, and P. Meehan, Surf. Sci., 175 (1986) 263.

89. J.M. MacLaren, D.D. Vvedensky, J.B. Pendry and R.W. Joyner, J. Chem. Soc. Faraday Trans. 1, 83 (1987) 1945.

90. T.B. Grimley, Proc. Phys. Soc., 90 (1967) 751.

91. T.B. Grimley and S.M. Walker, Surf. Sci., 14 (1969) 395.

92. T.E. Einstein and J.R. Schrieffer, Phys. Rev. B, 7 (1973) 3629.

93. P. Feibelman and D. Hamman, Phys. Rev. Lett., 52 (1984) 61.

94. P. Feibelman and D. Hamman, Surf. Sci., 149 (1985) 48.

95. J.K. Nørskov, S. Holloway and N.D. Lang, Surf. Sci., 137 (1984) 65.

96. N.D. Lang, S. Holloway and J.K. Nørskov, Surf. Sci., 150 (1985) 24.

97. S.J. Tauster, Accounts of Chemical Research, 20 (1987) 389.

98. G.L. Haller and D.E. Resasco, Adv. in Catalysis, 36 (1989) 173.

99. C.C. Kao, S.C. Tsai and Y.W. Chung, J. Catal., 73 (1982) 136.

100. Y.W. Chung, G. Xiong and C.C. Kao, J. Catal., 85 (1984) 237.

101. T. Engel and G. Ertl, The Chemical Physics of Solid Surfaces and Heterogeneous Catalysis; D.A. King and D.P. Woodruff, eds. (Elsevier: Amsterdam, 1982) Vol. 4.

102. a. R. Imbilhl, M.P. Cox and G. Ertl, J. Chem. Phys. 84 (1986) 3519.

b. G. Ertl, Adv. Catal. 37 (1990) 213.

103. M. Eiswirth, K. Krischer and G. Ertl, Surf. Sci. 202 (1988) 565.

104. M. Eiswirth, P. Möller and G. Ertl, Surf. Sci. 208 (1989) 13.

105. M. Ehsasi, C. Seidel, H. Ruppender, W. Drachsel, J.H. Block and K. Christmann, Surf. Sci. 210 (1989) L198.

106. S.H. Oh, G.B. Fischer, J.E. Carpenter and D.W. Goodman, J. Catal. 100 (1986) 360.

107. D.W. Goodman and C.H.F. Peden, J. Phys. Chem. 90 (1986) 4839.

108. C.H.F. Peden and D.W. Goodman, J. Phys. Chem. 90 (1986) 1360.

109. P.J. Berlowitz, C.H.F. Peden and D.W. Goodman, J. Phys. Chem. 92 (1988) 5213.

110. B.C. Sales, J.E. Turner and M.B. Maple, Surf. Sci. 114 (1982) 381.

111. R.C. Yeates, J.E. Turner A.J. Gellman and G.A. Somorjai, Surf. Sci. 149 (1985) 175.

112. C.H.F.Peden, D.W. Goodman, D.S. Blair, P.J. Berlowitz, G.B. Fisher and S.H. Oh, J. Phys. Chem. 92 (1988) 1563.

113. K.C. Taylor, in Catalysis: Science and Technology; J.R. Anderson and M. Boudart, eds. (Springer-Verlag: Berlin, 1984) Vol. 5.

114. J.C. Zomerdijk and M.W. Hall, Catal. Rev. Sci. Eng. 23 (1981) 163.

115. W.M.H. Sachtler, C. Backx and R.H. van Santen, Catal. Rev. Sci. Eng. 23 (1981) 127.

116. R.A. van Santen and H.P.C.E. Kuipers, Advan. Catal. 35 (1987) 265.

117. C.T. Campbell, J. Catal. 94 (1985) 436.

118. D.J. Sajkowski and M. Boudart, Catal. Rev. Sci. Eng. 29 (1987) 325.

119. H.R. Dettwiler, A. Baiker and W. Richarz, Helv. Chim. Acta 62 (1979) 1689.

120. C.T. Campbell, J. Vac. Sci. Technol. A 2 (1984) 1024.

121. S.A. Tan, R.B. Grant and R.M. Lambert, J. Catal. 100 (1986) 383.

122. a. R.B. Grant and R.M. Lambert, J. Chem. Soc. Chem. Commun. (1983) 662.

b. R.B. Grant, C.A.J. Harbach, R.M. Lambert and S.A. Tan, J. Chem. Soc., Faraday Trans. 1 83 (1987) 2035.

123. R.B. Grant and R.M. Lambert, J. Catal. 92 (1985) 364.

124. R.A. van Santen and C.P.M. de Groot, J. Catal. 98 (1986) 530.

125. P.J. van den Hoek, E.J. Baerends and R.A. van Santen, J. Phys. Chem. 93 (1989) 6469.

126. J.A. Rodriguez and C.T. Campbell, Surf. Sci. 206 (1988) 426.

127. a. E.A. Carter and W.A. Goddard, J. Catal. 112 (1988) 80.

b. E.A. Carter and W.A. Goddard, Surf. Sci. 209 (1989) 243.

128. C.T. Campbell and M.T. Paffett, Appl. Surf. Sci. 19 (1984) 28.

129. C.T. Campbell and B.E. Koel, J. Catal. 92 (1985) 272.

130. C.T. Campbell, J. Catal. 99 (1986) 28.

131. C.T. Campbell, J. Phys. Chem. 89 (1985) 5789.

132. R.B. Grant and R.M. Lambert, J. Catal. 93 (1985) 92.

133. R.B. Grant and R.M. Lambert, Langmuir, 1 (1985) 29.

134. B.C. Gates, J.R. Katzer and G.C.A. Shuit, Chemistry of Catalytic Processes (McGraw-Hill: New York, 1979).

135. F. Zaera, E.B. Kollin and J.L. Gland, Langmuir, 3 (1987) 555.

136. G.R. Schoofs, R.E. Preston and J.B. Benziger, Langmuir 1 (1985) 313.

137. J.T. Roberts and C.M. Friend, Surf. Sci. 186 (1987) 201.

138. F. Zaera, E.B. Kollin and J.L. Gland, Surf. Sci. 184 (1987) 75.

139. J.P. Fulmer, F. Zaera and W.T. Tysoe, J. Phys. Chem. 92 (1988) 4147.

140. B.A. Sexton, Surf. Sci. 163 (1985) 99.

141. J.A. Rodriguez, Surf. Sci. 234 (1990) 421.

142. A.J. Gellman, M.H. Farias and G.A. Somorjai, J. Catal. 88 (1984) 546.

143. M.E. Bussell and G.A. Somorjai, J. Catal. 106 (1987) 93.

144. A.J. Gellman, D. Neiman and G.A. Somorjai, J. Catal. 107 (1987) 92.

145. A.J. Gellman, M.E. Busell and G.A. Somorjai, J. Catal. 107 (1987) 103.

146. M.E. Bussell, A.J. Gellman and G.A. Somorjai, J. Catal. 110 (1988) 423.

147. J.E. Sinfelt, Adv. Catal. 23 (1980) 91.

148. D.W. Goodman, Surf. Sci. 123 (1982) L679.

149. G.A. Martin, J. Catal. 60 (1979) 345,452.

150. M.C. Desjonqueres and F. Cyrot-Lackmann, J. Chem. Phys. 64 (1976) 3707.

151. A.G. Sault and D.W. Goodman, Advan. Chem. Phys. 76 (1989) 153.

152. C.H.F. Peden and D.W. Goodman, ACS Symposium Series 288 (1985) 185.

153. C. Egawa and Y. Iwasawa, Surf. Sci. 198 (1988) L329.

154. E. Shincho, C. Egawa, S. Naito and K. Tamaru, Surf. Sci. 149 (1985) 1.

155. a. J.H. Sinfelt and D.J.C. Yeates, J. Catal. 8 (1967) 82.

b. J.H. Sinfelt, Catal. Rev. 3 (1969) 175.

156. J.R. Engstrom, D.W. Goodman and W.H. Weinberg, J. Am. Chem. Soc. 110 (1988) 8305.

157. a. C.M. Chan, M.A. Van Hove, W.H. Weinberg and D.E. Williams, Solid State Commun. 30 (1979) 47.

b. C.M. Chan, M.A. Van Hove, W.H. Weinberg and D.E. Williams, Surf. Sci. 91 (1980) 430.

158. J.A. Rodriguez and D.W. Goodman, J. Phys. Chem. 94 (1990) 5342.

159. F. Zaera and G.A. Somorjai, J. Phys. Chem. 89 (1985) 3211.

160. D.J. Godbey, F. Garin and G.A. Somorjai, J. Catal. 117 (1989) 144.

161. G. Leclerq, L. Leclerq and R. Maurel, J. Catal. 44

(1976) 68.

162. M.J. Wax, R.D. Kelley and T.E. Madey, J. Catal. 98 (1986) 487.

163. J.R. Anderson and B.G. Baker, Proc. Royal. Soc. A 271 (1963) 402.

164. K. Foger and J.R. Anderson, J. Catal. 59 (1979) 325.

165. A.K. Datye, B.F. Hegarty and D.W. Goodman, Faraday Discuss. Chem. Soc. 87 (1989) 18.

166. S.M. Davis, F. Zaera and G.A. Somorjai, J. Am. Chem. Soc. 104 (1982) 7453.

167. S.M. Davis, F. Zaera and G.A. Somorjai, J. Catal. 85 (1984) 206.

168. J.W.A. Sachtler and G.A. Somorjai, J. Catal. 81 (1983) 77.

169. R.C. Yeates and G.A. Somorjai, J. Catal. 103 (1987) 208.

170. D.W. Goodman, J. Vac. Sci. Technol. A 2 (1984) 873.

171. C.M. Machiels and R.B. Anderson, J. Catal. 58 (1979) 253.

172. R.A. Dalla Betta, J.A. Casumano and J.H. Sinfelt, J. Catal. 19 (1970) 343.

173. T.S. Sridhar and D.M. Ruthven, J. Catal. 24 (1972) 253.

174. A. Verma and D.M. Ruthven, J. Catal. 46 (1977) 160.

175. A. Verma and D.M. Ruthven, J. Catal. 19 (1970) 401.

176. D.S. Kellog, M.S. Touvelle and P.C. Stair, J. Catal. 120 (1989) 192.

177. J.R. Engstrom, D.W. Goodman and W.H. Weinberg, J. Phys. Chem. 94 (1990) 396.

178. W.D. Gillespie, R.K. Herz, E.E. Petersen and G.A. Somorjai, J. Catal. 70 (1981) 147.

179. F. Zaera, D. Godbey and G.A. Somorjai, J. Catal. 101 (1986) 73.

180. R.K. Herz, W.D. Gillespie, E.E. Petersen and G.A. Somorjai, J. Catal. 67 (1981) 371.

181. C.H.F. Peden and D.W. Goodman, J. Catal. 104 (1987) 347.

182. F. Garin, S. Aeiyach, P. Legare and G. Maire, J. Catal. 77 (1982) 323.

183. S.M. Davis and G.A. Somorjai, in: The Chemical Physics of Solid Surfaces and Heterogeneous Catalysis; D.A. King and D.P. Woodruff, Edts (Elsevier: Amsterdam, 1982) vol. 4, chp. 7.

184. A. Dauscher, F. Garin and G. Maire, J. Catal. 105 (1987) 233.

185. F. Zaera and G.A. Somorjai, Langmuir 2 (1986) 686.

186. F. Zaera and G.A. Somorjai, J. Am. Chem. Soc. 106 (1984) 2288.

187. J. Oudar, S. Pinol, C.M. Pradier and Y. Berthier, J. Catal. 107 (1987) 434, 445.

188. C.M. Pradier, E. Margot, Y. Berthier and J. Oudar, Applied Catal. 31 (1987) 243.

189. C.M. Pradier, E. Margot, Y. Berthier and J. Oudar, Applied Catal. 43 (1988) 177.

190. S.M. Davis and G.A. Somorjai, J. Catal. 65 (1980) 78.

191. J. Massardier and J.C. Bertolini, J. Catal. 90 (1984) 358.

192. G. Dalmai-Imelik and J. Massardier, in: Proc. 6th Int. Congr. Catal., London 1976 ; G.C. Bond, P.B. Wells and F.C. Tomkins, Edts. (The Chemical Society, London, 1977) p. 90.

193. J.R. Engstrom, W. Tsai and W.H. Weinberg, J. Chem. Phys. 87 (1987) 3104.

194. E. Segal, R.J. Madon and M. Boudart, J. Catal. 52 (1978) 45.

195. C.M. Tsai, C.M. Friend and E.L. Muetterties, J. Am. Chem. Soc. 104 (1982) 2539.

196. A.P. Hitchcock, D.C. Newbury, I. Ishii, J. Stohr, J.A. Horsley, R.D. Redwing, A.L. Johnson and F. Sette, J. Chem. Phys. 85 (1986) 4849.

197. J. Stohr, F. Sette and A.L. Johnson, Phys. Rev. Lett. 53 (1984) 1684.

198. L.E. Firment and G.A. Somorjai, J. Chem. Phys. <u>66</u> (1977) 2901.

199. J.E. Demuth, H. Ibach and S. Lehwald, Phys. Rev. Lett. <u>40</u> (1978) 1044.

200. D.B. Kang and A.B. Anderson, J. Am. Chem. Soc. <u>107</u> (1985) 7858.

201. a. J.A. Rodriguez and C.T. Campbell, J. Phys. Chem. <u>93</u> (1989) 826.

b. C.T. Campbell, to be published.

202. C.T. Campbell, J.A. Rodriguez, F.C. Henn, J.M. Campbell, P.J. Dalton and S. Seimanides, J. Chem. Phys. <u>88</u> (1988) 6585.

203. J.W.A. Sachtler and G.A. Somorjai, J. Catal. <u>89</u> (1984) 35.

204. A. Sault and D.W. Goodman, J. Catal. <u>126</u> (1990) 57.

205. T.G. Rucker, M.A. Logan, T.M. Gentle, E.L. Muetterties and G.A. Somorjai, J. Phys. Chem. <u>90</u> (1986) 2703.

206. W.T. Tysoe, G.L. Nyberg and R.M. Lambert, Surf. Sci. <u>135</u> (1983) 128.

207. W. Sesselman, B. Woratschek, G. Ertl, J. Kupers and H. Haberland, Surf. Sci. <u>130</u> (1983) 245.

208. B. Marchon, Surf. Sci. <u>162</u> (1985) 382.

209. a. C.H. Patterson, J.M. Mundenar, P.Y. Timbrell, A.J. Gellman and R.M. Lambert, Surf. Sci. <u>208</u> (1989) 93.

b. C.H. Patterson and R.M. Lambert, J. Phys. Chem. <u>92</u> (1988) 1266.

210. G.N. Schrauzer, P. Glockner and S. Eichler, Angew. Chem., Int. Ed. Engl. <u>3</u> (1964) 185.

211. K.P.C. Vollhardt, Acc. Chem. Res. <u>10</u> (1977) 1.

212. P.M. Maitlis, Acc. Chem. Res. <u>9</u> (1976) 93.

213. D.S. Newsome, Catal. Rev. Sci. Eng., <u>21</u> (1980) 275.

214. C.T. Campbell and K. Daube, J. Catal., <u>104</u> (1987) 109.

215. J. Nakamura, J.M. Campbell and C.T. Campbell, J. Chem.

Soc. Faraday Trans. 86 (1990) 2725.

216. G.C. Chinchen, M.S. Spencer, K.C. Waugh and D.A. Whan, J. Chem. Soc., Faraday Trans. 1, 83 (1987) 2193.

217. S. Kinnaird, G. Webb and G.C. Chinchen, J. Chem. Soc., Faraday Trans. 1, 83 (1987) 3399.

218. E.G.M. Kuijpers, R.B. Tjepkema, W. Van der Wal, C.M. Mesters, S.F. Spronck and J.W. Geus, App. Catal., 25 (1986) 139.

219. K. Bange, D.E. Grider, T.E. Madey and J.K. Sass, Surf. Sci., 137 (1984) 38.

220. W.D. Clendening, J.A. Rodriguez, J.M. Campbell and C.T. Campbell, Surf. Sci., 216 (1989) 429.

221. C.T. Campbell and B.E. Koel, Surf. Sci., 183 (1987) 100.

222. D.C. Bybell, P.P. Deutsch, R.G. Herman, P.B. Himelfarb, J.G. Nunan, C.W. Young, C.E. Bogdan, G.W. Simmons and K. Klier, Prep. Petrol. Div., Am. Chem. Soc., 31 (1986) 282.

223. K. Klier, C.W. Young and J.G. Nunan, Ind. Eng. Chem. Fundam., 25 (1986) 36.

224. C.T. Campbell and B.E. Koel, Surf. Sci., 186 (1987) 393.

225. J.A. Rodriguez, W.D. Clendening and C.T. Campbell, J. Phys. Chem., 93 (1989) 5238.

226. J.A. Rodriguez, W.D. Clendening, J.M. Campbell, W. Min and C.T. Campbell, J. Vac. Sci. Technol. A, 7 (1989) 2118.

227. J. Nakamura, J.M. Campbell and C.T. Campbell, in preparation.

228. H.H. Kung, Catal. Rev. Sci. Eng., 22 (1980) 235.

229. K. Klier, Adv. in Catal., 31 (1982) 243.

230. J. H. Lunsford, Chem. Ind., 22 (1985) 95.

231. P.J. Berlowitz and D.W. Goodman, J. Catal., 108 (1987) 364.

232. C.T. Campbell, K.A. Daube and J.M. White, Surf. Sci., 182 (1987) 458.

233. Y.A. Ryndin, R.F. Hicks, A.T. Bell and Y.I. Yermakov, J. Catal., 70 (1981) 287.

234. R.F. Hicks and A.T. Bell, J. Catal., 91 (1985) 104.

235. F. Fajula, R.G. Anthony and J.H. Lunsford, J. Catal., 73 (1982) 237.

236. J. Szanyi and D. W. Goodman, Catalysis Lett., submitted for publication.

237. R. Burch and R.J. Chappel, Appl. Catal., 45 (1988) 131.

238. C.A. Leon y Leon and M.A. Vannice, Appl. Catal. 69 (1991) 291.

FIGURE CAPTIONS

Figure 1. (a) Schematic representation of five Fe single crystal surfaces. The coordination number for each surface atoms is indicated. (b) rate of NH_3 synthesis over five different faces of iron (from ref. [21]).

Figure 2. Structure sensitivity in the ammonia synthesis over Re single-crystal faces. The turnover frequencies (TF) are given as NH_3 molecules $cm^{-2}s^{-1}$. Schematics of the atomic structure of each surface are given above each bar (from ref. [22]).

Figure 3. (a) A comparison of the rate of methane formation (CH_4 molecules/site-s) over single crystal nickel catalysts and supported Ni/Al_2O_3. Reaction conditions: 120 Torr, H_2/CO ratio = 4 (from ref. [25]). (b) Atomic configuration of a Ni(100) surface. (c) Atomic configuration of a Ni(111) surface.

Figure 4. (a) Arrhenius plot of CH_4 synthesis on a Ni(100) catalyst at total reactant pressures of 1, 10 and 120 Torr. The ratio H_2 / CO is 4 (from ref. [25]). (b) Arrhenius plot of CH_4 synthesis on a Ru(110) catalyst at total reactant pressures of 1, 10 and 120 Torr. The ratio H_2 / CO is 4. Data at two temperatures for a Ru(001) catalyst at 120 Torr are plotted with the symbol X (from ref. [25]).

Figure 5. Methane production rate (molecules/Ni surface atom-s) at 625K over a Ni(100) catalyst versus surface carbon coverage (under steady-state conditions). The H_2 / CO ratio and the total pressure (Torr) for each point are indicated in the insert (from ref. [25]).

Figure 6. (a) The methanation activity for W(110) compared to that for Ni(100), plotted in an Arrhenius fashion (from ref. [34]). (b) The H_2 dependence of the methanation activity for W(110) compared to that of Ni(100) (from ref. [34]).

Figure 7. (a) Arrhenius plot for CO methanation on Mo(100) (from ref. [38]). (b) Rate of formation of methane over Mo(100) versus the partial pressure of each reactant. Constant H_2 pressure of 3 atm for determination of CO dependence, and constant CO pressure of 3 atm for determination of H_2 pressure dependence. In all the cases the total pressure was 6 atm, with nitrogen or argon used as a buffer gas (from ref. [38]).

Figure 8. (a) Arrhenius plot for CH_4 synthesis over several different Ni coverages on W(110) and W(100) at a total reactant pressure of 120 Torr (H_2/CO = 4) (from ref. [51]). (b) Arrhenius plot for CH_4 synthesis over several different Ni coverages on W(110) at total reactant pressures of 1, 10 and 120 Torr (H_2/CO = 4) (from ref. [51]).

Figure 9. Variation of the saturation coverage of CO (part (a)) and H_2 (part (b)) on Ni(100) with the precoverage of Cl, S and P (from ref. [63]).

Figure 10. Plot of the rate of methanation (CH_4 molecules/site-s) over a sulfide and phosphided Ni(100) catalyst at 120 Torr and a pressure ratio of H_2 to CO of 4 (from ref. [63]).

Figure 11. Methanation rate as a function of sulfur coverage on: (a) Ru(001) (from ref. [68]), and (b) Rh(111) (from ref. [58]) catalysts. Pressure = 120 Torr, $H_2/CO = 4$, reaction temperature = 600K.

Figure 12. Relative change in methanation rate over W(110) as a function of sulfur coverage (from ref. [69]). For comparison the data for Ni(100) is also shown (from ref. [63]).

Figure 13. (a) Relative methanation rate as a function of potassium coverage at various reaction conditions: (◇) $P_{CO} = 1.0$ Torr, $P_{H2} = 99.9$ Torr, T = 600K; (O) $P_{CO} = 24$ Torr, $P_{H2} = 97.6$, T = 538K; (△) $P_{CO} = 24$ Torr, $P_{H2} = 96$ Torr, T = 600K; (□) $P_{CO} = 24$ Torr, $P_{H2} = 96$ Torr, T = 594K (from ref. [70]). (b) A comparison of the rate of methane synthesis over a clean single crystal Ni(100) catalyst with the rate over a potassium doped catalyst. Total reactant pressure is 120 Torr, $H_2/CO = 4$ (from ref. [70]).

Figure 14. A comparison of the product distributions (weight percent) observed for clean and K-doped catalysts at T = 500K, $H_2/CO = 4$, and a total pressure of 120 Torr. Potassium coverage = 0.10 ML (from ref. [70]).

Figure 15. The relative initial rate of reactive carbon formation from CO disproportionation as a function of potassium coverage. $P_{CO} = 24$ Torr, T = 500K. (From ref. [70]).

Figure 16. (a) The methane yield from $Ni/TiO_2(100)$ as a function of the average Ni thickness. $P_{H2} = 60$ Torr, $P_{CO} = 20$ Torr, T = 190°C (from ref. [99]). (b) Arrhenius plots of the methane turnover number (CH_4 molecules/site-s) for Ni(111) and 5Å $Ni/TiO_2(100)$, $P_{H2} = 60$ Torr, $P_{CO} = 20$ Torr (from ref. [99]).

Figure 17. (a) Comparison of the specific rates of the CO + O_2 reaction measured over Rh(100), Rh(111) and Rh/Al_2O_3 (from refs. [106,107]). (b) Measured rates of the CO + O_2 reaction over Rh(111) at various partial pressures of CO, an O_2 partial pressure of 8 Torr and a temperature of 500K (from ref. [107]). (c) Rates of CO oxidation over Rh(111) at various partial pressures of O_2, a CO partial pressure of 16 Torr and a temperature of 500K (from ref. [107]).

Figure 18. (a) Arrhenius plot of the rate of CO_2 formation over Ru(001) and Ru/SiO_2 catalysts (from ref. [107]). (b) Effect of

CO partial pressure on the rate of CO oxidation on Ru(001), P_{O2} = 8 torr, T = 500K (from ref. [107]). (c) Effect of O_2 partial pressure on the rate of CO oxidation on Ru(001), P_{CO}= 16 Torr, T = 500K (from ref. [107]).

Figure 19. Specific rates of CO_2 formation as a function of inverse temperature for single-crystal and supported catalysts (from ref. [109]).

Figure 20. O_2 (part a) and CO (part b) partial pressure dependence of CO oxidation over Pt(100) at several temperatures (from ref. [109]).

Figure 21. Dependence in CO and O_2 partial pressures for CO oxidation on Ir(111) (from ref. [109]).

Figure 22. Arrhenius plot of the CO_2 formation rate from the CO + NO reaction on Rh(111) and Rh(100). $P_{CO} = P_{NO}$ = 8 Torr (from ref. [112]).

Figure 23. NO and CO partial pressure dependences of the CO + NO reaction on Rh(111) and Rh(100) catalysts (from ref. [112]).

Figure 24. Arrhenius plot of the steady-state rates of CO_2 and ethylene epoxide (EtO) production on Ag(110) at P_{Et} = 20 Torr and P_{O2} = 150 Torr (from ref. [8]). Shown for comparison is the rate of EtO production on a silica supported Ag catalyst (form ref. [119]).

Figure 25. Effects of O_2 (part a) and C_2H_4 (part b) partial pressures on the rates of production of ethylene epoxide (EtO)and CO_2 on Ag(110). The selectivity for ethylene conversion into EtO is defined as: $S_{EtO} = TON_{EtO} / (TON_{EtO} + \frac{1}{2}TON_{CO2})$ (from ref. [8]).

Figure 26. (a) Variations in the steady-state reaction rates and selectivity with Cl coverage on Ag(111) at 490K, 4.1 Torr of C_2H_4 and 150 Torr O_2 (from ref. [130]). (b) Selectivity variations on Ag(111) and Ag(110) as a function of Cl coverage (from ref. [130]).

Figure 27. Influence of chlorine coverage upon the kinetic parameters for CO_2 and ethylene epoxide (EtO) production on Ag(110) (from ref. [129]).

Figure 28. Rates of ethylene epoxide (EtO) and CO_2 production as a function of Cs precoverage on Ag(111). The selectivity to produce EtO is defined as: $S_{EtO} = TON_{EtO}/(TON_{EtO} + \frac{1}{2}TON_{CO2})$ (from ref. [131]).

Figure 29. (a) Arrhenius plot of the rate of product appearance during thiophene HDS over Mo(100). P_{H2}= 780 Torr, $P_{thiophene}$= 2.5 Torr (from ref. [144]). (b) Comparison of the product

Figure 39. Ethane hydrogenolysis activity of Re/Pt(111) (a) and Pt/Re(001) (b). P_{ethane}= 10 Torr, P_{H2}= 100 Torr and T= 573K (from ref. [160]).

Figure 40. Relative rate of ethane hydrogenolysis over Ru(001) as a function of copper or sulfur coverage. P_{H2}= 99 Torr, P_{ethane}= 1 Torr, T= 550K (from ref. [152]).

Figure 41. Specific reaction rates for propane hydrogenolysis on Ir(111) and Ir(110)-(1x2). (○)= methane, (□)= ethane. P_{H2}= 100 Torr, $P_{propane}$= 1.0 Torr (from ref. [156]).

Figure 42. Specific reaction rates for n-butane hydrogenolysis on Ir(111) and Ir(110)-(1x2). (○)= methane, (□)= ethane, (△)= propane. P_{H2}= 100 Torr, P_{butane}= 1.0 Torr (from ref. [156]).

Figure 43. Selectivity for ethane production (mol % of total products) from the reaction of n-butane with hydrogen on Ir catalysts plotted as a function of the mean Ir particle size (from ref. [156]). The abscissae for the two single crystals were determined by a calculated "effective particle size" (see ref. [156]).

Figure 44. Specific reaction rates for the hydrogenolysis of n-butane over Rh(110) (part a) and Rh(111) (part b). (□)= methane, (♦)= ethane, (△)= propane. P_{butane}= 10 Torr, P_{H2}= 200 Torr (from ref. [165]).

Figure 45. (a) Product accumulation curves for isobutane hydrogenolysis over platinum single-crystal surfaces. T= 573K, P_{H2}= 200 Torr, $P_{isobutane}$= 20 Torr (from ref. [166]). (b) Idealized atomic surface structures for the flat (100) and (111), stepped (332), (557) and (13,1,1) and kinked (10,8,7) platinum single-crystal surfaces (from refs. [166,178]).

Figure 46. Arrhenius plots for n-hexane hydrogenolysis catalyzed over platinum single crystal surfaces. P_{H2}= 200 Torr, P_{C6H14}= 20 Torr (from ref. [167]). The atomic configurations of the Pt surfaces are shown in Fig. 45b .

Figure 47. Product formation from the reaction of cyclopropane with hydrogen over Ni(111) and Ni(100) surfaces. Total pressure= 100 Torr, H_2/cyclopropane= 100 (from ref. [170]).

Figure 48. Product distribution as a function of S coverage for the reaction of cyclopropane with hydrogen over Ni(111) at 550K and Ni(100) at 450K . P_{total}= 100 Torr, H_2/cyclopropane= 100 (from ref. [170]).

Figure 49. Time evolution of ethane formation on initially clean Mo(100) at 323, 423 and 523K (from ref. [176]).

Figure 50. Arrhenius plots for ethane formation from cyclopropane hydrogenolysis on clean, C- and O-modified Mo(100). P_{H2}= 715 Torr, P_{C3H6}= 40 Torr (from ref. [176]).

Figure 51. Arrhenius plot for the hydrogenolysis of cyclopropane on Pt(s)-[6(111)x(100)]. P_{C3H6}= 135 Torr, P_{H2}= 675 Torr (from ref. [4]).

Figure 52. Specific reaction rates for the reaction of cyclopropane and hydrogen on Ir(111) (part a) and Ir(110)-(1x2) (part b) surfaces. P_{H2}= 100 Torr, P_{C3H6}= 2.0 Torr (from ref. [177]).

Figure 53. Specific rates for the reaction of cyclopropane and hydrogen on Ir(111) at T= 575K. (a) Effect of H_2 partial pressure, P_{C3H6}= 2.0 Torr. (b) Effect of cyclopropane partial pressure, P_{H2}= 100 Torr (from ref. [177]).

Figure 54. (a) Relative selectivity for hydrogenation/isomerization (C_3) and hydrogenolysis (C_1+C_2) from the reaction of cyclopropane and hydrogen on Ir(111) at 575K. The reaction conditions are identical with those given in fig. 53 . (b) The fractional surface coverage of the carbonaceous residue at the corresponding reaction conditions (from ref. [177]).

Figure 55. N-hexane (part a) and light alkane (part b) production from cyclohexane hydrogenolysis as a function of surface structure and time (from ref. [180]). The atomic configurations of the Pt surfaces are shown in Fig. 45b .

Figure 56. Effect of hydrogen pressure upon dehydrogenation and hydrogenolysis rates over Pt(111) (part a) and Pt(10,8,7) (part b, from ref. [180]).

Figure 57. Cyclohexane hydrogenolysis rates over Ru(001) at 650K as a function of reactant partial pressures: a) P_{H2}= 100 Torr, and b) $P_{c-C6H12}$= 1 Torr (from ref. [181]).

Figure 58. Product accumulation curves determined as a function of reaction time for isobutane isomerization over Pt single-crystal surfaces (from ref. [166]). P_{H2}= 200 Torr, $P_{isobutane}$= 20 Torr, and T= 573K . The atomic configurations of the platinum surfaces are shown in Fig. 45b .

Figure 59. Arrhenius plots for the initial rates of isobutane isomerization over the flat (100) and kinked (10,8,7) platinum single-crystal surfaces (from ref. [166]).

Figure 60. Product accumulation curves measured as a function of reaction time for neopentane isomerization over Pt single-crystal surfaces (from ref. [166]).

Figure 61. Arrhenius plots for n-hexane isomerization to 2-methylpentane (below) and 3-methylpentane (above) catalyzed over several Pt surfaces (from ref. [167]). The atomic configurations of the platinum surfaces are shown in Fig. 45b .

Figure 62. Arrhenius plots for n-hexane C_5-cyclization (part a) and aromatization (part b) catalyzed over five Pt surfaces (from ref. [167]).

Figure 63. Plot of the initial turnover frequencies per surface atom (platinum and gold) versus the surface atom fraction of gold (from ref. [169]).

Figure 64. Toluene formation from n-heptane over four Pt single-crystal surfaces (from ref. [178]).

Figure 65. The dependence of initial rates (top) and selectivities (bottom) with respect to atomic surface structure at 15 Torr n-heptane, 480 Torr hydrogen and 573K (from ref. [178]).

Figure 66. Structure sensitivities of alkane isomerization reactions catalyzed over platinum single-crystal surfaces (from ref. [166]). The atomic configurations of the Pt surfaces are displayed in Fig. 45b .

Figure 67. Arrhenius plots for ethylene hydrogenation with H_2 and D_2 over Pt(111). P_{C2H4}= 10 Torr, P_{H2} or P_{D2}= 20 Torr, and P_{N2}= 80 Torr (from ref. [186]).

Figure 68. Deuterium atom distribution in the resulting ethane from the hydrogenation of ethylene with deuterium over Pt(111) (from ref. [186]).

Figure 69. Specific reaction rates for the reaction of propylene and hydrogen on Ir(111) (part a) and Ir(110)-(1x2) (part b). The partial pressure of propylene was 2 Torr, whereas that of hydrogen was 100 Torr (from ref. [177]).

Figure 70. (a) Specific reaction rates for the reaction of propylene and hydrogen on the Ir(111) surface at a temperature of 575K. The partial pressure of hydrogen was maintained at 100 Torr as the partial pressure of propylene was varied. (b) The fractional coverage of the carbonaceous residue at the corresponding reaction conditions (from ref. [177]).

Figure 71. 1,3-Butadiene hydrogenation reaction on Pt(111): (a) composition of the gas phase as a function of time; (b) selectivity as a function of conversion. "B-1" = 1-butene, "B-2-cis" = 2-cis-butene, and "B-2-trans" = 2-trans-butene. T= 413K, P_{H2}= 495 Torr and P_{C4H6}= 20.3 Torr (from ref. [189]).

Figure 72. Initial rates of 1,3-butadiene hydrogenation on Pt(100) (part a, from ref. [188]) and Pt(111) (part b, from ref. [189]).

Figure 73. Rates of 1,3-butadiene hydrogenation as a function of S coverage (from refs. [188,189]).

Figure 74. Conversion versus time for 1,3-butadiene hydrogenation on: (a) Pt(111) and (b) $Pt_{0.5}Ni_{0.5}(111)$. P_{H2}= 660 Torr, P_{C4H6}= 4.5 Torr and T= 300K (from ref. [191]).

Figure 75. Product accumulation versus reaction time for cyclohexene hydrogenation over Pt(223) at several temperatures (from ref. [190]).

Figure 76. Correlation of cyclohexene reaction rates and reaction probabilities over a ten-order-of-magnitude pressure range. The reactions were performed at 423K over Pt(223) with P_{H2}/P_{C4H6}= 10 (from ref. [190]).

Figure 77. Arrhenius plot for cyclohexene hydrogenation over Pt(223) (from ref. [190]). For comparison results for a high-surface area Pt/SiO_2 catalyst are included (from ref. [194]).

Figure 78. Product accumulation curves for the reaction of cyclohexane + hydrogen on the Pt(10,8,7) surface (from ref. [180]).

Figure 79. Benzene (part a) and cyclohexene (part b) production from the $c\text{-}C_6H_{12} + H_2$ reaction on several platinum surfaces (from ref. [180]).

Figure 80. Influence of Au surface content on the amount of benzene and cyclohexene produced from cyclohexane dehydrogenation over Au-Pt(111) in 123 min reaction time (from ref. [203]).

Figure 81. Part a: amount of benzene (1) and lower carbon number alkanes (2) formed from the $c\text{-}C_6H_{12} + H_2$ reaction on Ru(001) as a function of time; (3) Relative quantities of carbonaceous material present on the surface following reaction. Part b: relative rates of cyclohexane dehydrogenation (4) and hydrogenolysis (5) as a function of relative carbon coverage present on the surface following reaction at T= 650K, H_2/C_6H_{12}= 100, P_{Total}= 101 Torr (from ref. [181]).

Figure 82. (a) Arrhenius plot of the rate of cyclohexane dehydrogenation to benzene over Ru(001) under steady-state reaction conditions, H_2/C_6H_{12}= 100 and P_{total}= 101 Torr. (b) Cyclohexane dehydrogenation rates over Ru(001) at 650K as a function of reactant partial pressure: (1) P_{H2}= 100 Torr and (2) P_{C6H12}= 1 Torr (from ref. [181]).

Figure 83. Relative rate of cyclohexane dehydrogenation as a function of surface Cu coverage on Ru(001) at T= 650K, H_2/C_6H_{12}= 25 and P_{Total}= 104 Torr (from ref. [181]).

Figure 84. Relative amount of benzene formed from acetylene cyclotrimerization on Pd single crystals in UHV and at atmospheric pressures (from ref. [205]).

Figure 85. (a) Apparent activation energy for acetylene cyclotrimerization over Pd. The same value was obtained on all three low-Miller-index planes of palladium [205]. (b) Turnover frequency for acetylene cyclization as a function of acetylene partial pressure (from ref. [205]).

Figure 86. Variation of the water-gas shift reaction rates on Cu(110) and Cu(111) with temperature, in Arrhenius form. P_{H2O} = 10 Torr and P_{CO} = 26 Torr. (from ref. [214] and [215]).

Figure 87. Potential energy diagram of the water-gas shift reaction on Cu(110) (from ref. [215]).

Figure 88. Rate of water-gas shift reaction over Cu(111) as a function of sulfur coverage (from ref. [221]).

Figure 89. The water-gas shift reaction rate as function of Cs coverage (θ_{Cs}) on Cs/Cu(110) at 493, 523 and 573K. P_{H2O} = 10 Torr and P_{CO} = 26 Torr (from ref. [215]).

Figure 90. (a) Turnover frequency (CH_3OH molecules produced/Pd surface atom-s) versus inverse temperature at a total pressure of 244 kPa and a 3.9:1 H_2/CO mixture (from ref. [231]). (b) Turnover frequency plotted as a function of total pressure at 553K, for a 3.9:1 H_2/CO mixture (from ref. [231]).

Figure 91. The temperature dependence of methanol turnover frequencies for Cu(100) (•) [236], oxidized Cu(100) (▲) [236], Cu/SiO_2 (∇) [237,238], CuO/ZnO (Δ,○) [232], $CuO/ZnO/Al_2O_3$ (○) [232], and Raney Cu-Zn (◊) [232]. Filled symbols represent data obtained under the actual experimental conditions: P_T = 750 Torr, $CO_2/CO/H_2$ = 1/2/12. Open symbols represent data extrapolated to 14.8 atm (from ref. [236]).

TABLE I

Metal Single Crystal Catalysts: Specific Activities and Activation Energies in CO Methanation

Catalyst	T (K)	P_{H2} (Torr)	P_{CO} (Torr)	TOF[a] ($site^{-1}s^{-1}$)	E_a (kJ/mol)	Ref.
Ni(100)	450-700	96	24	0.0002 - 8	103	[25]
Ni(111)	550-700	96	24	0.04 - 5	103	[25]
	440-540	60	20	0.0002 - 0.05	111	[99]
Ru(110)	500-700	96	24	0.002 - 10	123	[25]
Ru(001)	550-650	96	24	0.01 - 0.8	~120	[25]
W(110)	480-750	100	0.1	0.002 - 0.5	56	[34]
Mo(100)	510-640	1100	220	0.001 - 0.2	100	[38]
Co(001)	490-550	500	250	0.01 - 0.07	~70	[40]

[a] TOF = turnover frequency = CH_4 molecules/site-s

Table II

CO Oxidation by O_2

Activation Energies

Catalyst	P_{CO} (Torr)	P_{O2} (Torr)	Temp (K)	TOF[a]	E_a (kJ mol^{1})	ref.
Rh(100)	8	8	450-600	0.1-1000	108.8	[107]
Rh(111)						
Ru(0001)	16	8	380-550	0.05-50	81.6	[108]
Pt(100)	16	8	500-725	0.1-500	137.7	[109]
Pd(110)	16	8	475-625	0.05-400	138.6	[109]
Ir(110)	16	8	425-625	0.02-100	92.1	[109]
Ir(111)						

Reaction Orders[b]

Catalyst	Temp (K)	in CO	in O_2	ref.
Rh(111)	500K	~ -1.0	~ 1.0	[107]
Ru(0001)	500K	--	~ 0.0	[108]
Pt(100)	650K	-0.9 ± 0.2	1.0 ± 0.1	[109]
Pd(110)	525K	-1.0 ± 0.1	1.0 ± 0.1	[109]
Ir(111)	525K	-0.9 ± 0.2	0.9 ± 0.2	[109]

[a] TOF = Turnover frequency = CO_2 molecules metal surface site•second

[b] P_{CO} = 16 Torr, P_{O2} = 8 Torr.

TABLE III

Metal Single Crystal Catalysts: Specific Activities and Activation Energies in Ethane Hydrogenolysis.

Catalyst	T (K)	P_{H2} (Torr)	P_{ethane} (Torr)	TOF[a] ($site^{-1}s^{-1}$)	E_a (kJ/mol)	Ref.
Ni(100)	450-600	99	0.99	0.0005 - 0.3	100.5	[148]
Ni(111)	520-600	99	0.99	0.0005 - 0.1	192.6	[148]
Ru(001)	500-600	20	1	0.2 - 3	~84	[152]
	500-600	99	1	0.04 - 1	~84	[152]
Ru(1,1,10)	475-510	39.8	5.6	-	92	[153]
Ir(111)	450-550	100	1	0.0004 - 0.3	145.2	[156]
	575-650	100	1	0.9 - 8	82.5	[156]
Ir(110)-(1x2)	475-575	100	1	0.0003 - 2	206.7	[156]
	575-700	100	1	2 - 75	95.4	[156]
Pt(111)	550-640	100	1	0.0003 - 0.02	153.2	[158]
	570-625	100[b]	10	0.02 - 0.25	144	[159]
Re(001)	573-623	100	10	0.55 - 2	75.3	[160]
W(100)	553-613	100	1	0.004 - 0.05	113	[162]

[a] TOF= turnover frequency = CH_4 molecules/site s

[b] D_2 pressure

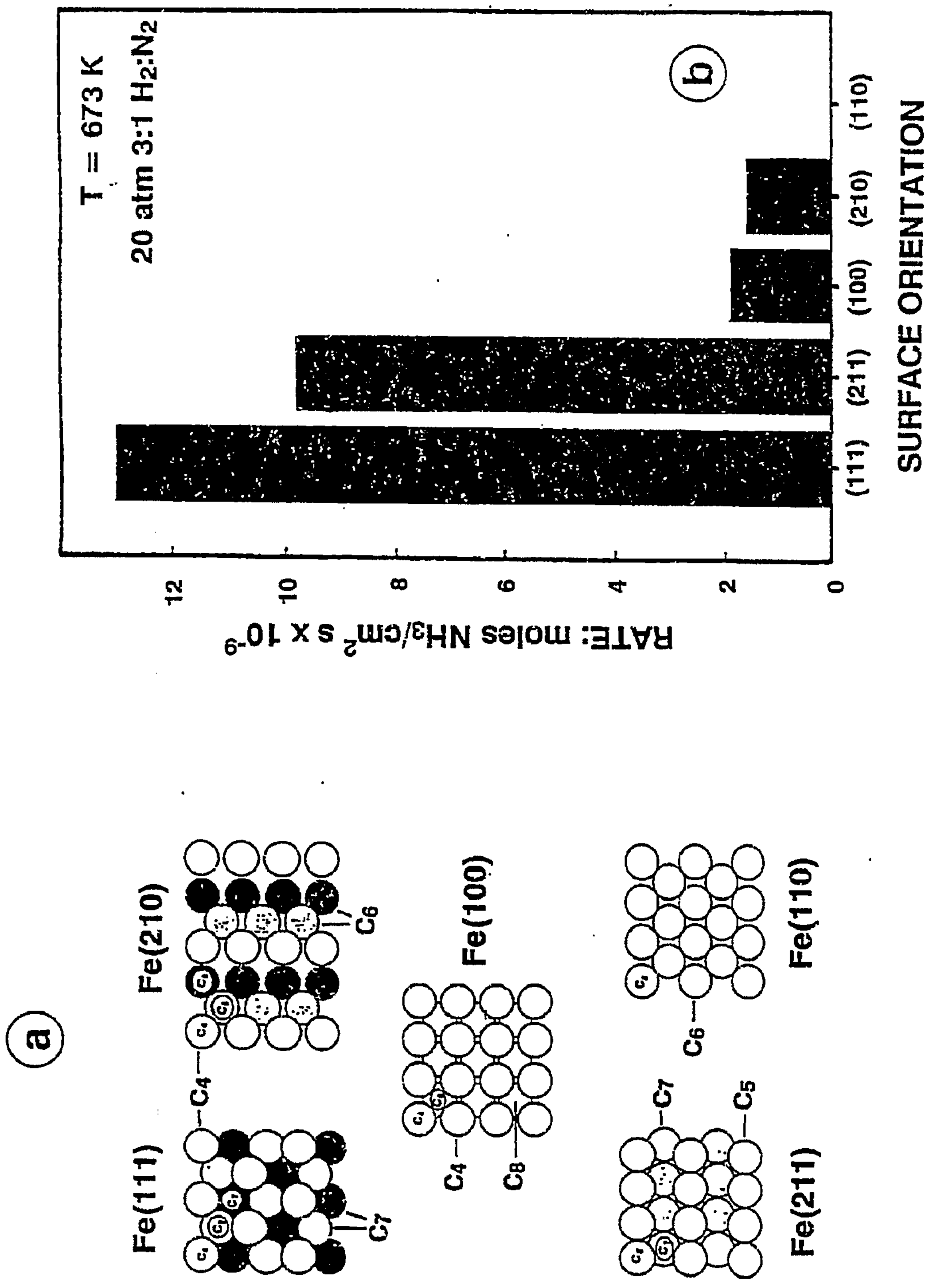
a
Fe(111)
C4
C7
Fe(210)
C6
Fe(100)
C4
C8
Fe(211)
C7
C5
Fe(110)
C6
b
T = 673 K
20 atm 3:1 H₂:N₂
RATE: moles NH₃/cm² s x 10⁻⁹
0
2
4
6
8
10
12
(111)
(211)
(100)
(210)
(110)
SURFACE ORIENTATION

Fig. 1

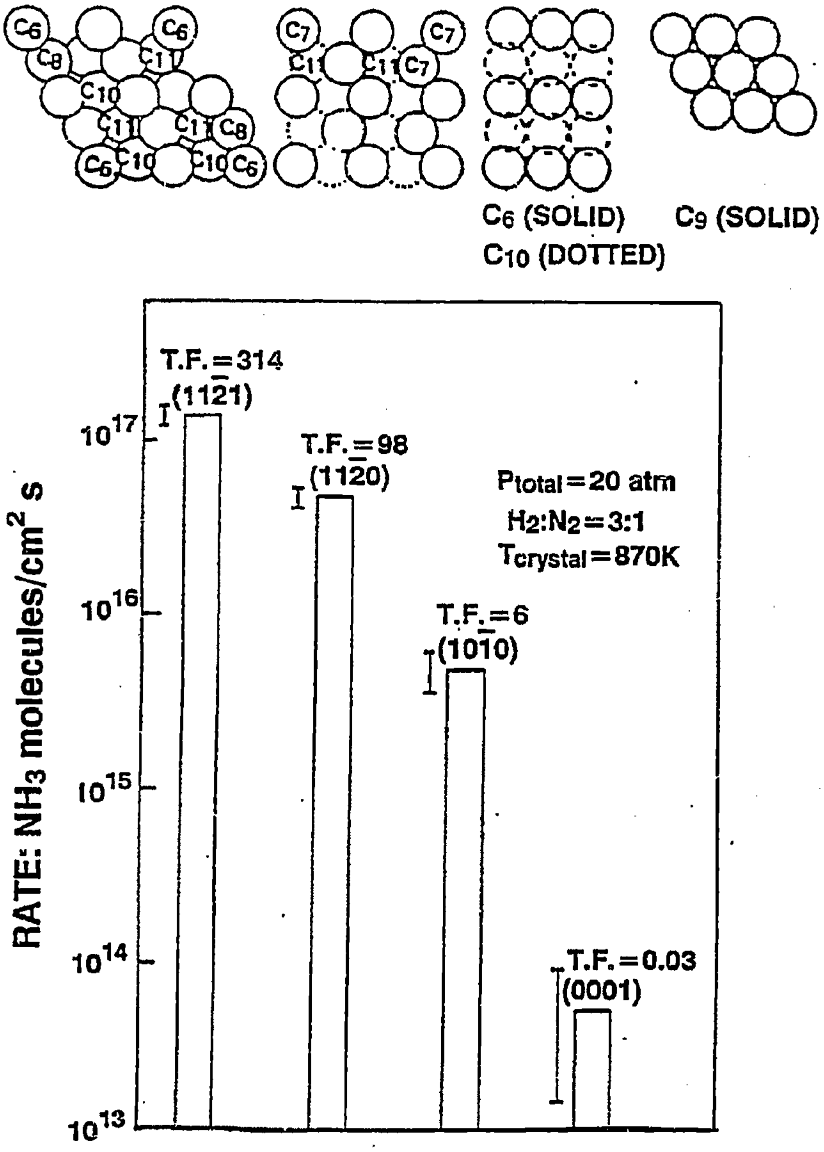
C6
C8
C6
C11
C10
C11
C11
C8
C6
C10
C10
C6
C7
C7
C11
C11
C7
C6 (SOLID)
C10 (DOTTED)
C9 (SOLID)
RATE: NH_3 molecules/cm^2 s
10^{17}
10^{16}
10^{15}
10^{14}
10^{13}
T.F. = 314
(11$\bar{2}$1)
T.F. = 98
(11$\bar{2}$0)
T.F. = 6
(10$\bar{1}$0)
T.F. = 0.03
(0001)
P_{total} = 20 atm
H_2:N_2 = 3:1
$T_{crystal}$ = 870K

Fig. 2

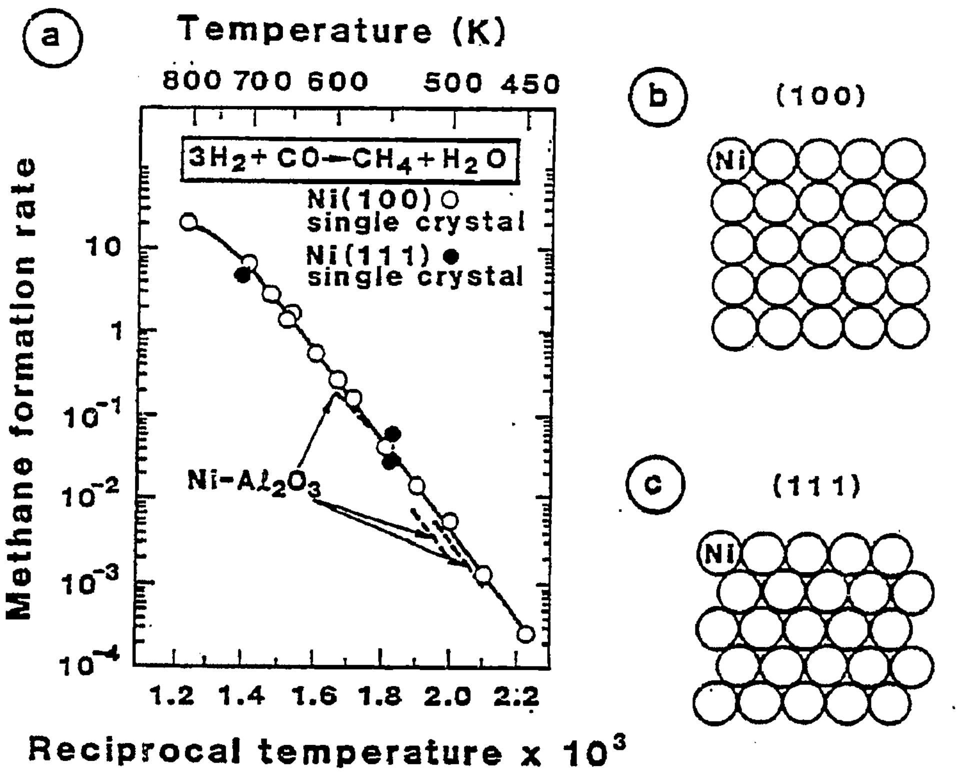
a
Temperature (K)
800 700 600 500 450
$3H_2 + CO \rightarrow CH_4 + H_2O$
Ni(100) ○ single crystal
Ni(111) ● single crystal
Methane formation rate
10
1
10^{-1}
10^{-2}
10^{-3}
10^{-4}
$Ni\text{-}Al_2O_3$
1.2 1.4 1.6 1.8 2.0 2.2
Reciprocal temperature x 10^3
b
(100)
Ni
c
(111)
Ni

Fig. 3

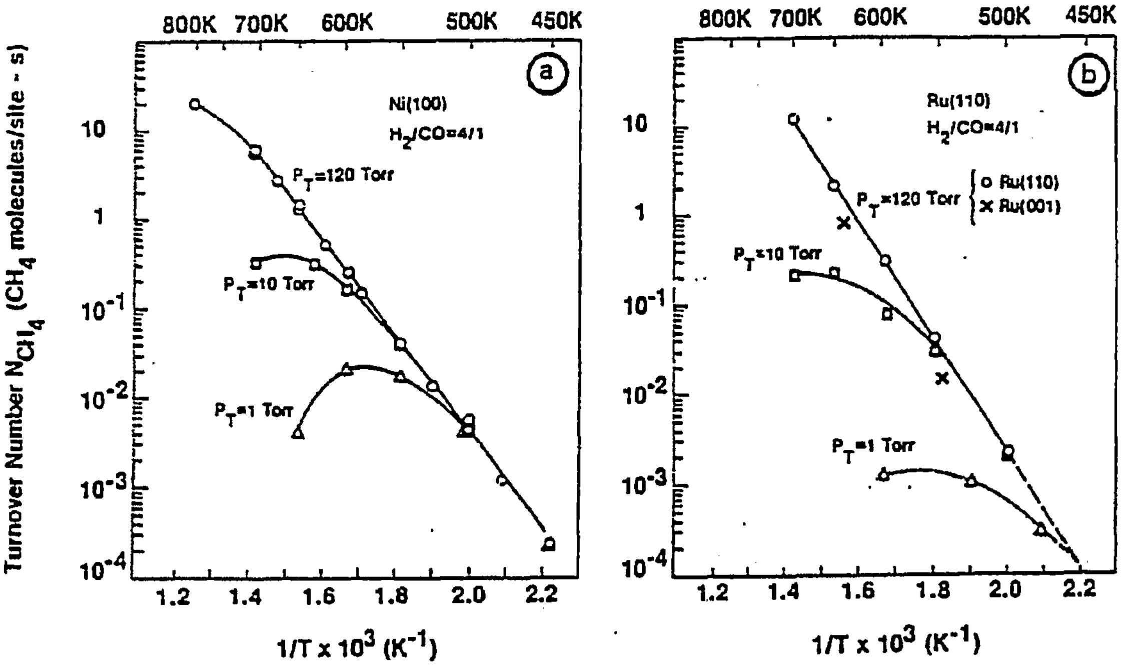
800K
700K
600K
500K
450K
Turnover Number N_{CH_4} (CH_4 molecules/site - s)
10
1
10^{-1}
10^{-2}
10^{-3}
10^{-4}
a
Ni(100)
$H_2/CO=4/1$
$P_T=120$ Torr
$P_T=10$ Torr
$P_T=1$ Torr
1.2
1.4
1.6
1.8
2.0
2.2
1/T x 10^3 (K^{-1})
b
Ru(110)
$H_2/CO=4/1$
$P_T=120$ Torr
o Ru(110)
x Ru(001)
$P_T=10$ Torr
$P_T=1$ Torr

Fig. 4

Methanation Rate Versus Surface Carbon Level

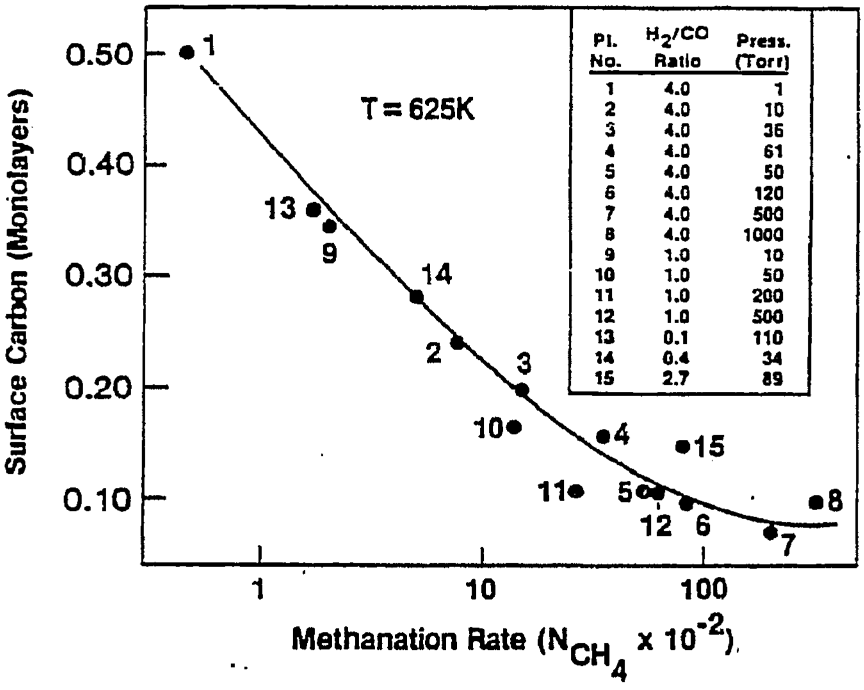

Pt. No.	H_2/CO Ratio	Press. (Torr)
1	4.0	1
2	4.0	10
3	4.0	36
4	4.0	61
5	4.0	50
6	4.0	120
7	4.0	500
8	4.0	1000
9	1.0	10
10	1.0	50
11	1.0	200
12	1.0	500
13	0.1	110
14	0.4	34
15	2.7	89

Fig. 5

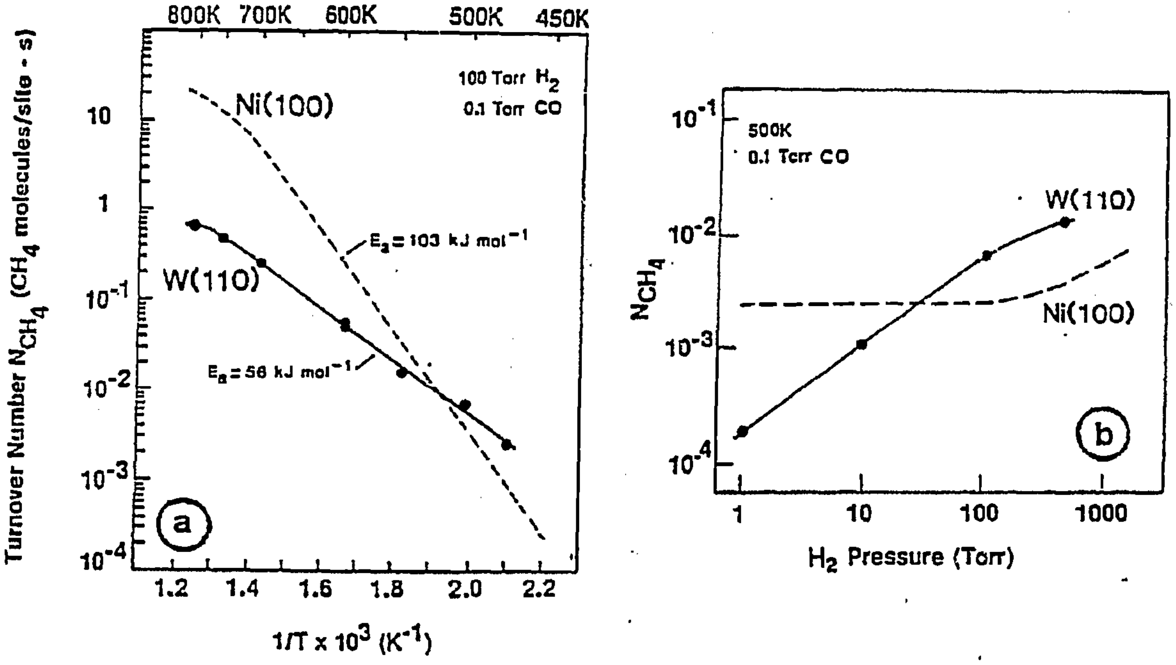
800K
700K
600K
500K
450K
100 Torr H_2
0.1 Torr CO
Ni(100)
W(110)
$E_a = 103$ kJ mol^{-1}
$E_a = 56$ kJ mol^{-1}
Turnover Number N_{CH_4} (CH_4 molecules/site · s)
10
1
10^{-1}
10^{-2}
10^{-3}
10^{-4}
1.2
1.4
1.6
1.8
2.0
2.2
$1/T \times 10^3$ (K^{-1})
a
500K
0.1 Torr CO
W(110)
Ni(100)
N_{CH_4}
10^{-1}
10^{-2}
10^{-3}
10^{-4}
1
10
100
1000
H_2 Pressure (Torr)
b

Fig. 6

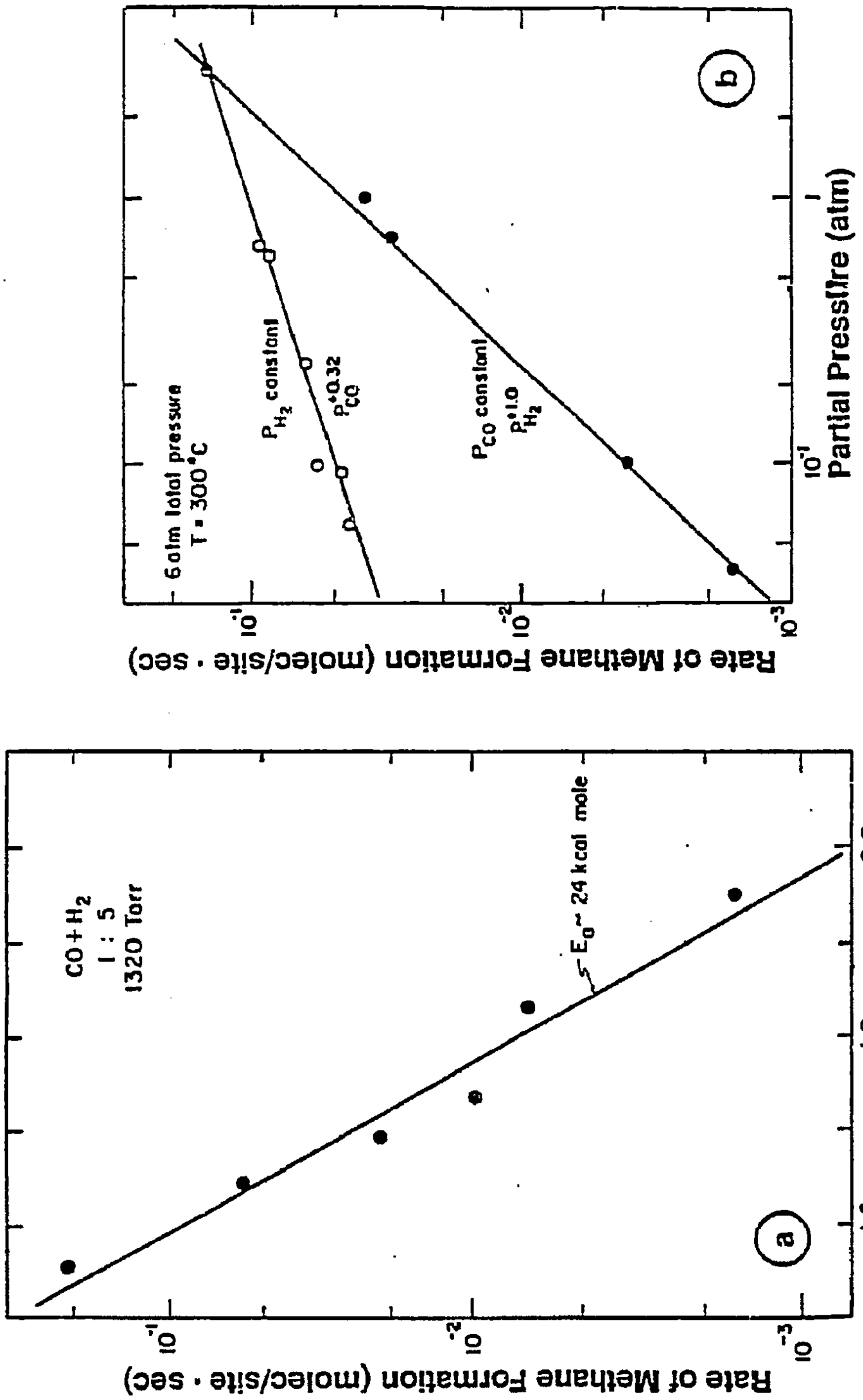
a
CO + H_2
1 : 5
1320 Torr
$E_a \sim 24$ kcal mole
Rate of Methane Formation (molec/site · sec)
10^{-1}
10^{-2}
10^{-3}
1.6
1.8
2.0
1/T x 10^3 (K^{-1})
b
6 atm total pressure
T = 300°C
P_{H_2} constant
$P_{CO}^{+0.32}$
P_{CO} constant
$P_{H_2}^{+1.0}$
Rate of Methane Formation (molec/site · sec)
10^{-1}
10^{-2}
10^{-3}
10^{-1}
1
Partial Pressure (atm)

Fig. 7

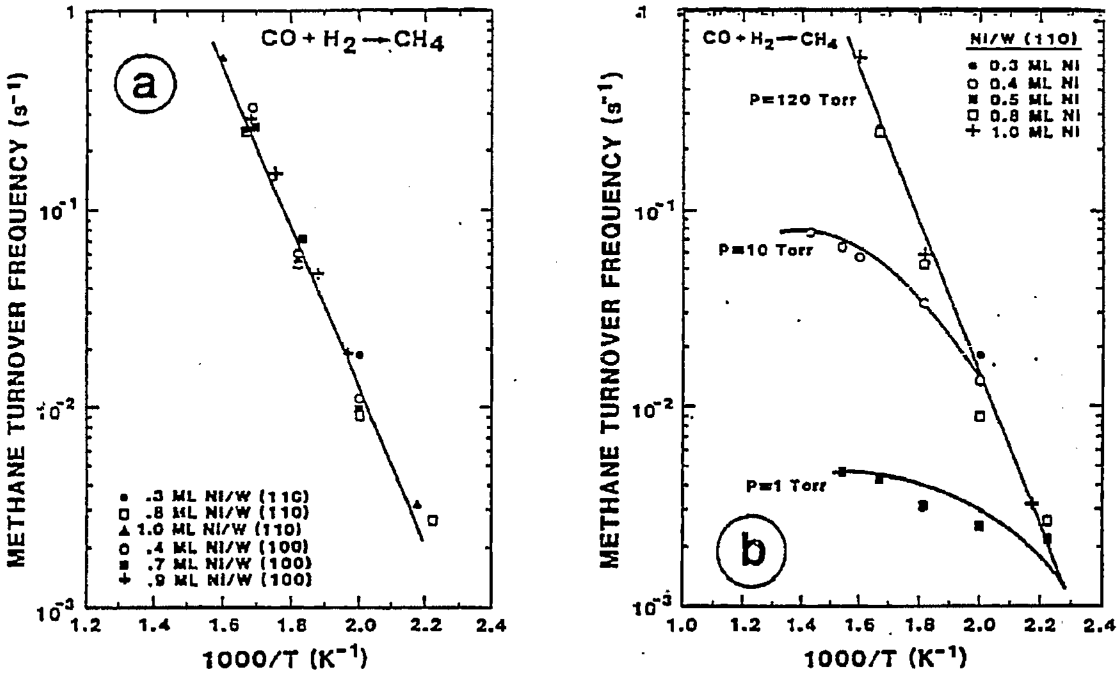
a
CO + H_2 → CH_4
METHANE TURNOVER FREQUENCY (s^{-1})
1
10^{-1}
10^{-2}
10^{-3}
1.2
1.4
1.6
1.8
2.0
2.2
2.4
1000/T (K^{-1})
● .3 ML Ni/W (110)
□ .8 ML Ni/W (110)
▲ 1.0 ML Ni/W (110)
○ .4 ML Ni/W (100)
■ .7 ML Ni/W (100)
+ .9 ML Ni/W (100)
b
CO + H_2 → CH_4
Ni/W (110)
● 0.3 ML Ni
○ 0.4 ML Ni
■ 0.5 ML Ni
□ 0.8 ML Ni
+ 1.0 ML Ni
P=120 Torr
P=10 Torr
P=1 Torr
METHANE TURNOVER FREQUENCY (s^{-1})
1
10^{-1}
10^{-2}
10^{-3}
1.0
1.2
1.4
1.6
1.8
2.0
2.2
2.4
1000/T (K^{-1})

Fig. 8

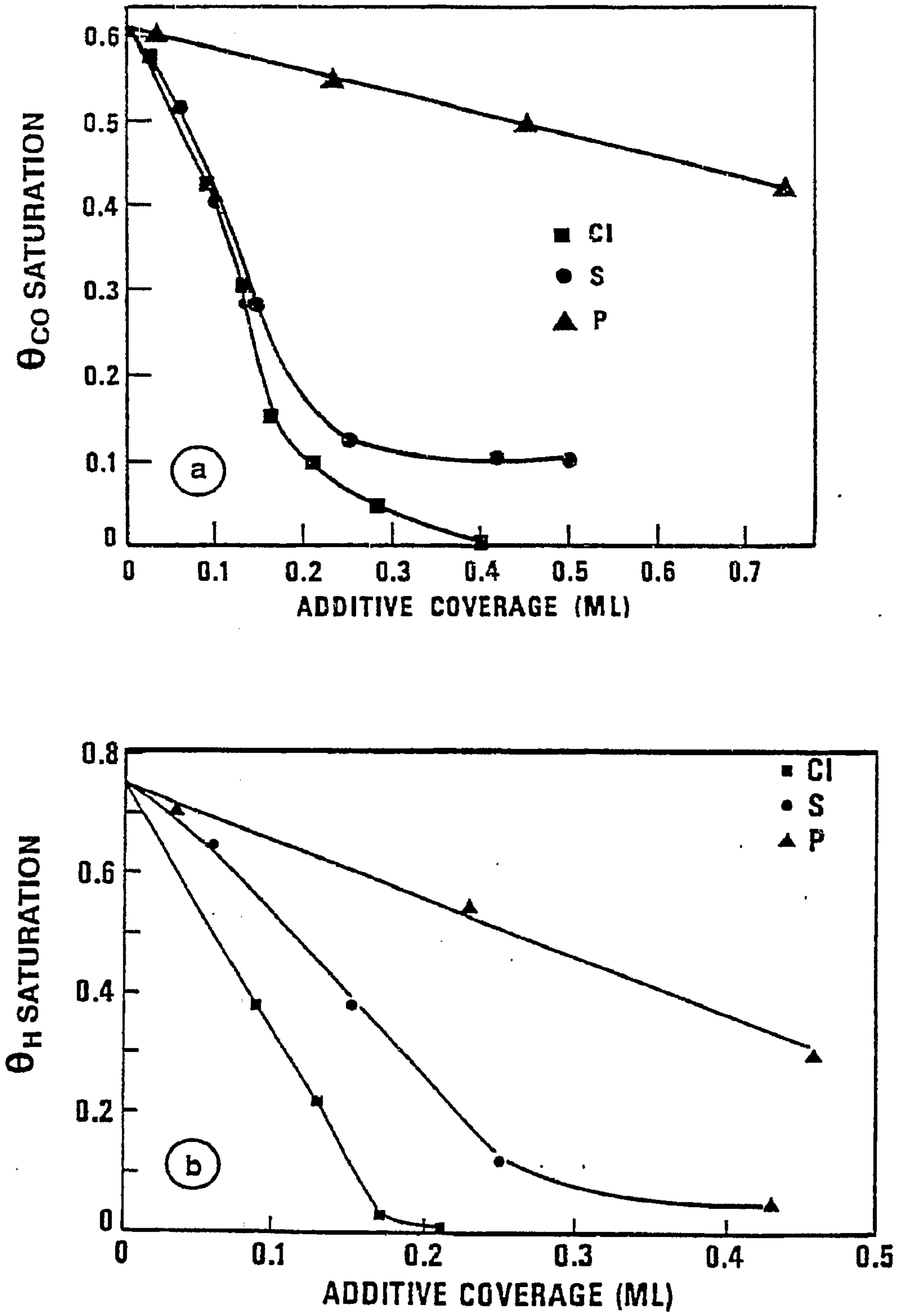
θ_CO SATURATION
0.6
0.5
0.4
0.3
0.2
0.1
0
■ Cl
● S
▲ P
a
0
0.1
0.2
0.3
0.4
0.5
0.6
0.7
ADDITIVE COVERAGE (ML)
θ_H SATURATION
0.8
0.6
0.4
0.2
0
■ Cl
● S
▲ P
b
0
0.1
0.2
0.3
0.4
0.5
ADDITIVE COVERAGE (ML)

Fig. 9

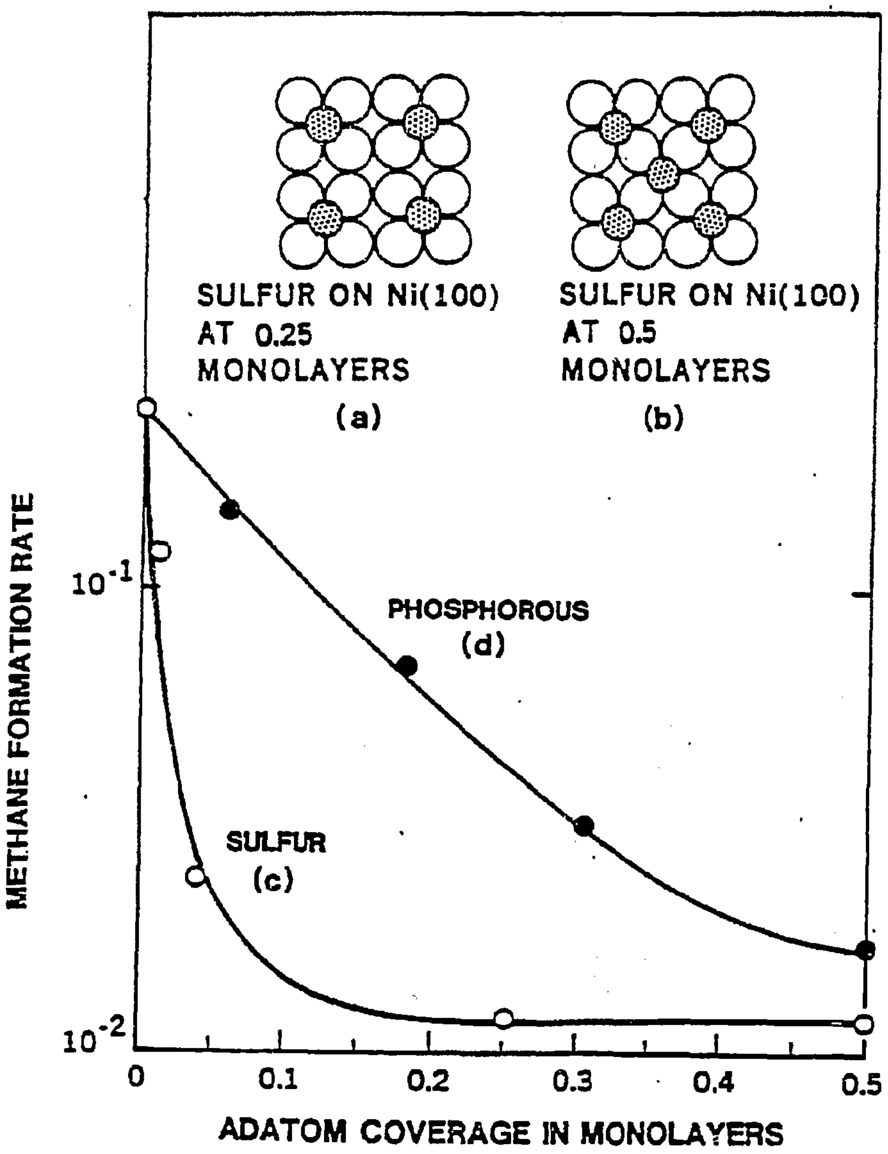
SULFUR ON Ni(100)
AT 0.25
MONOLAYERS
(a)
SULFUR ON Ni(100)
AT 0.5
MONOLAYERS
(b)
METHANE FORMATION RATE
10^-1
10^-2
PHOSPHOROUS
(d)
SULFUR
(c)
0
0.1
0.2
0.3
0.4
0.5
ADATOM COVERAGE IN MONOLAYERS

Fig. 10

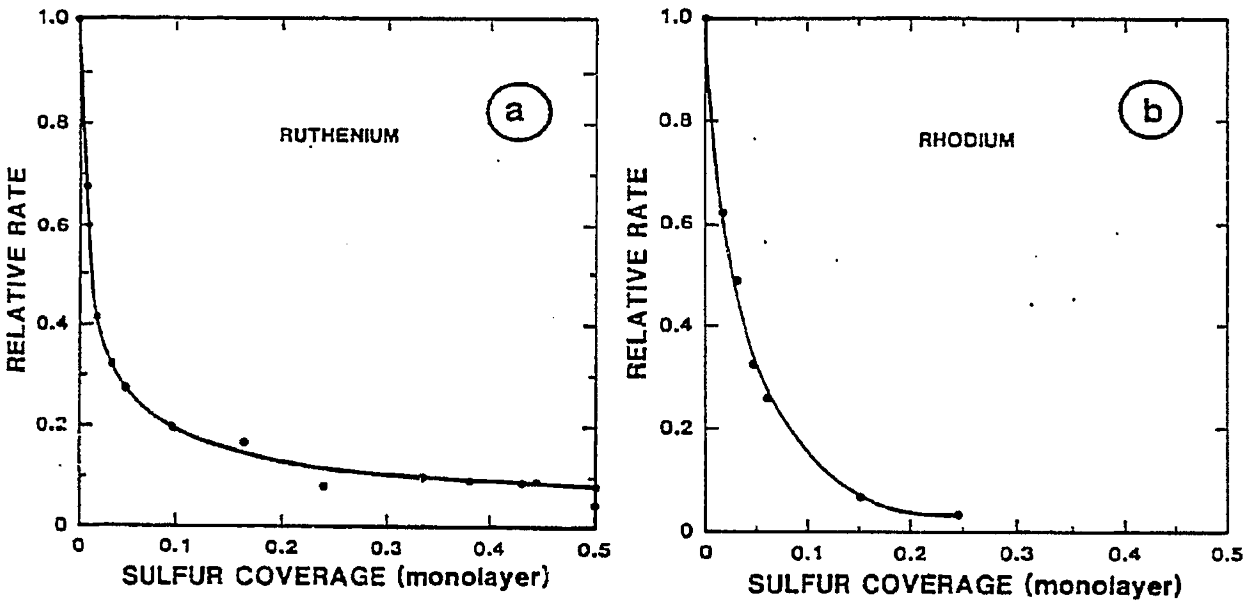
1.0
0.8
0.6
0.4
0.2
0
RELATIVE RATE
a
RUTHENIUM
0
0.1
0.2
0.3
0.4
0.5
SULFUR COVERAGE (monolayer)
b
RHODIUM
SULFUR COVERAGE (monolayer)

Fig. 11

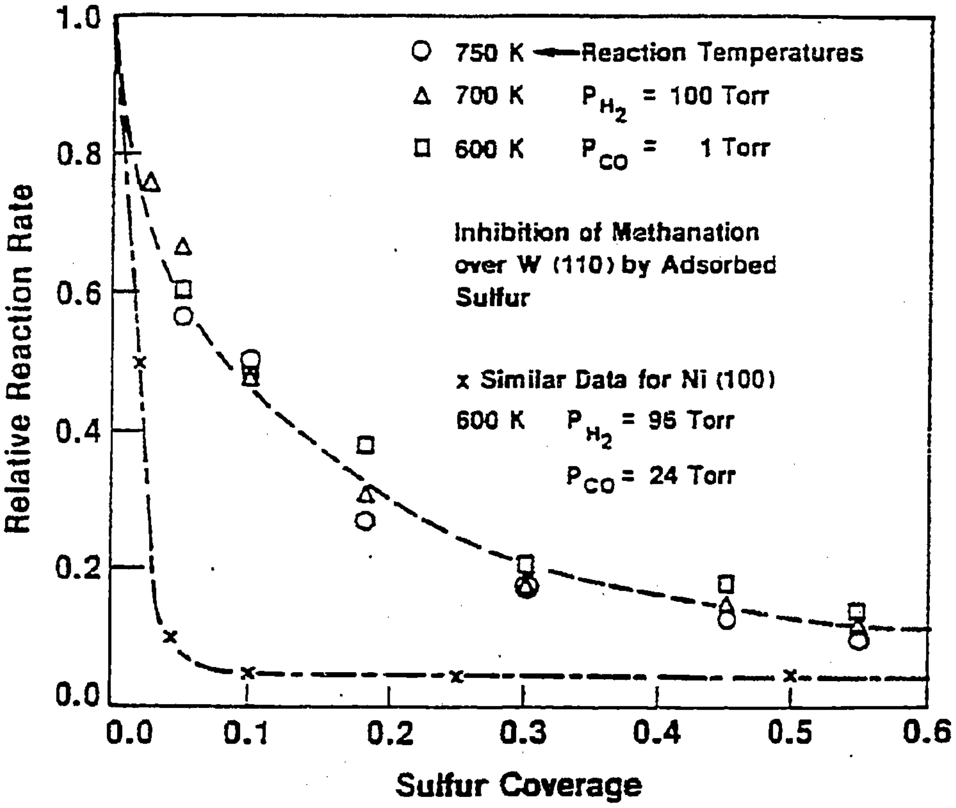

1.0
0.8
0.6
0.4
0.2
0.0
Relative Reaction Rate
0.0
0.1
0.2
0.3
0.4
0.5
0.6
Sulfur Coverage
○ 750 K ← Reaction Temperatures
△ 700 K P_{H_2} = 100 Torr
□ 600 K P_{CO} = 1 Torr
Inhibition of Methanation over W (110) by Adsorbed Sulfur
x Similar Data for Ni (100)
600 K P_{H_2} = 95 Torr
P_{CO} = 24 Torr

Fig. 12

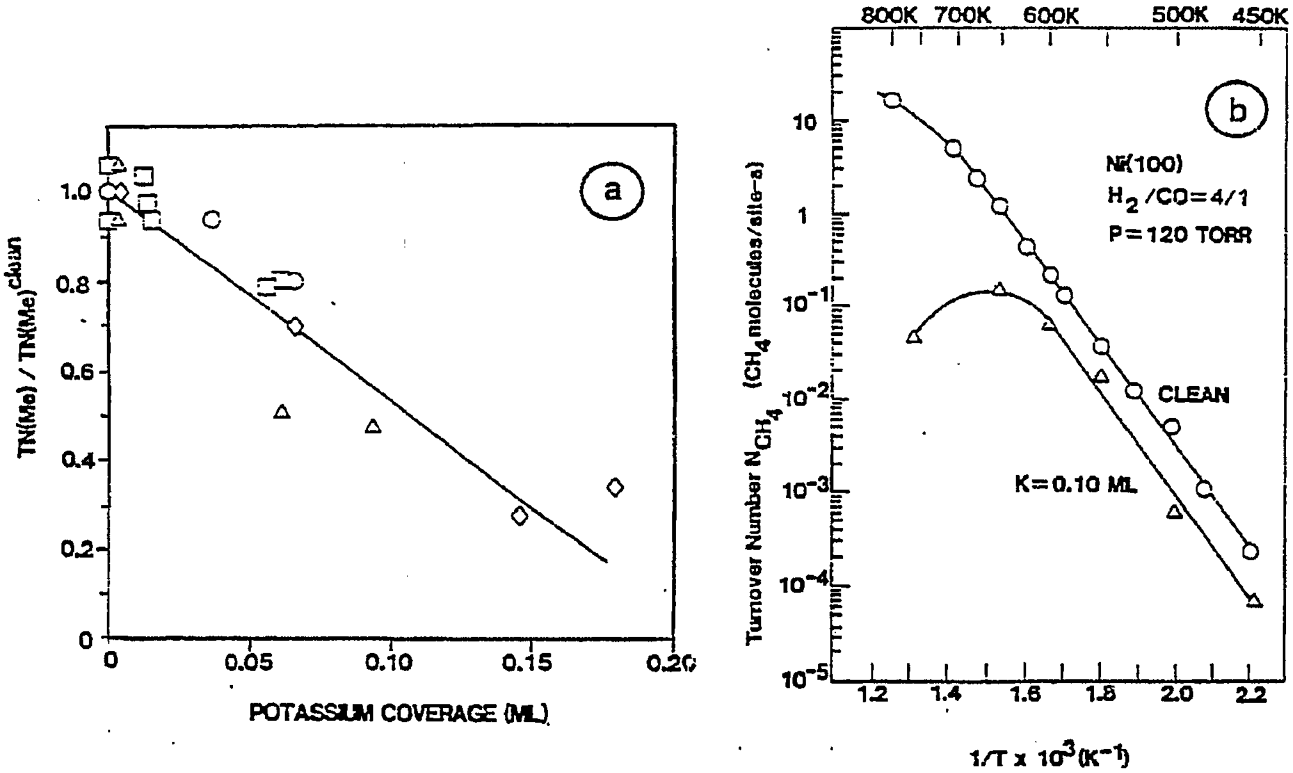
a
1.0
0.8
0.6
0.4
0.2
0
TN(Me) / TN(Me)^{clean}
0
0.05
0.10
0.15
0.20
POTASSIUM COVERAGE (ML)
b
800K
700K
600K
500K
450K
10
1
10^{-1}
10^{-2}
10^{-3}
10^{-4}
10^{-5}
Turnover Number N_{CH_4} (CH_4 molecules/site-s)
Ni(100)
H_2/CO=4/1
P=120 TORR
CLEAN
K=0.10 ML
1.2
1.4
1.6
1.8
2.0
2.2
1/T x 10^3(K^{-1})

Fig. 13

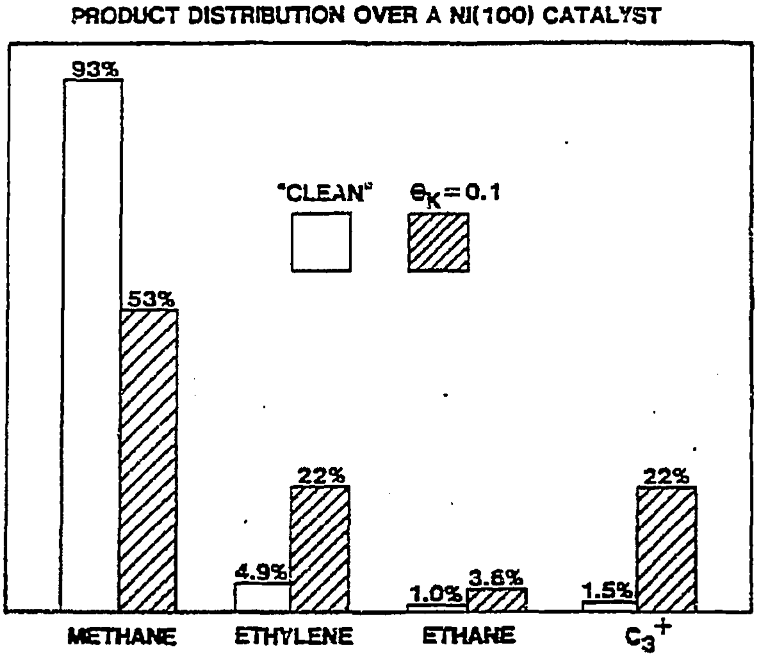
PRODUCT DISTRIBUTION OVER A NI(100) CATALYST
"CLEAN"
$\theta_K = 0.1$
93%
53%
4.9%
22%
1.0%
3.6%
1.5%
22%
METHANE
ETHYLENE
ETHANE
C_3^+

Fig. 14

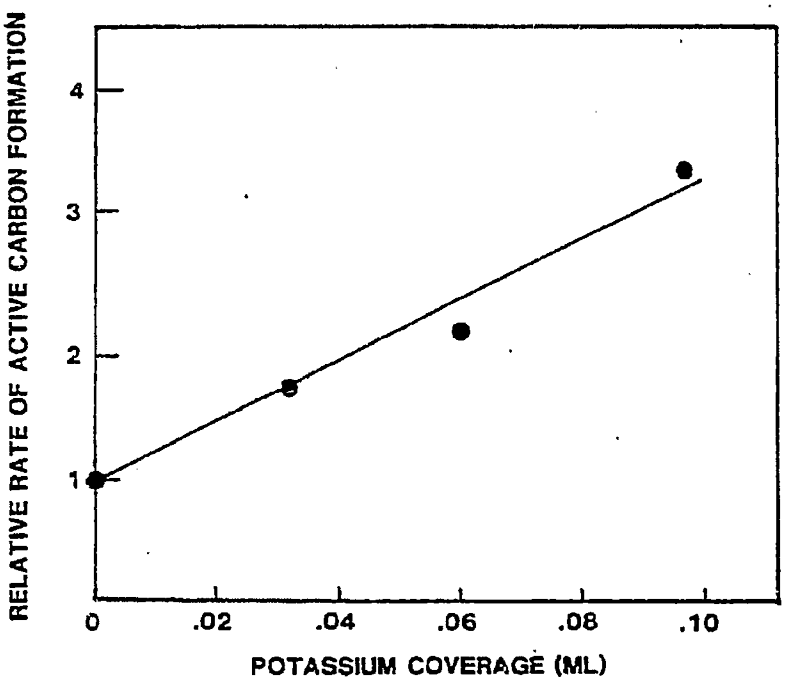

RELATIVE RATE OF ACTIVE CARBON FORMATION
4
3
2
1
0
.02
.04
.06
.08
.10
POTASSIUM COVERAGE (ML)

Fig. 15

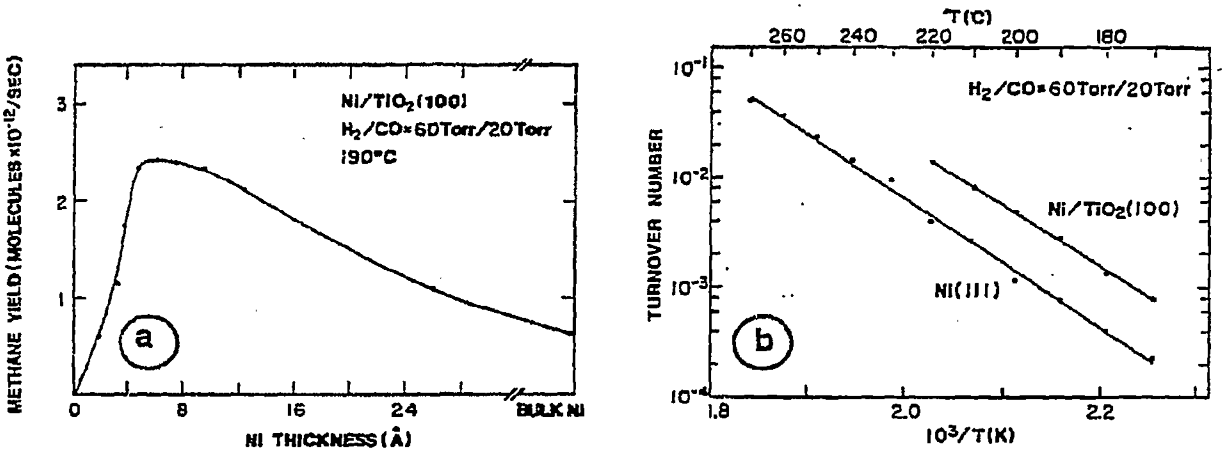
METHANE YIELD (MOLECULES×10^{-12}/SEC)
3
2
1
0
8
16
24
BULK Ni
Ni THICKNESS (Å)
Ni/TiO$_2$(100)
H$_2$/CO=60Torr/20Torr
190°C
a
T(°C)
260
240
220
200
180
10^{-1}
10^{-2}
10^{-3}
10^{-4}
TURNOVER NUMBER
1.8
2.0
2.2
10^3/T(K)
H$_2$/CO=60Torr/20Torr
Ni/TiO$_2$(100)
Ni(111)
b

Fig. 16

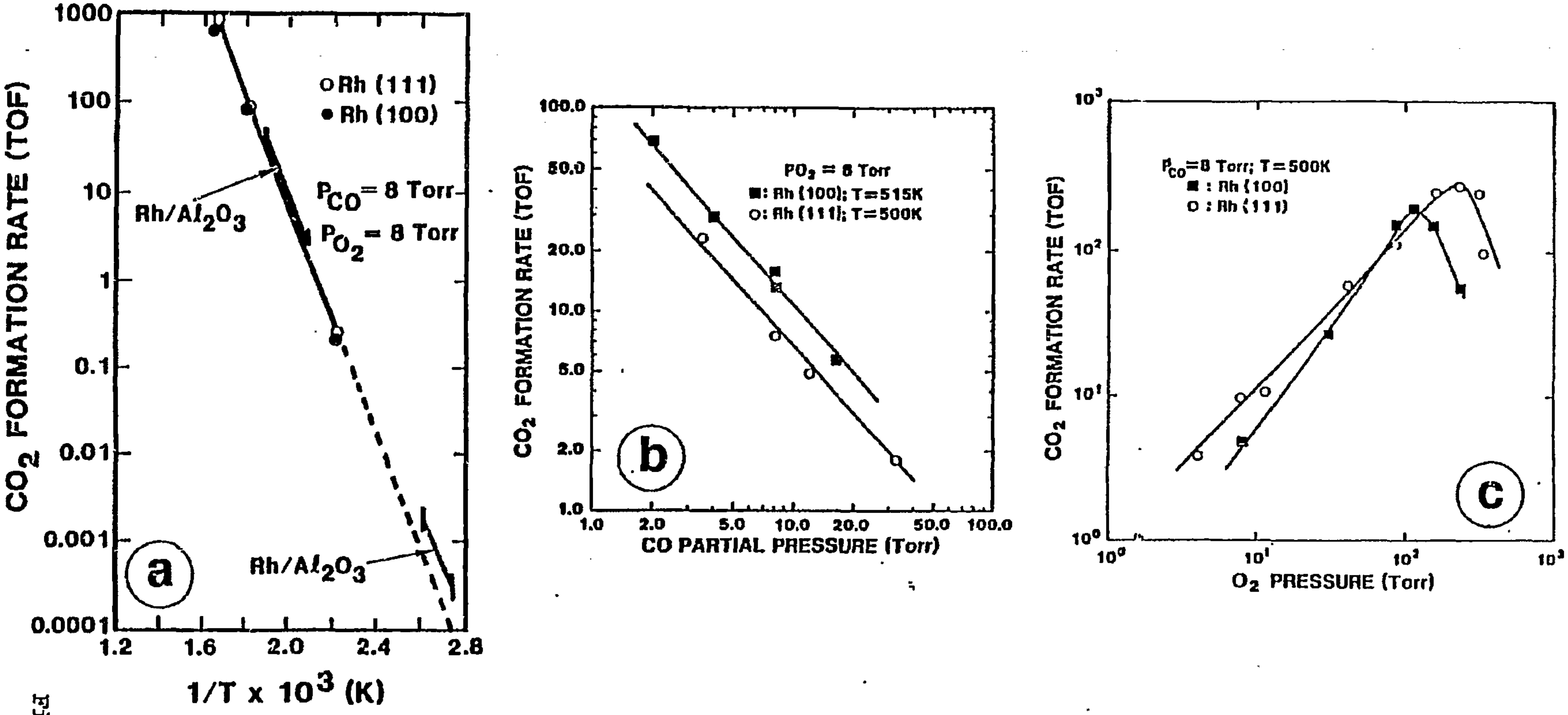
CO$_2$ FORMATION RATE (TOF)
1000
100
10
1
0.1
0.01
0.001
0.0001
1.2
1.6
2.0
2.4
2.8
1/T x 10^3 (K)
○ Rh (111)
● Rh (100)
P_{CO} = 8 Torr
P_{O_2} = 8 Torr
Rh/Al$_2$O$_3$
Rh/Al$_2$O$_3$
a
CO$_2$ FORMATION RATE (TOF)
100.0
50.0
20.0
10.0
5.0
2.0
1.0
1.0
2.0
5.0
10.0
20.0
50.0
100.0
CO PARTIAL PRESSURE (Torr)
P_{O_2} = 8 Torr
■: Rh (100); T=515K
○: Rh (111); T=500K
b
CO$_2$ FORMATION RATE (TOF)
10^3
10^2
10^1
10^0
10^0
10^1
10^2
10^3
O$_2$ PRESSURE (Torr)
P_{CO}=8 Torr; T=500K
■ : Rh (100)
○ : Rh (111)
c

Fig. 17

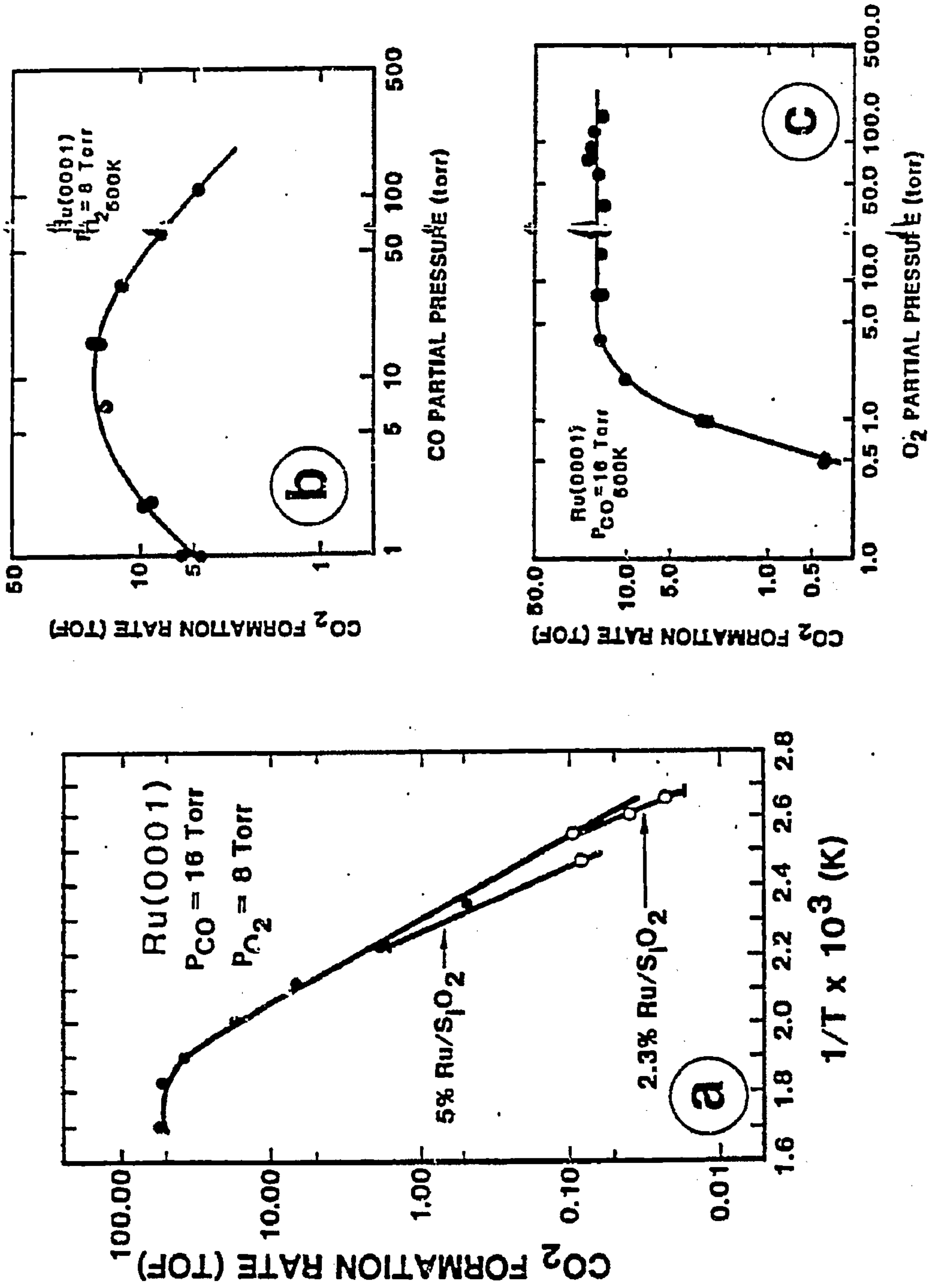
a
Ru(0001)
P_CO = 16 Torr
P_O2 = 8 Torr
5% Ru/SiO2
2.3% Ru/SiO2
CO2 FORMATION RATE (TOF)
100.00
10.00
1.00
0.10
0.01
1/T x 10^3 (K)
1.6
1.8
2.0
2.2
2.4
2.6
2.8
b
Ru(0001)
P_O2 = 8 Torr
600K
CO2 FORMATION RATE (TOF)
50
10
5
1
CO PARTIAL PRESSURE (torr)
1
5
10
50
100
500
c
Ru(0001)
P_CO = 16 Torr
600K
CO2 FORMATION RATE (TOF)
50.0
10.0
5.0
1.0
0.5
0.1
O2 PARTIAL PRESSURE (torr)
0.1
0.5
1.0
5.0
10.0
50.0
100.0
500.0

Fig. 18

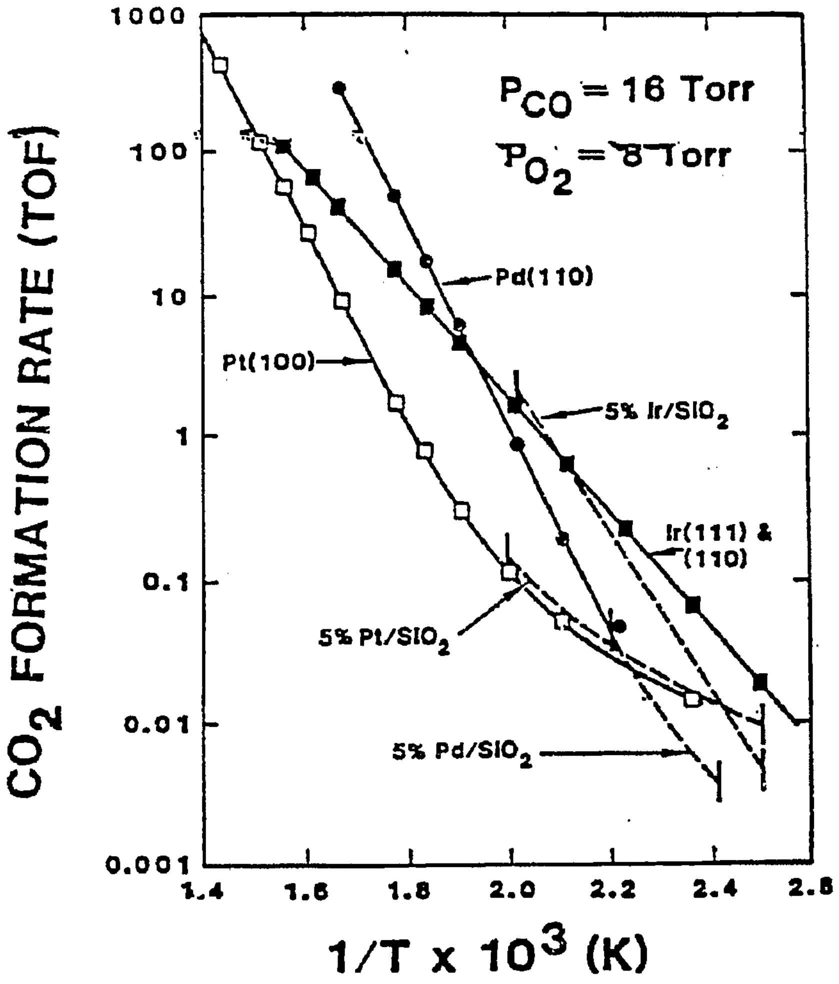
P_{CO} = 16 Torr
P_{O_2} = 8 Torr
Pd(110)
Pt(100)
5% Ir/SiO$_2$
Ir(111) & (110)
5% Pt/SiO$_2$
5% Pd/SiO$_2$
CO$_2$ FORMATION RATE (TOF)
1000
100
10
1
0.1
0.01
0.001
1.4
1.6
1.8
2.0
2.2
2.4
2.8
1/T x 10^3 (K)

Fig. 19

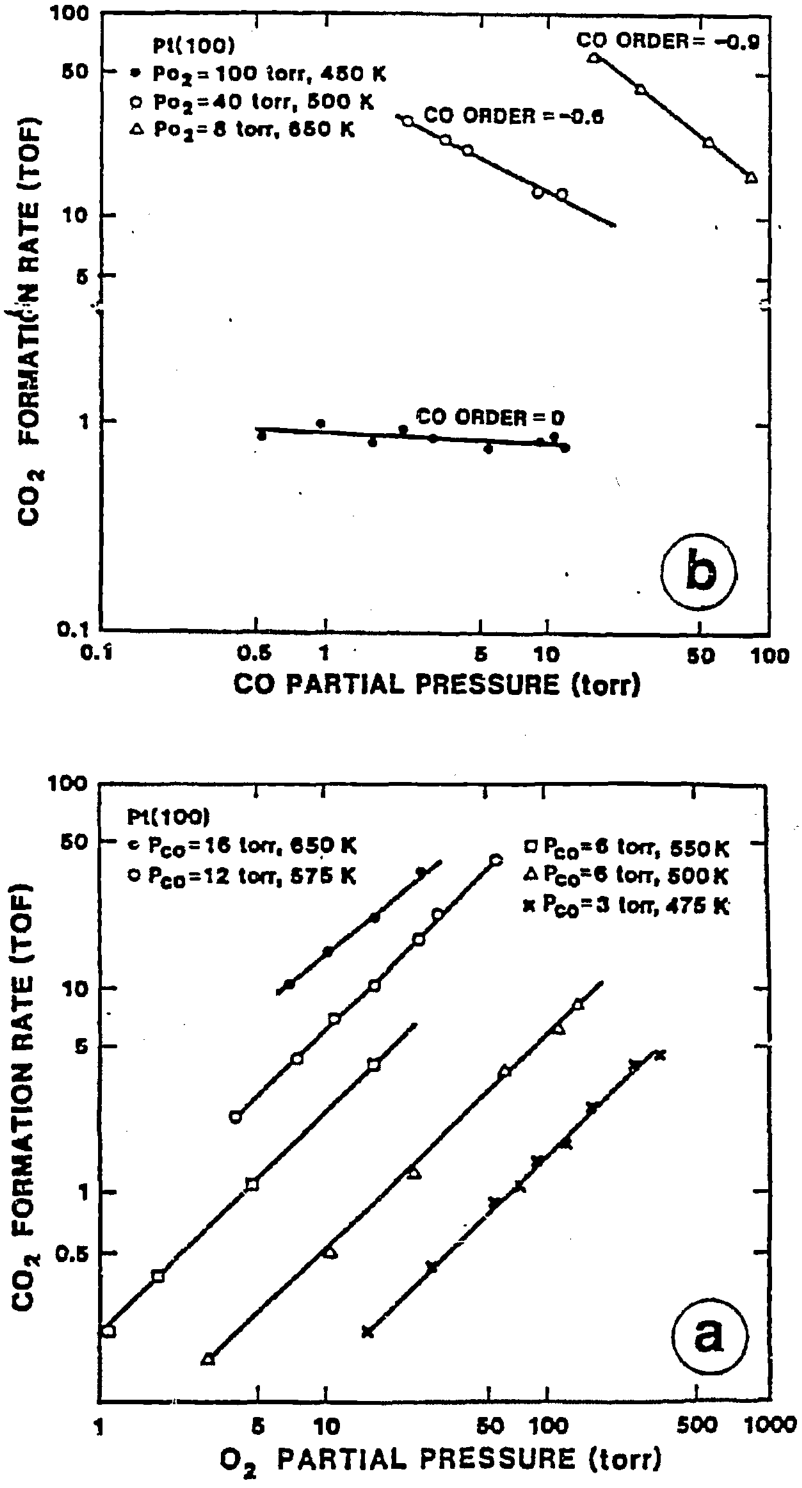Pt(100)
• P_{O_2} = 100 torr, 450 K
○ P_{O_2} = 40 torr, 500 K
△ P_{O_2} = 8 torr, 650 K
CO ORDER = −0.9
CO ORDER = −0.6
CO ORDER = 0
b
CO_2 FORMATION RATE (TOF)
100
50
10
5
1
0.1
0.1
0.5
1
5
10
50
100
CO PARTIAL PRESSURE (torr)
Pt(100)
• P_{CO} = 16 torr, 650 K
○ P_{CO} = 12 torr, 575 K
□ P_{CO} = 6 torr, 550 K
△ P_{CO} = 6 torr, 500 K
× P_{CO} = 3 torr, 475 K
a
CO_2 FORMATION RATE (TOF)
100
50
10
5
1
0.5
1
5
10
50
100
500
1000
O_2 PARTIAL PRESSURE (torr)

Fig. 20

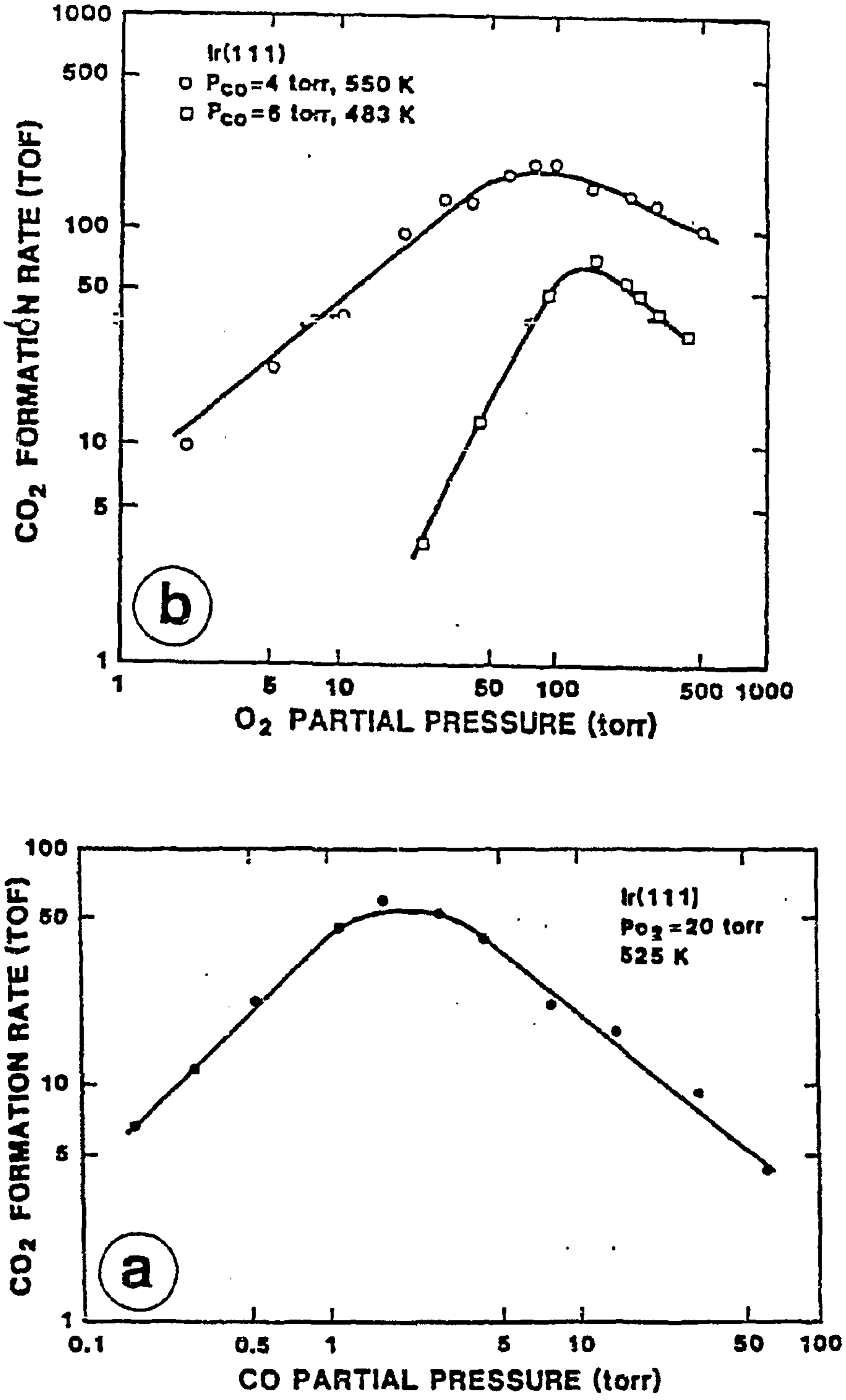

1000
500
100
50
10
5
1
CO2 FORMATION RATE (TOF)
Ir(111)
○ PCO=4 torr, 550 K
□ PCO=6 torr, 483 K
b
1
5
10
50
100
500
1000
O2 PARTIAL PRESSURE (torr)
100
50
10
5
1
CO2 FORMATION RATE (TOF)
Ir(111)
PO2=20 torr
525 K
a
0.1
0.5
1
5
10
50
100
CO PARTIAL PRESSURE (torr)

Fig. 21

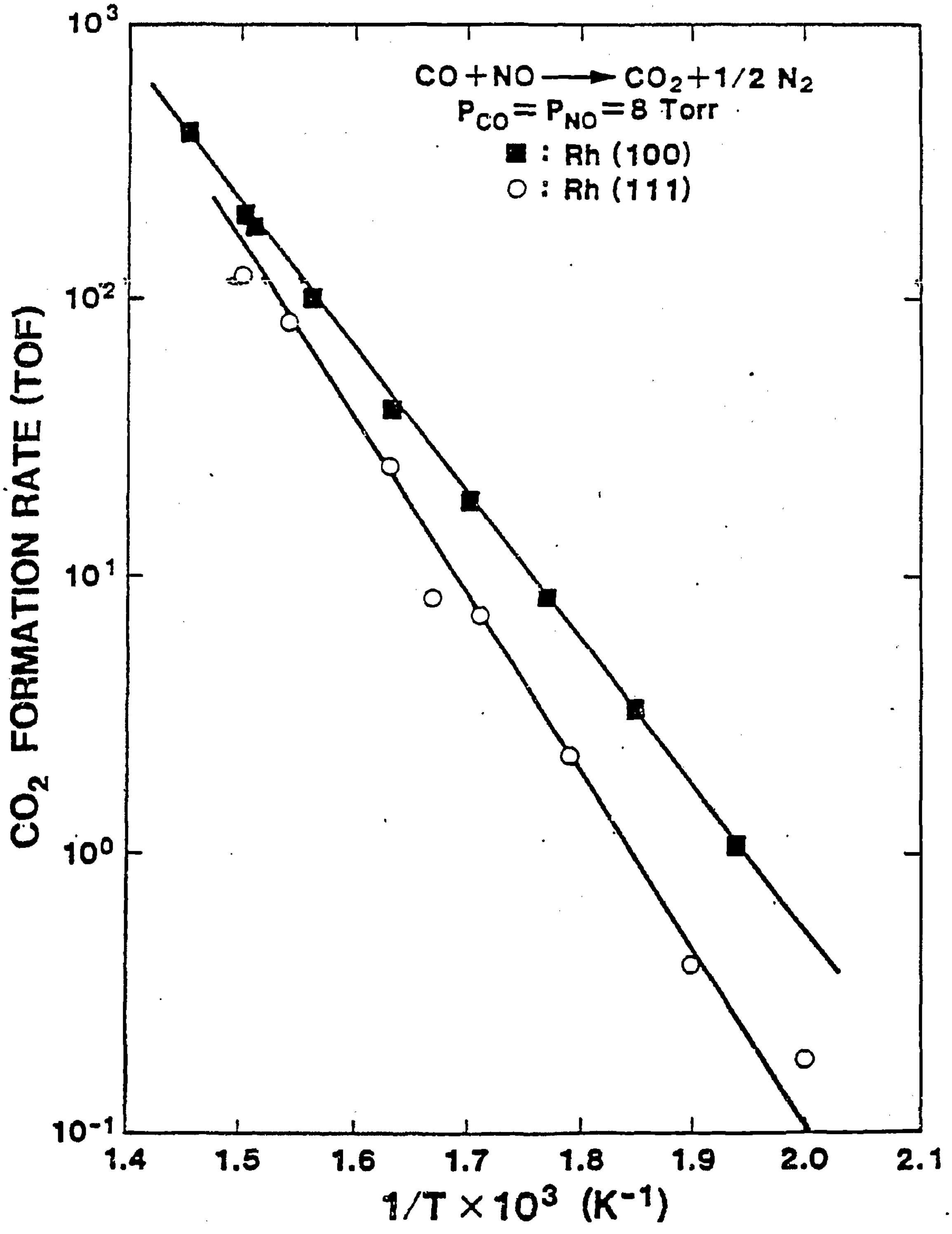
CO + NO → CO_2 + 1/2 N_2
$P_{CO} = P_{NO}$ = 8 Torr
■ : Rh (100)
○ : Rh (111)
CO_2 FORMATION RATE (TOF)
10^3
10^2
10^1
10^0
10^{-1}
1.4
1.5
1.6
1.7
1.8
1.9
2.0
2.1
1/T × 10^3 (K^{-1})

Fig. 22

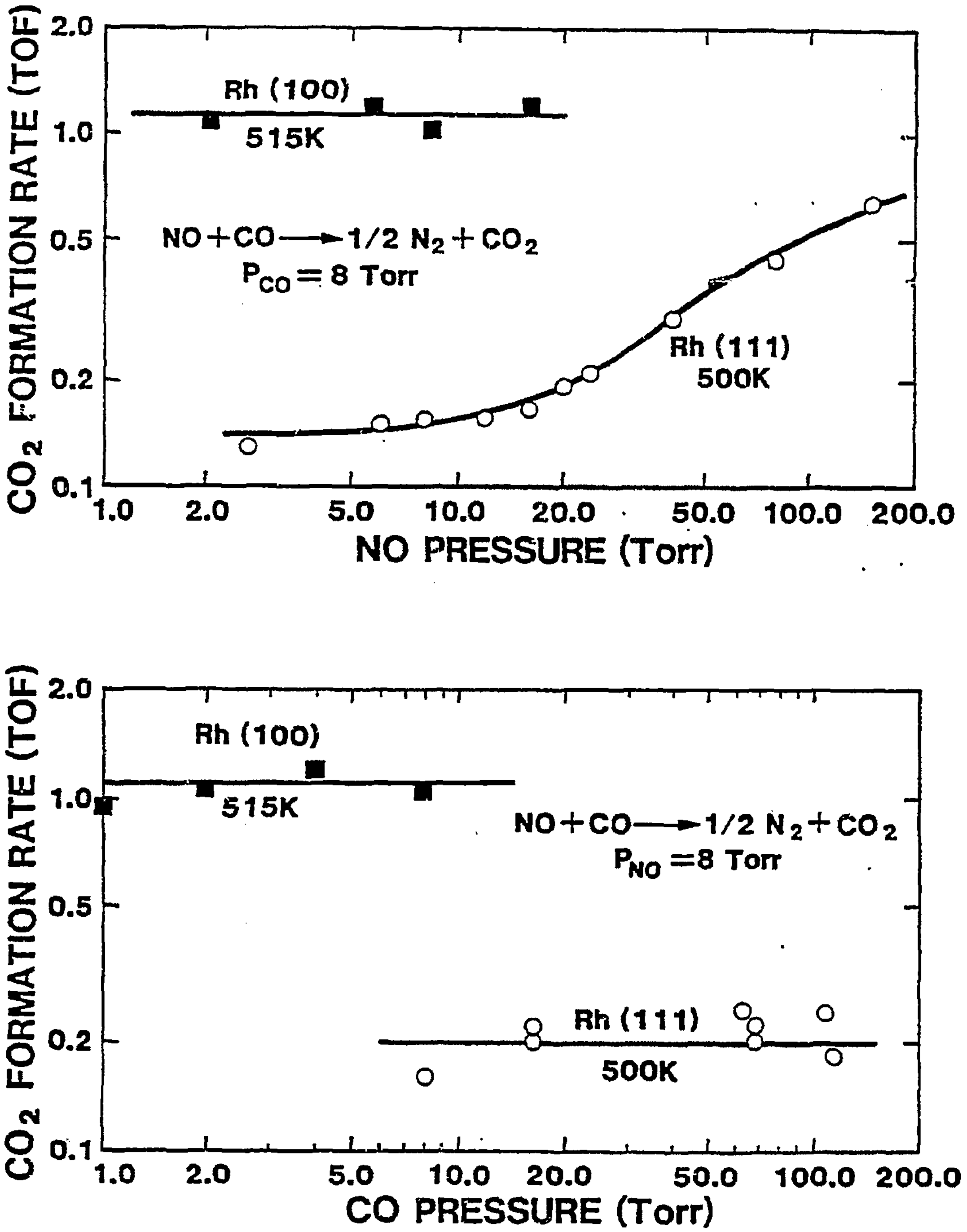
CO₂ FORMATION RATE (TOF)
2.0
1.0
0.5
0.2
0.1
Rh (100)
515K
NO+CO⟶1/2 N₂+CO₂
P_CO = 8 Torr
Rh (111)
500K
1.0
2.0
5.0
10.0
20.0
50.0
100.0
200.0
NO PRESSURE (Torr)
CO₂ FORMATION RATE (TOF)
2.0
1.0
0.5
0.2
0.1
Rh (100)
515K
NO+CO⟶1/2 N₂+CO₂
P_NO =8 Torr
Rh (111)
500K
1.0
2.0
5.0
10.0
20.0
50.0
100.0
200.0
CO PRESSURE (Torr)

Fig. 23

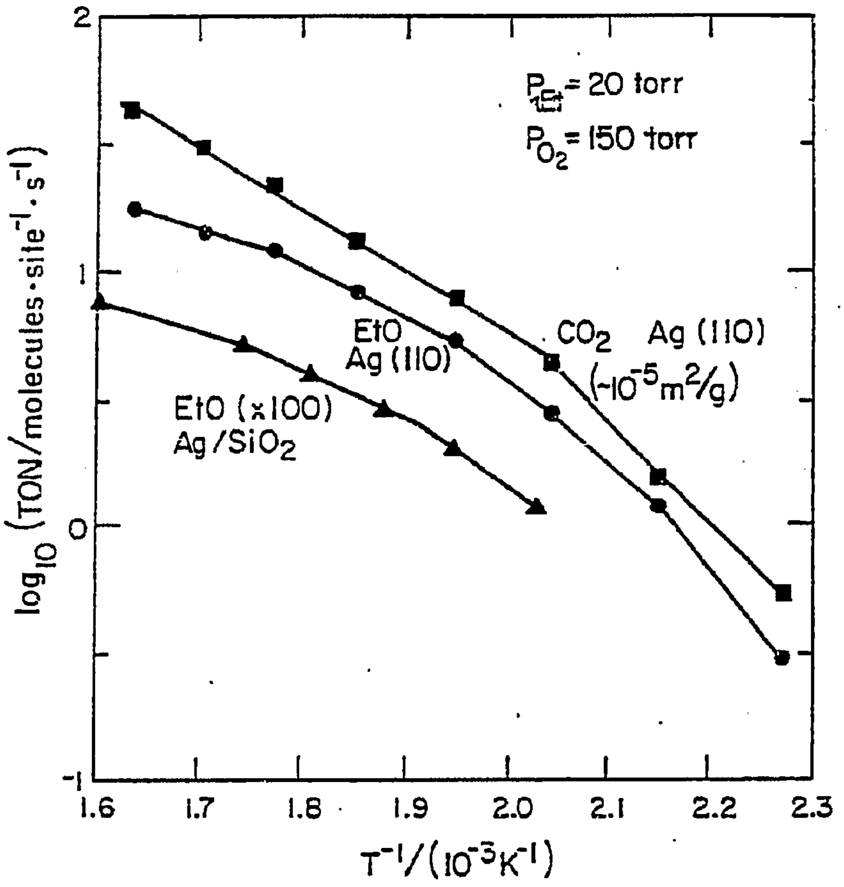
P_{Et} = 20 torr
P_{O_2} = 150 torr
CO_2 Ag (110)
(~10^{-5} m^2/g)
EtO
Ag (110)
EtO (x100)
Ag/SiO_2
$\log_{10}$ (TON/molecules · site^{-1} · s^{-1})
$T^{-1}/(10^{-3}K^{-1})$
2
1
0
-1
1.6
1.7
1.8
1.9
2.0
2.1
2.2
2.3

Fig. 24

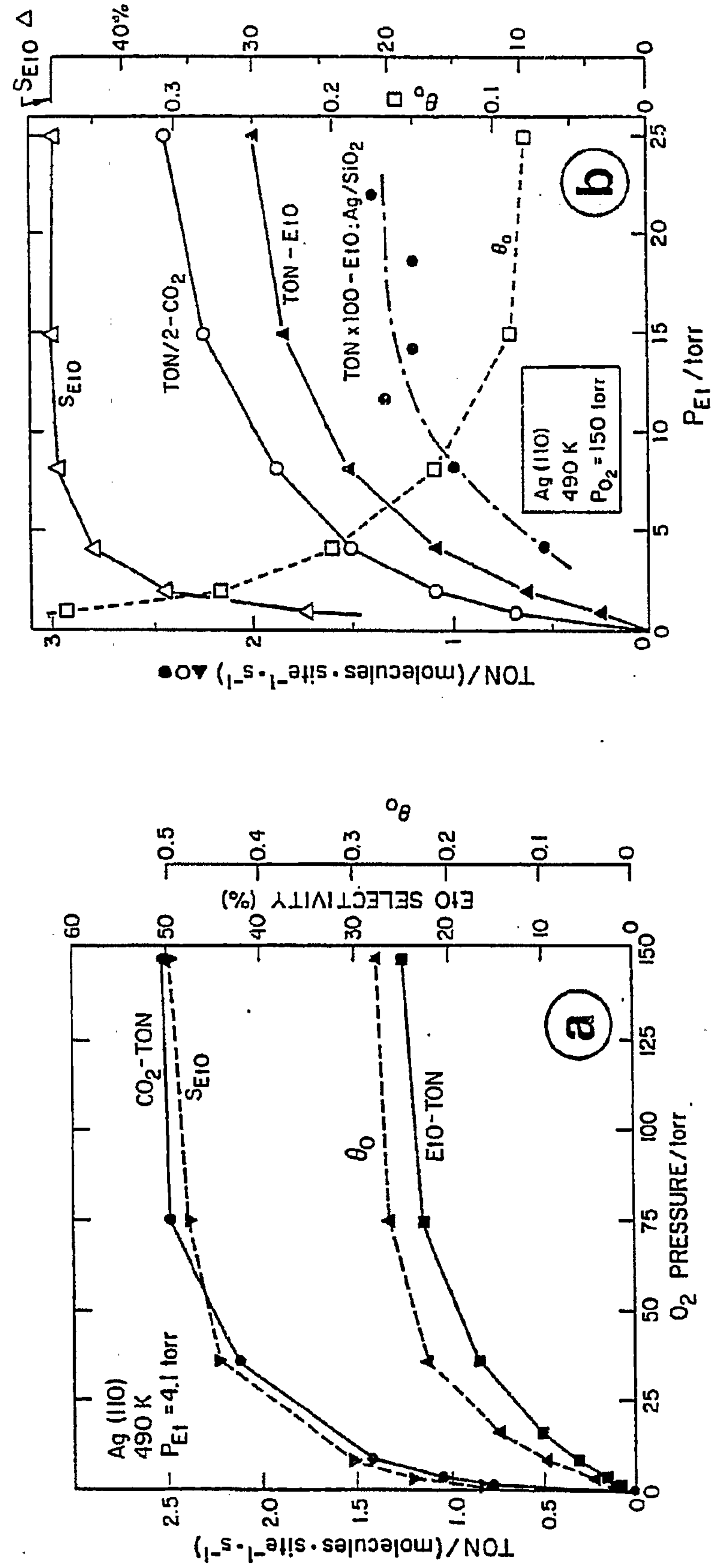
a
Ag (110)
490 K
P_{EI} = 4.1 torr
CO_2-TON
S_{EIO}
θ_O
EIO-TON
TON/(molecules·site^{-1}·s^{-1})
0
0.5
1.0
1.5
2.0
2.5
O_2 PRESSURE/torr
0
25
50
75
100
125
150
EIO SELECTIVITY (%)
0
10
20
30
40
50
60
θ_O
0
0.1
0.2
0.3
0.4
0.5
b
Ag (110)
490 K
P_{O_2} = 150 torr
S_{EIO}
TON/2-CO_2
TON - EIO
TON x 100 - EIO : Ag/SiO$_2$
θ_O
TON/(molecules·site^{-1}·s^{-1}) ▲○●
0
1
2
3
P_{EI}/torr
0
5
10
15
20
25
θ_O □
0
0.1
0.2
0.3
S_{EIO} △
0
10
20
30
40%

Fig. 25

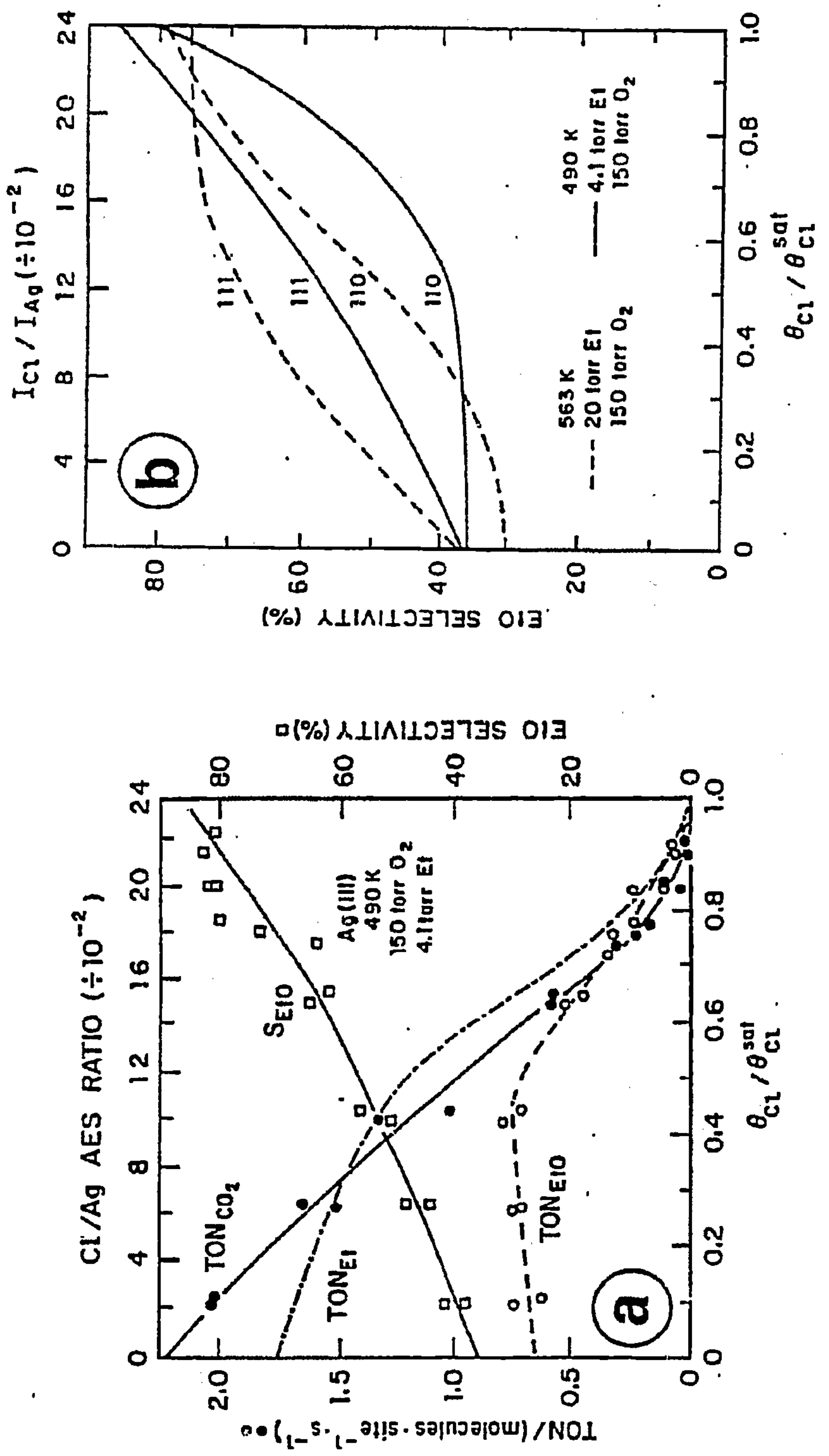
b
$I_{Cl} / I_{Ag} (\div 10^{-2})$
0
4
8
12
16
20
24
E1O SELECTIVITY (%)
0
20
40
60
80
111
111
110
110
563 K
20 torr Et
150 torr O2
490 K
4.1 torr Et
150 torr O2
$\theta_{Cl} / \theta_{Cl}^{sat}$
0
0.2
0.4
0.6
0.8
1.0
a
Cl/Ag AES RATIO (÷10⁻²)
0
4
8
12
16
20
24
TON/(molecules·site⁻¹·s⁻¹)●○
0
0.5
1.0
1.5
2.0
EIO SELECTIVITY (%)□
0
20
40
60
80
S_{EIO}
TON_{CO_2}
TON_{Et}
TON_{EIO}
Ag(111)
490 K
150 torr O2
4.1 torr Et
$\theta_{Cl} / \theta_{Cl}^{sat}$
0
0.2
0.4
0.6
0.8
1.0

Fig. 26

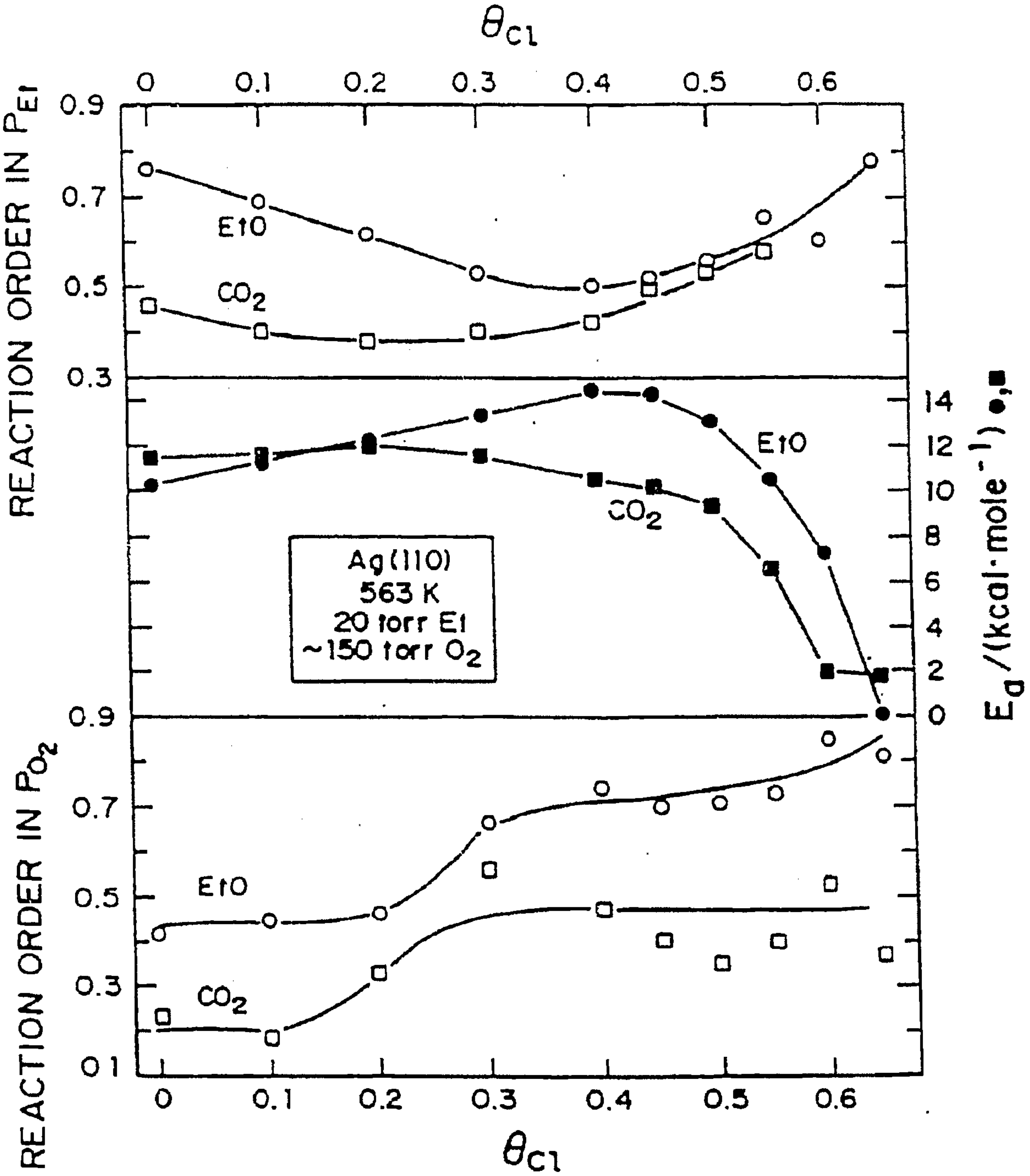

θ_{Cl}
0
0.1
0.2
0.3
0.4
0.5
0.6
REACTION ORDER IN P_{Et}
0.9
0.7
0.5
0.3
EtO
CO_2
E_a /(kcal·mole^{-1}) ●,■
14
12
10
8
6
4
2
0
Ag(110)
563 K
20 torr Et
~150 torr O_2
REACTION ORDER IN P_{O_2}
0.9
0.7
0.5
0.3
0.1

Fig. 27

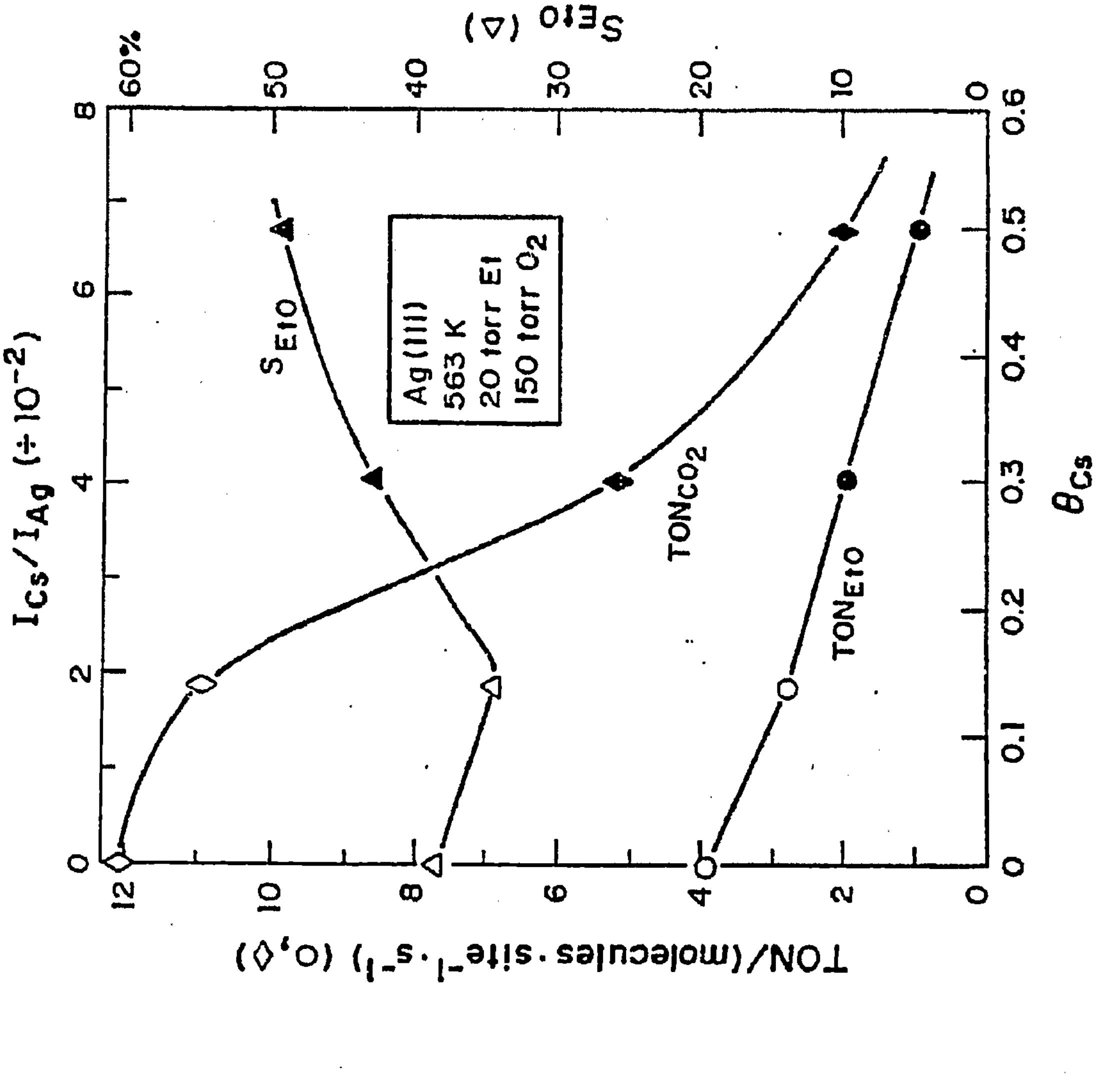
I_Cs/I_Ag (÷10^-2)
0
2
4
6
8
TON/(molecules·site^-1·s^-1) (○,◊)
12
10
8
6
4
2
0
S_EtO (△)
60%
50
40
30
20
10
0
θ_Cs
0
0.1
0.2
0.3
0.4
0.5
0.6
S_EtO
TON_CO2
TON_EtO
Ag(111)
563 K
20 torr Et
150 torr O2

Fig. 28

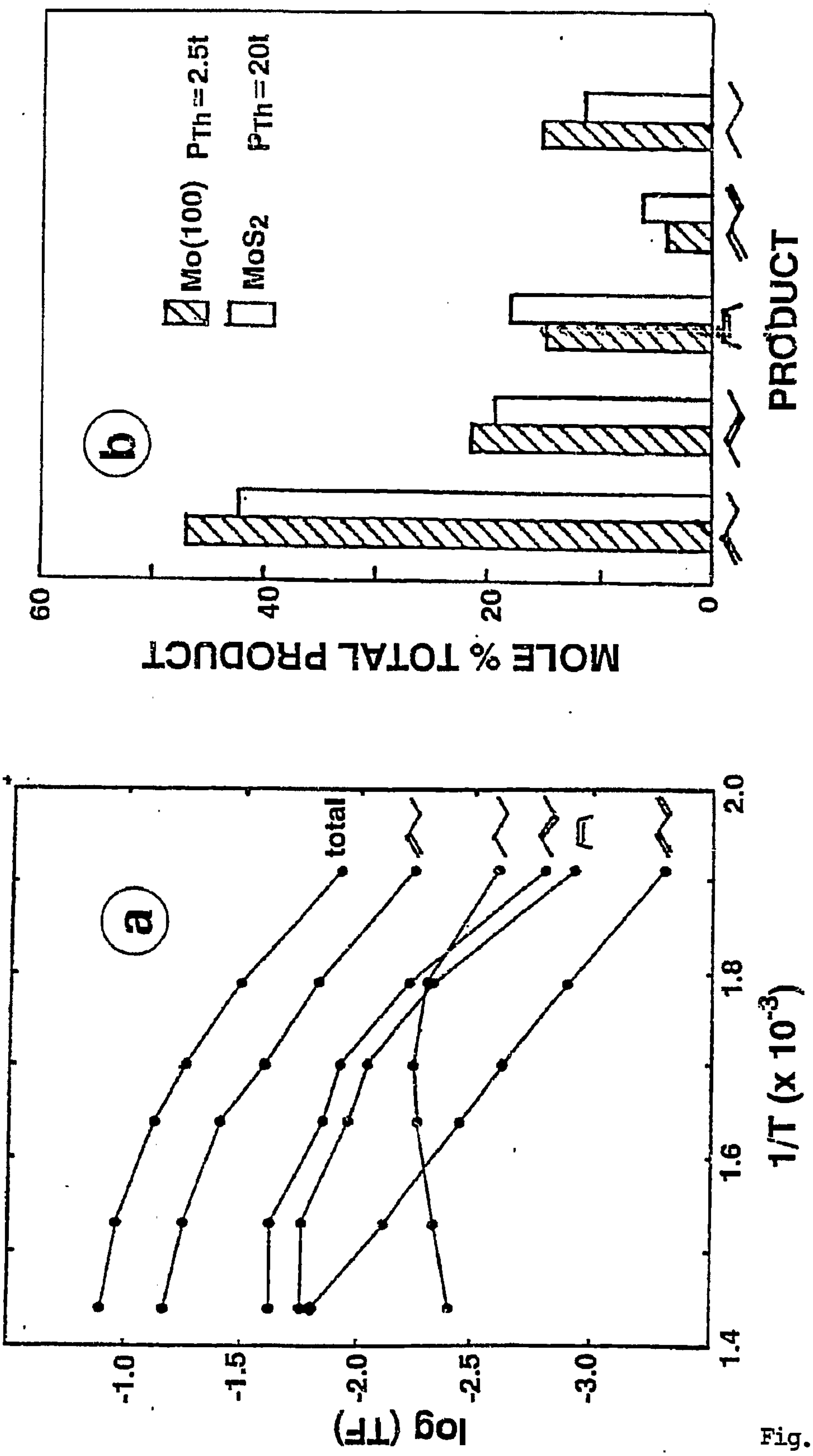
a
log (TF)
-1.0
-1.5
-2.0
-2.5
-3.0
1.4
1.6
1.8
2.0
1/T (x 10^-3)
total
b
MOLE % TOTAL PRODUCT
0
20
40
60
PRODUCT
Mo(100) PTh=2.5t
MoS2 PTh=20t

Fig. 29

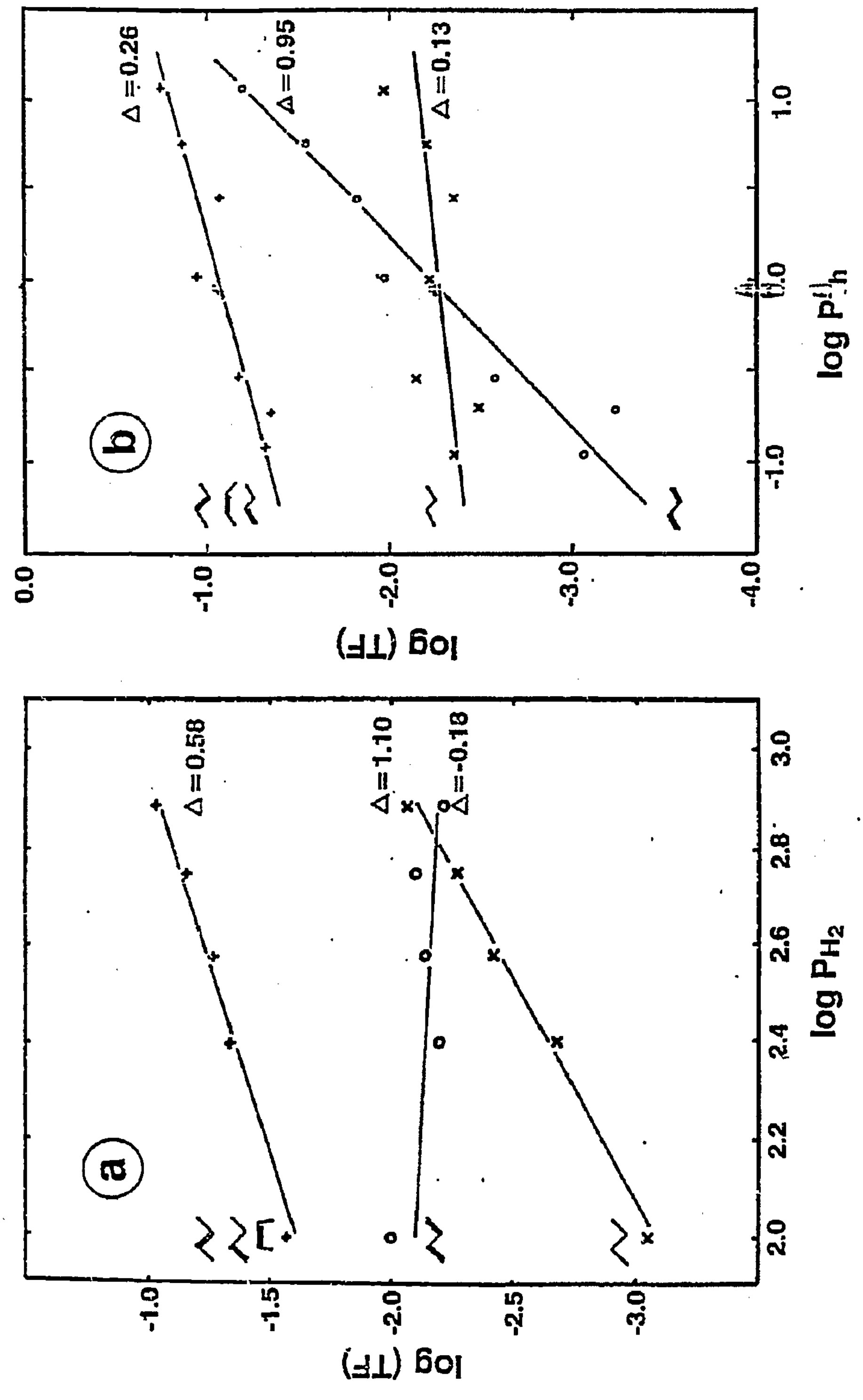
a
Δ=0.58
Δ=1.10
Δ=-0.18
log (TF)
-1.0
-1.5
-2.0
-2.5
-3.0
2.0
2.2
2.4
2.6
2.8
3.0
log P_{H_2}
b
Δ=0.26
Δ=0.95
Δ=0.13
log (TF)
0.0
-1.0
-2.0
-3.0
-4.0
-1.0
0.0
1.0
log P_h

Fig. 30

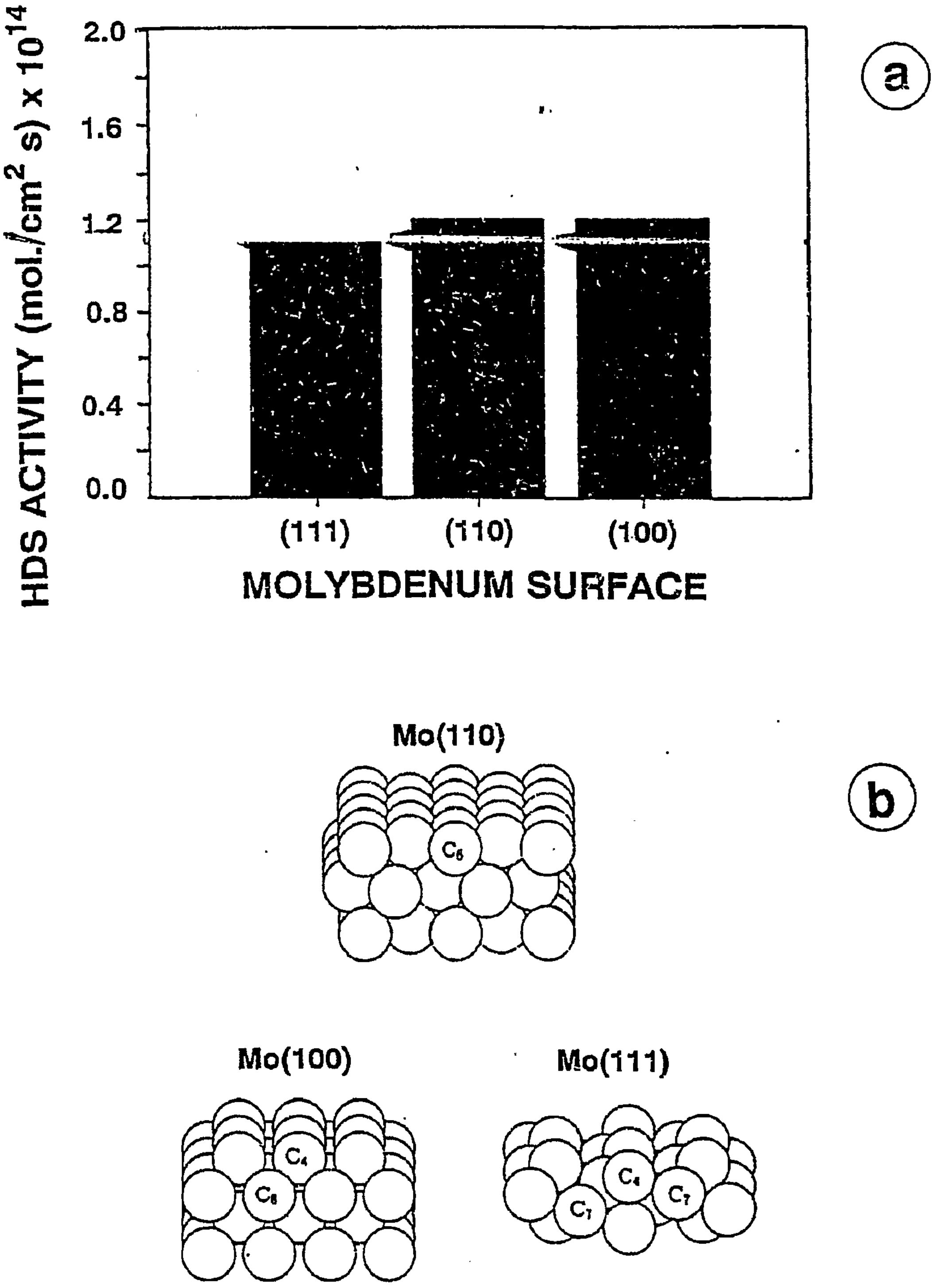
a
HDS ACTIVITY (mol./cm^2 s) x 10^{14}
2.0
1.6
1.2
0.8
0.4
0.0
(111)
(110)
(100)
MOLYBDENUM SURFACE
b
Mo(110)
C$_8$
Mo(100)
C$_4$
C$_8$
Mo(111)
C$_4$
C$_7$
C$_7$

Fig. 31

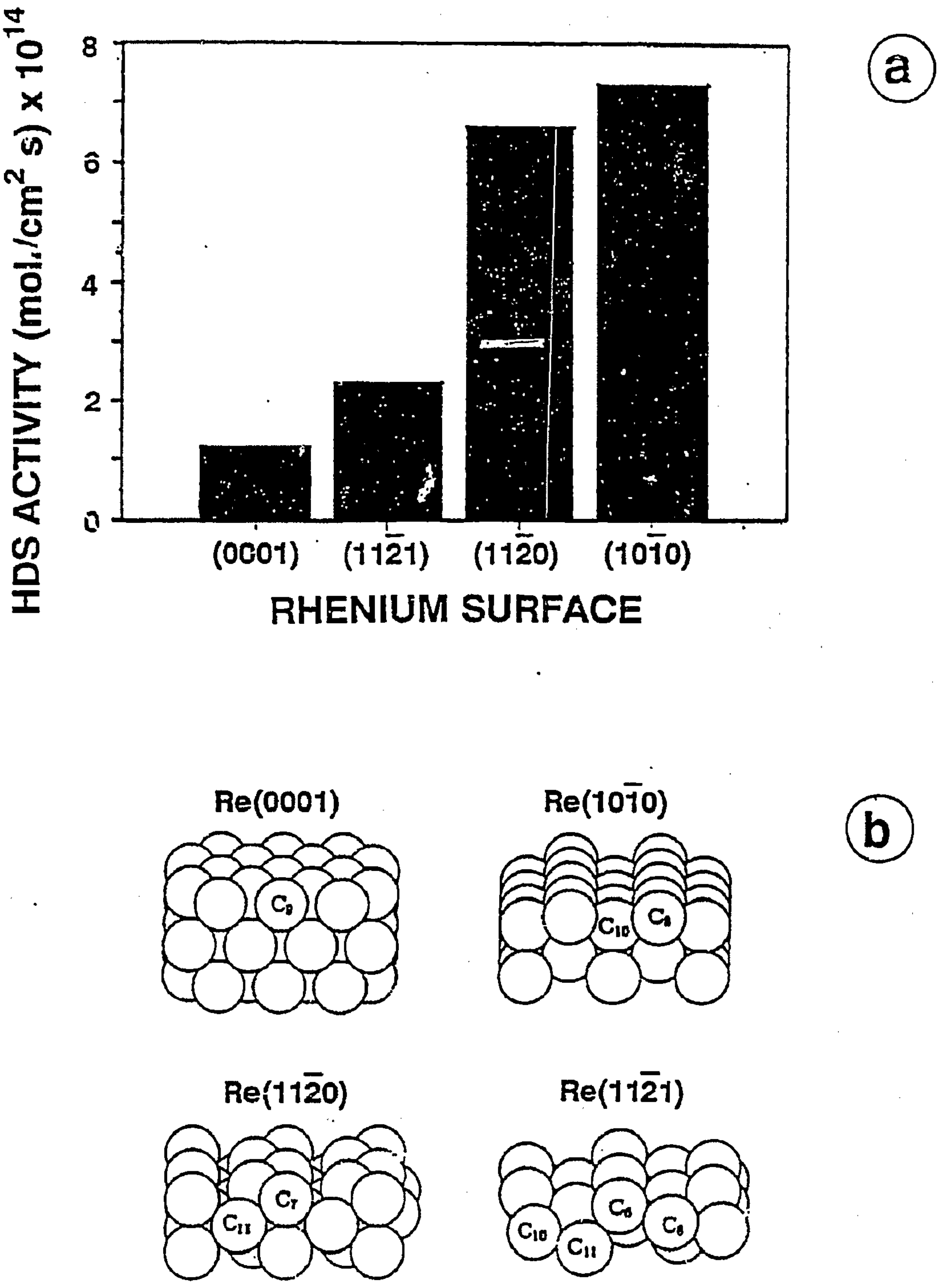
a
HDS ACTIVITY (mol./cm^2 s) x 10^{14}
0
2
4
6
8
(0001)
(11$\bar{2}$1)
(11$\bar{2}$0)
(10$\bar{1}$0)
RHENIUM SURFACE
b
Re(0001)
C$_9$
Re(10$\bar{1}$0)
C$_{10}$
C$_8$
Re(11$\bar{2}$0)
C$_7$
C$_{11}$
Re(11$\bar{2}$1)
C$_{10}$
C$_{11}$
C$_6$
C$_8$

Fig. 32

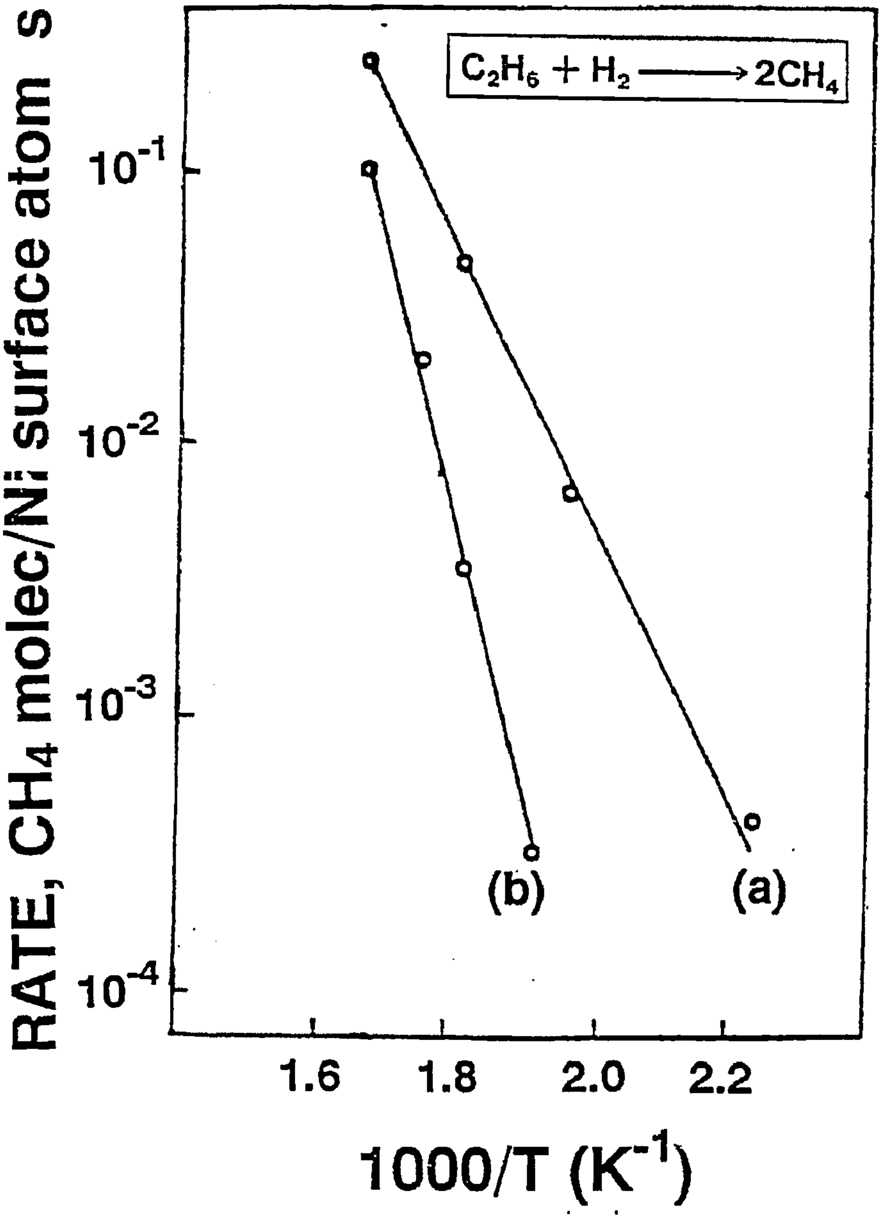

$C_2H_6 + H_2 \longrightarrow 2CH_4$
RATE, CH_4 molec/Ni surface atom s
10^{-1}
10^{-2}
10^{-3}
10^{-4}
(b)
(a)
1.6
1.8
2.0
2.2
1000/T (K^{-1})

Fig. 33

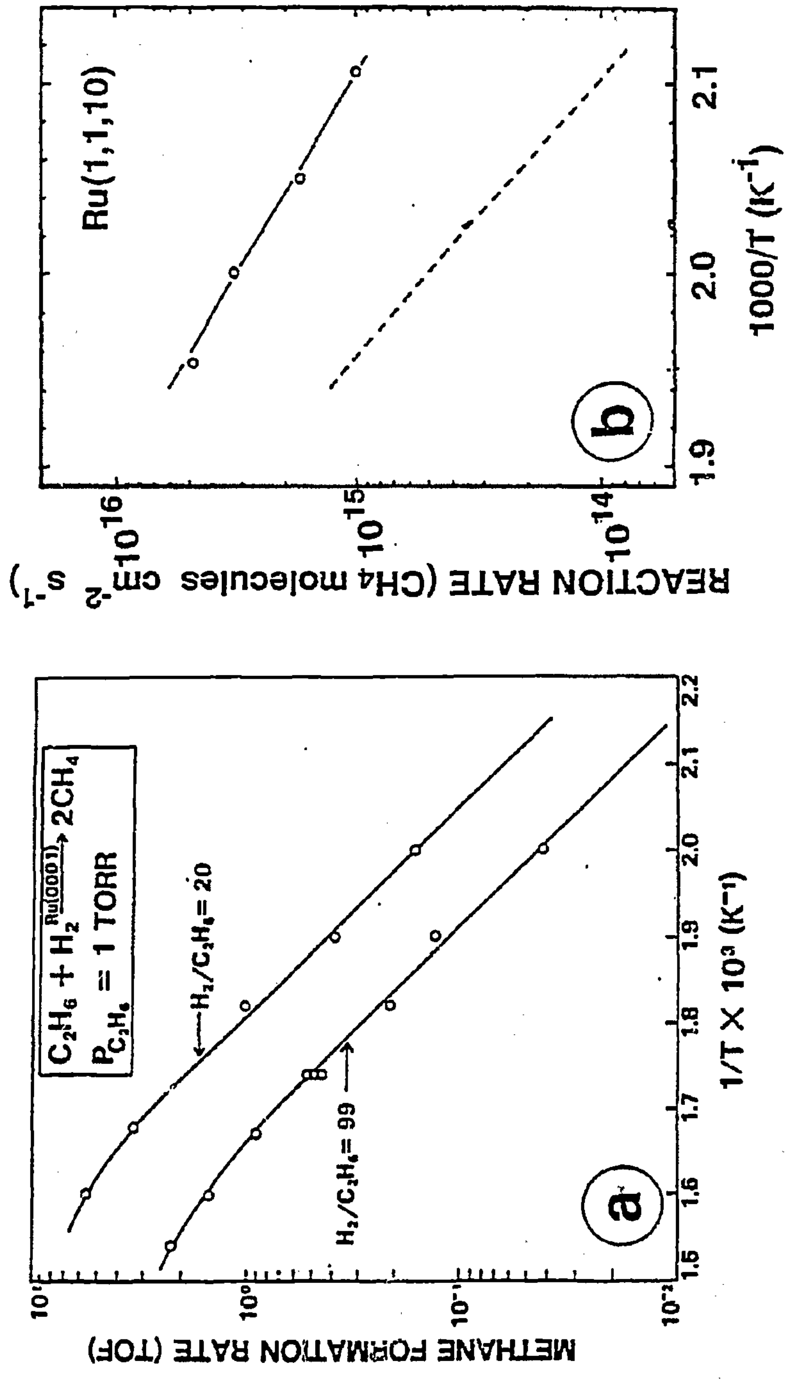
a
$C_2H_6 + H_2 \xrightarrow{Ru(0001)} 2CH_4$
$P_{C_2H_6}$ = 1 TORR
H_2/C_2H_6 = 20
H_2/C_2H_6 = 99
METHANE FORMATION RATE (TOF)
10^1
10^0
10^{-1}
10^{-2}
1.5
1.6
1.7
1.8
1.9
2.0
2.1
2.2
1/T × 10^3 (K^{-1})
b
Ru(1,1,10)
REACTION RATE (CH_4 molecules cm^{-2} s^{-1})
10^{16}
10^{15}
10^{14}
1.9
2.0
2.1
1000/T (K^{-1})

Fig. 34

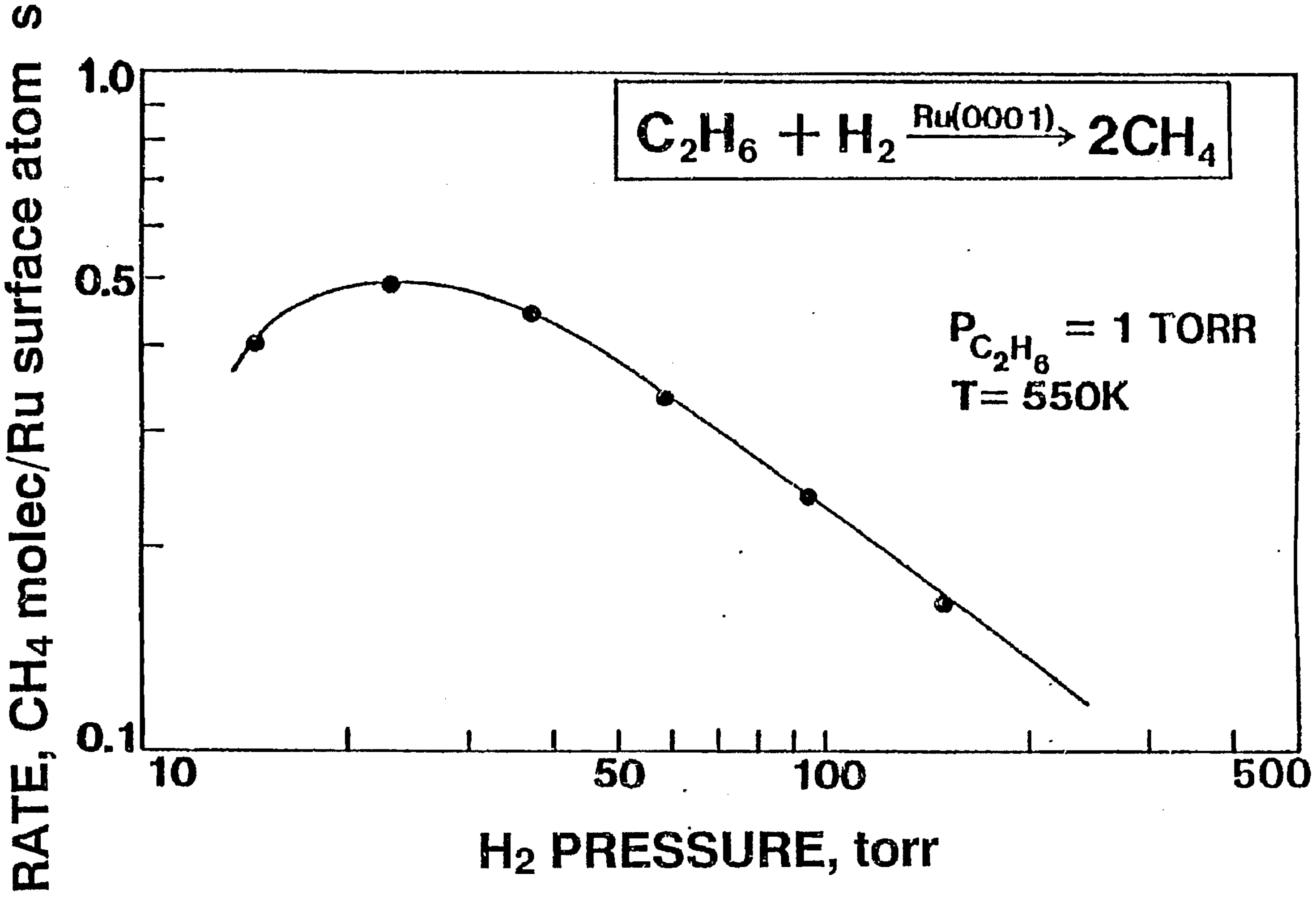
$C_2H_6 + H_2 \xrightarrow{Ru(0001)} 2CH_4$
$P_{C_2H_6}$ = 1 TORR
T= 550K
RATE, CH_4 molec/Ru surface atom s
1.0
0.5
0.1
10
50
100
500
H_2 PRESSURE, torr

Fig. 35

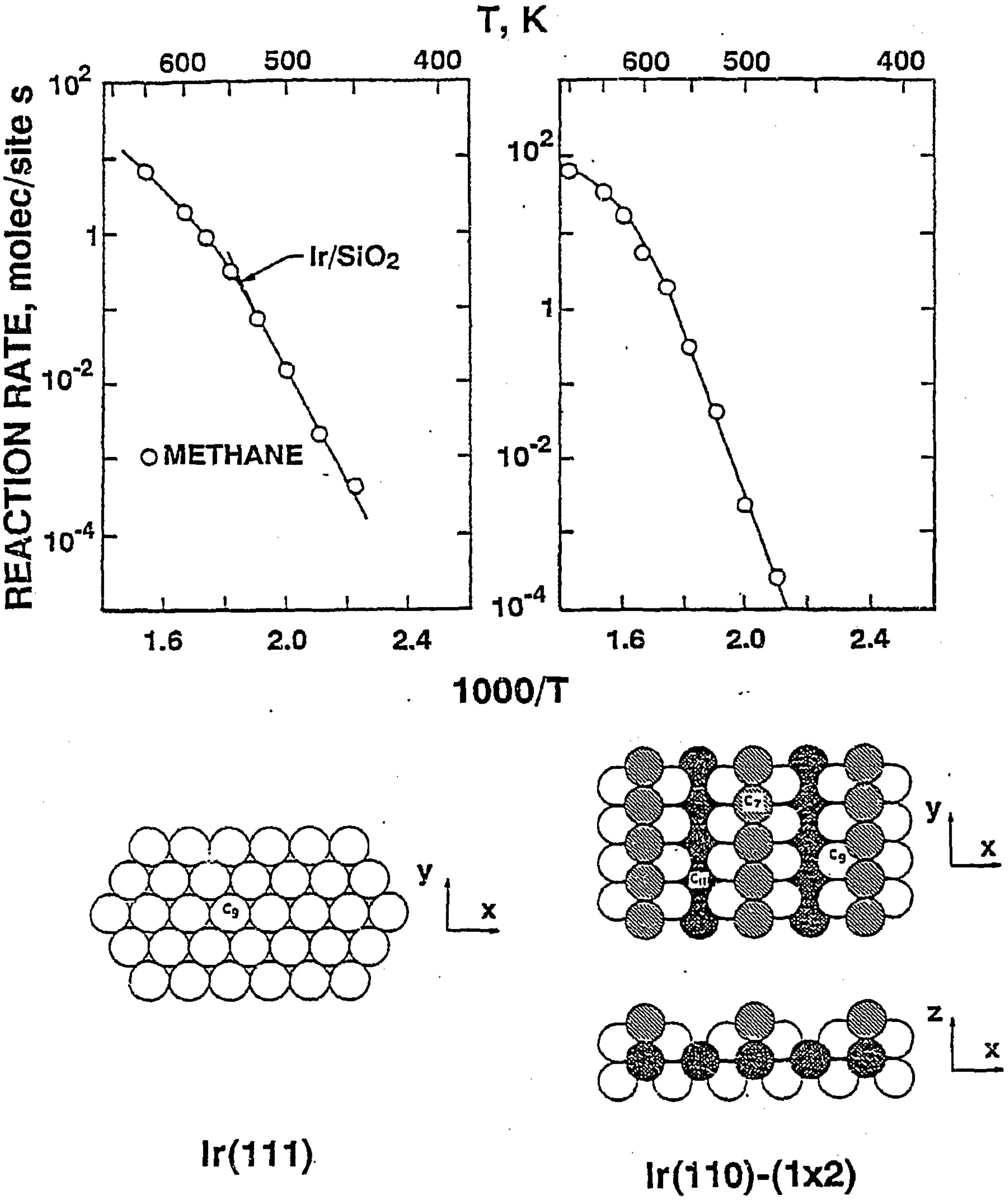
T, K
600
500
400
REACTION RATE, molec/site s
10^2
1
10^{-2}
10^{-4}
Ir/SiO2
METHANE
1.6
2.0
2.4
1000/T
c9
c7
c11
y
x
z
Ir(111)
Ir(110)-(1x2)

Fig. 36

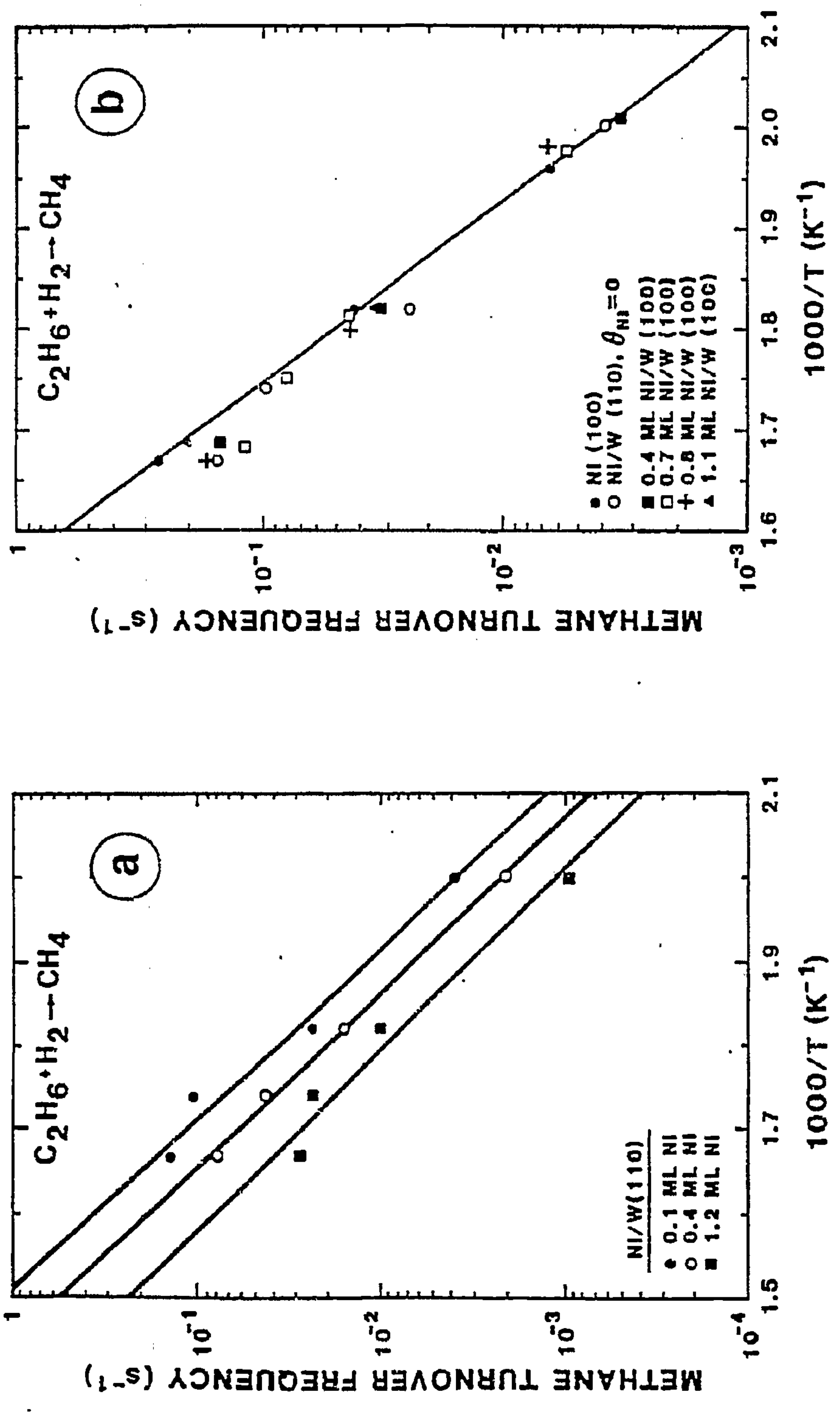
b
C2H6+H2→CH4
METHANE TURNOVER FREQUENCY (s-1)
1
10-1
10-2
10-3
1.6
1.7
1.8
1.9
2.0
2.1
1000/T (K-1)
● Ni (100)
○ Ni/W (110), θNi=0
■ 0.4 ML Ni/W (100)
□ 0.7 ML Ni/W (100)
+ 0.8 ML Ni/W (100)
▲ 1.1 ML Ni/W (100)
a
C2H6+H2→CH4
METHANE TURNOVER FREQUENCY (s-1)
1
10-1
10-2
10-3
10-4
1.5
1.7
1.9
2.1
1000/T (K-1)
Ni/W(110)
● 0.1 ML Ni
○ 0.4 ML Ni
■ 1.2 ML Ni

Fig. 37

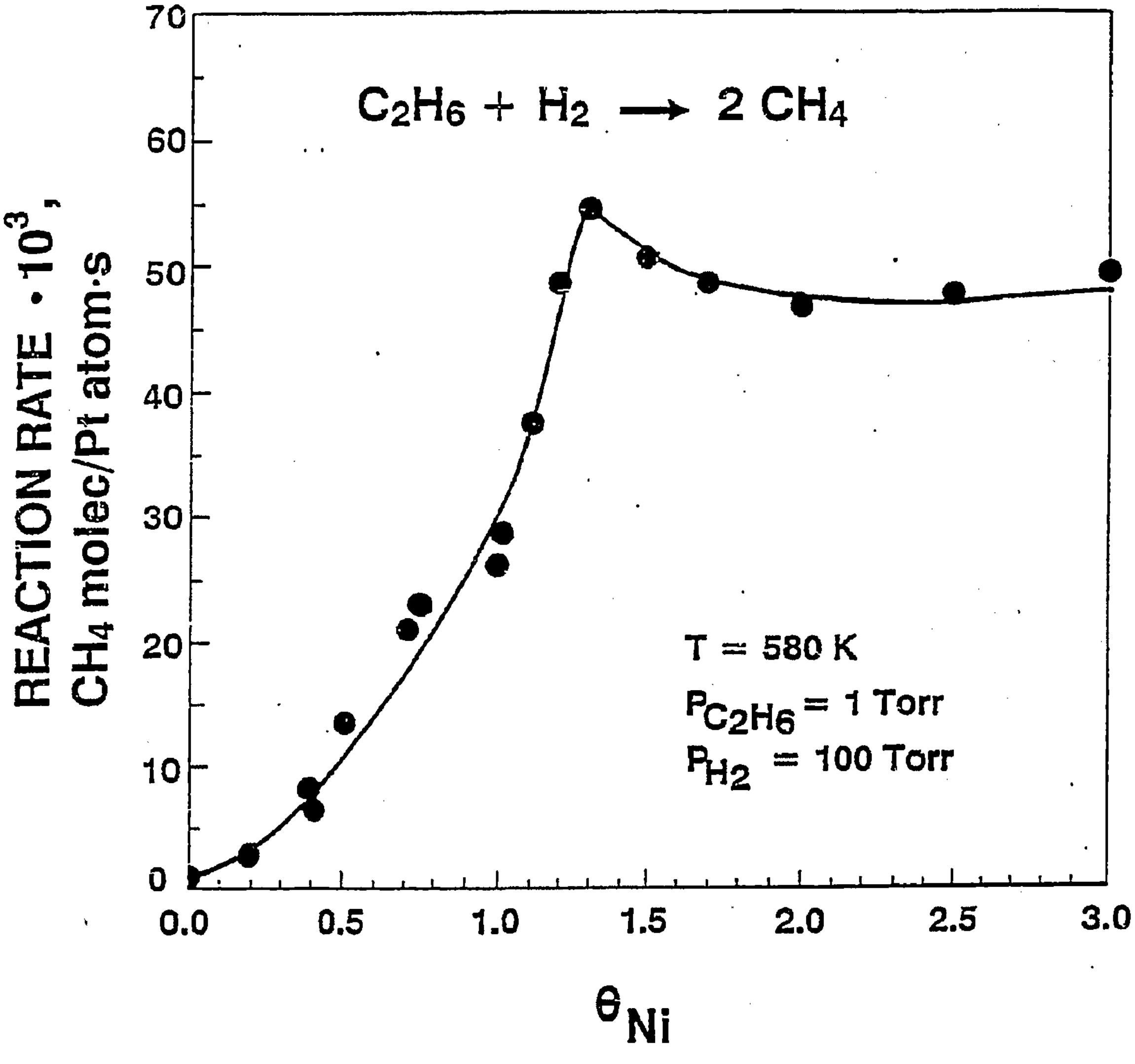

$C_2H_6 + H_2 \longrightarrow 2\ CH_4$
T = 580 K
$P_{C_2H_6}$ = 1 Torr
P_{H_2} = 100 Torr
REACTION RATE · 10^3, CH_4 molec/Pt atom·s
0
10
20
30
40
50
60
70
0.0
0.5
1.0
1.5
2.0
2.5
3.0
θ_{Ni}

Fig. 38

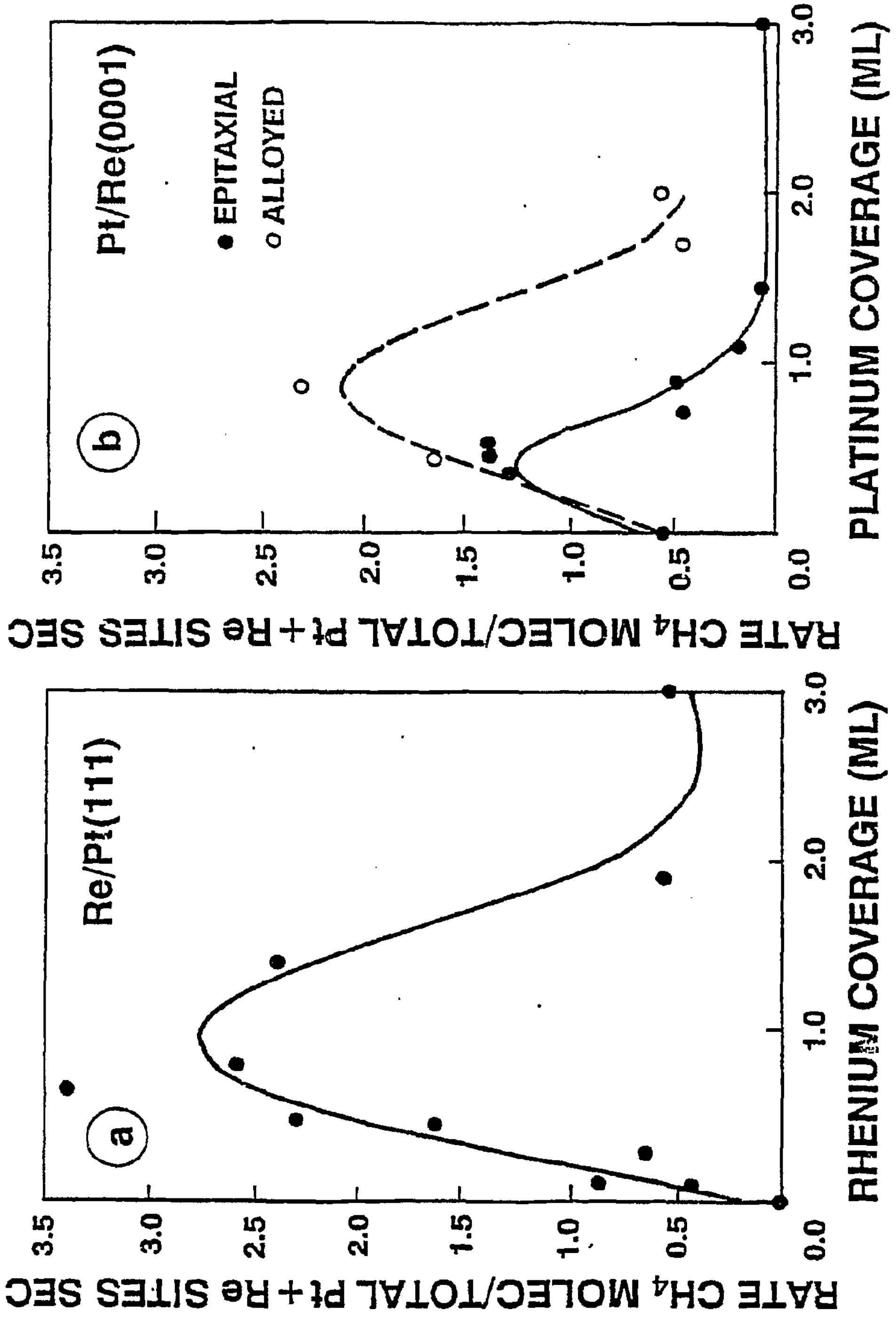a
Re/Pt(111)
RATE CH$_4$ MOLEC/TOTAL Pt+Re SITES SEC
0.0
0.5
1.0
1.5
2.0
2.5
3.0
3.5
1.0
2.0
3.0
RHENIUM COVERAGE (ML)
b
Pt/Re(0001)
● EPITAXIAL
○ ALLOYED
RATE CH$_4$ MOLEC/TOTAL Pt+Re SITES SEC
0.0
0.5
1.0
1.5
2.0
2.5
3.0
3.5
1.0
2.0
3.0
PLATINUM COVERAGE (ML)

Fig. 39

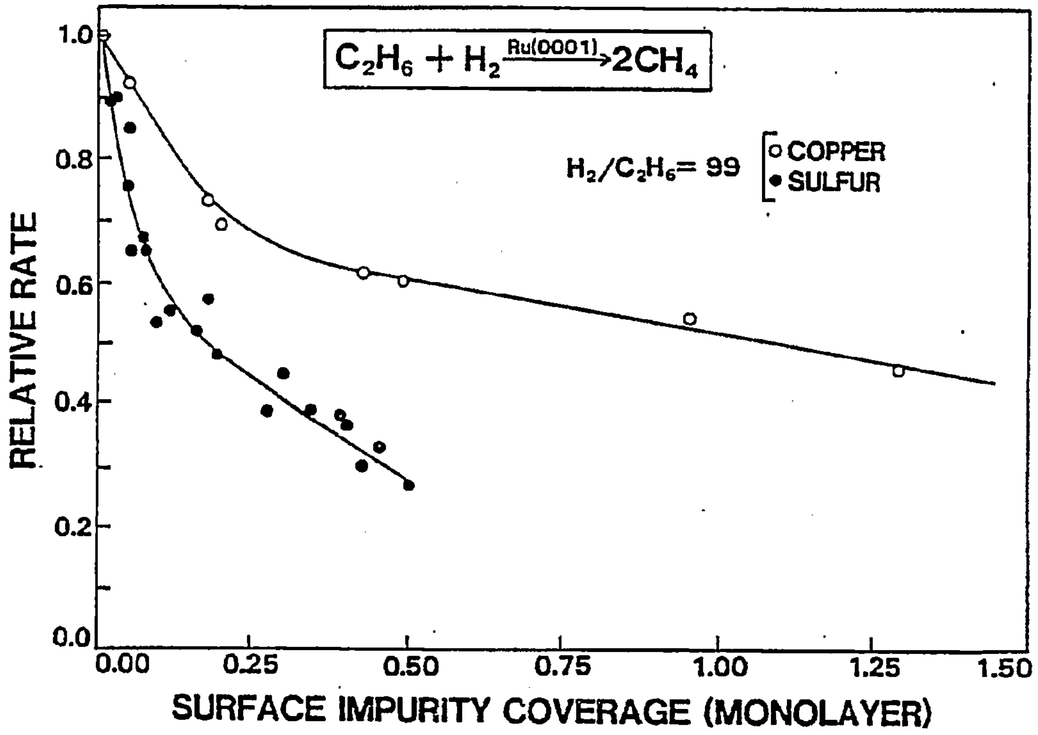

$C_2H_6 + H_2 \xrightarrow{Ru(0001)} 2CH_4$
$H_2/C_2H_6 = 99$
○ COPPER
● SULFUR
RELATIVE RATE
1.0
0.8
0.6
0.4
0.2
0.0
0.00
0.25
0.50
0.75
1.00
1.25
1.50
SURFACE IMPURITY COVERAGE (MONOLAYER)

Fig. 40

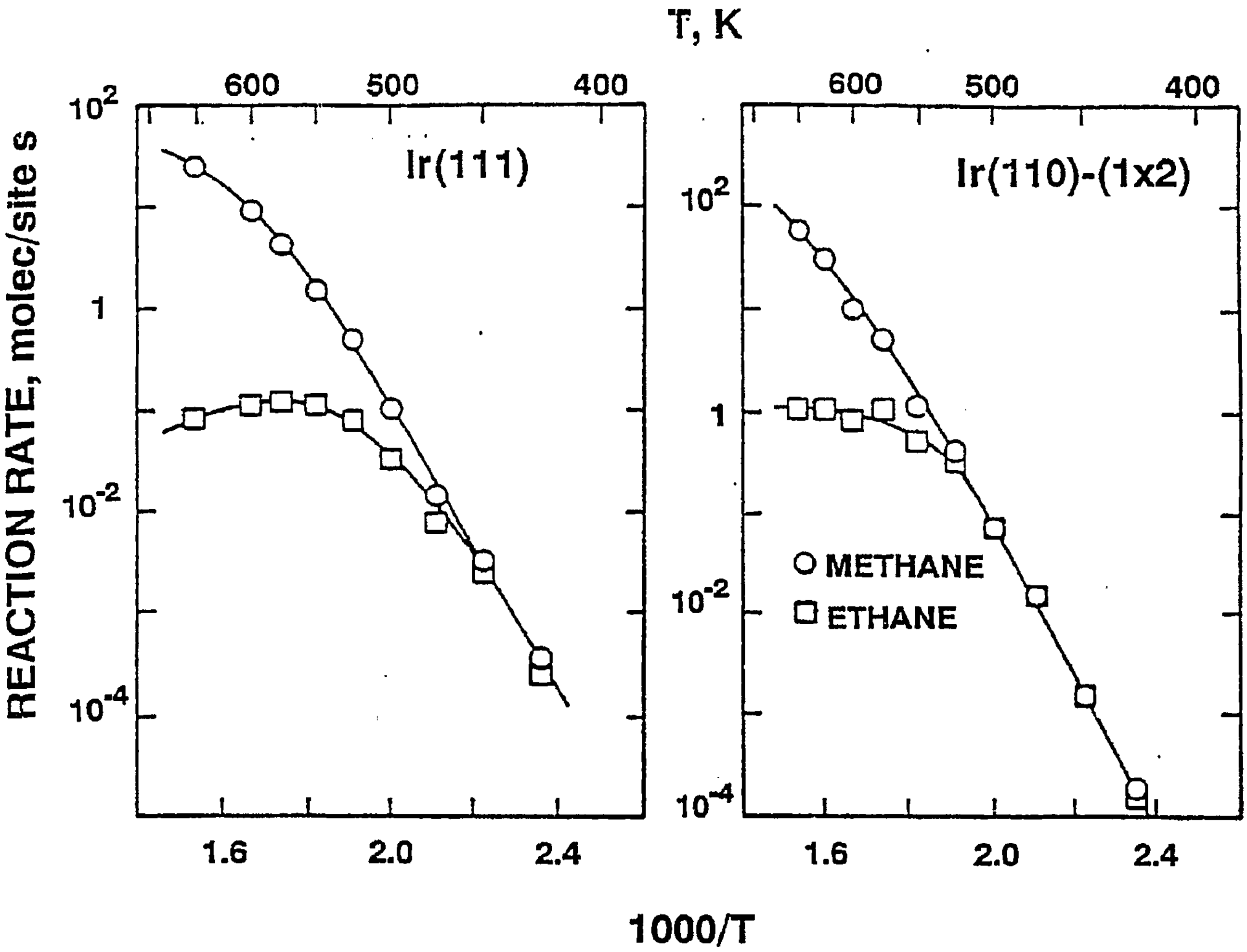
T, K
600
500
400
600
500
400
REACTION RATE, molec/site s
10^2
1
10^{-2}
10^{-4}
Ir(111)
10^2
1
10^{-2}
10^{-4}
Ir(110)-(1x2)
○ METHANE
□ ETHANE
1.6
2.0
2.4
1.6
2.0
2.4
1000/T

Fig. 41

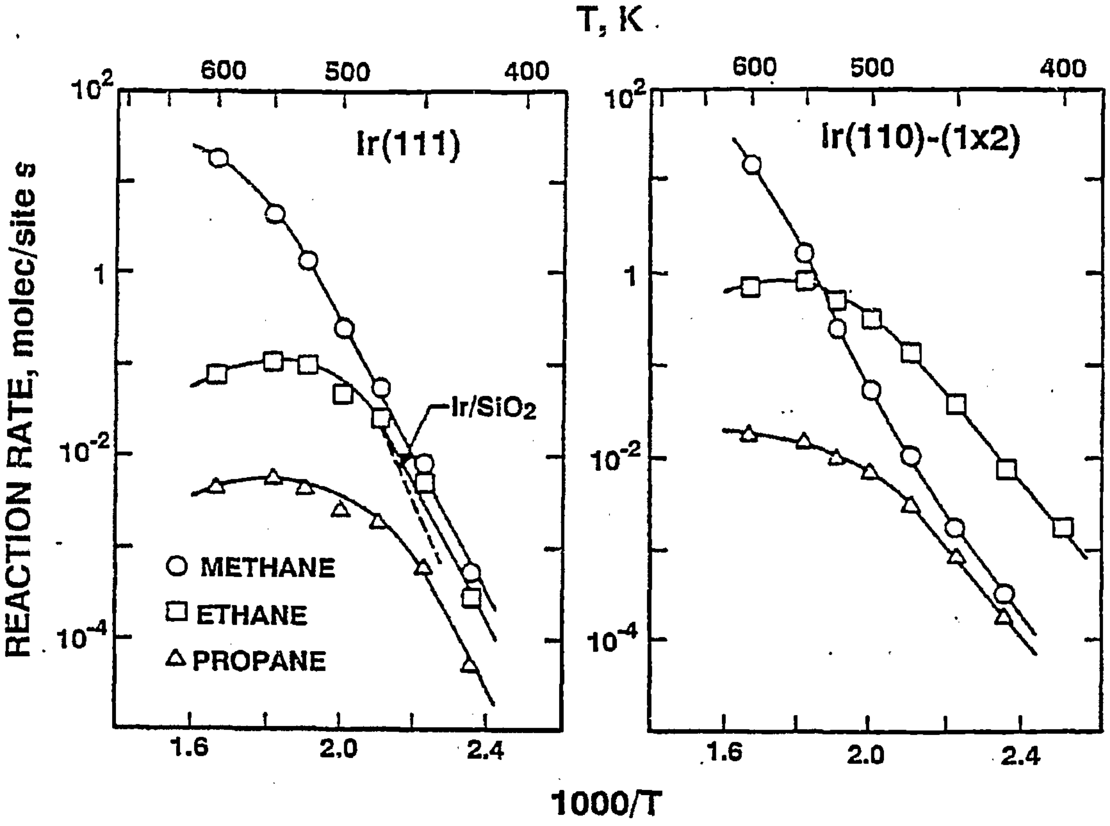
T, K
600
500
400
600
500
400
Ir(111)
Ir(110)-(1x2)
Ir/SiO2
REACTION RATE, molec/site s
10^2
1
10^{-2}
10^{-4}
○ METHANE
□ ETHANE
△ PROPANE
1.6
2.0
2.4
1000/T

Fig. 42

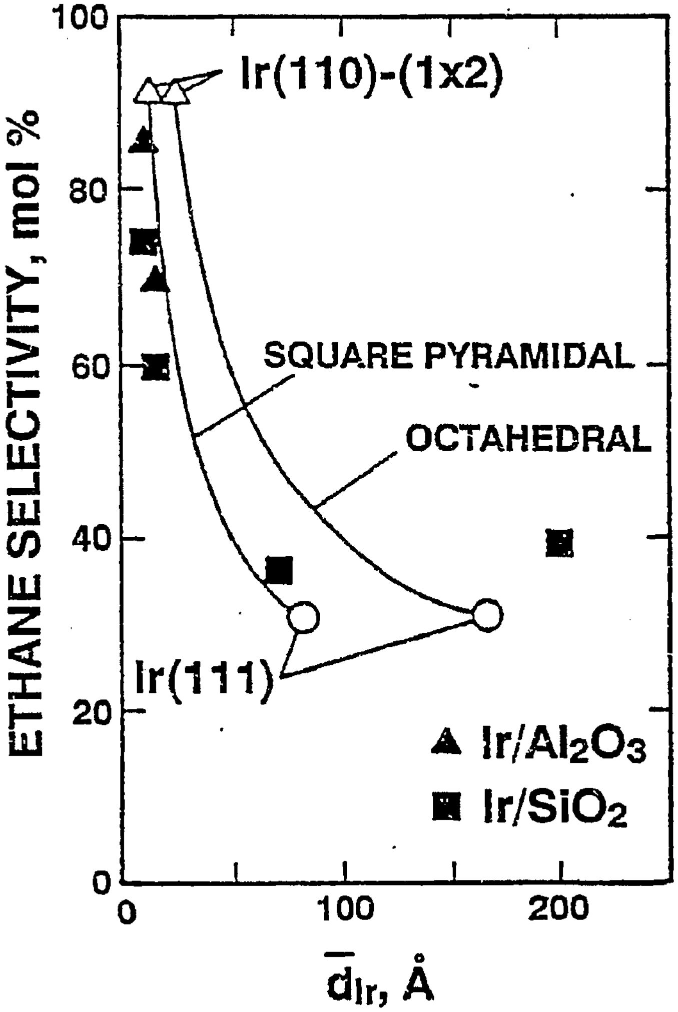
100
80
60
40
20
0
0
100
200
ETHANE SELECTIVITY, mol %
$\bar{d}_{Ir}$, Å
Ir(110)-(1x2)
SQUARE PYRAMIDAL
OCTAHEDRAL
Ir(111)
▲ Ir/Al_2O_3
■ Ir/SiO_2

Fig. 43

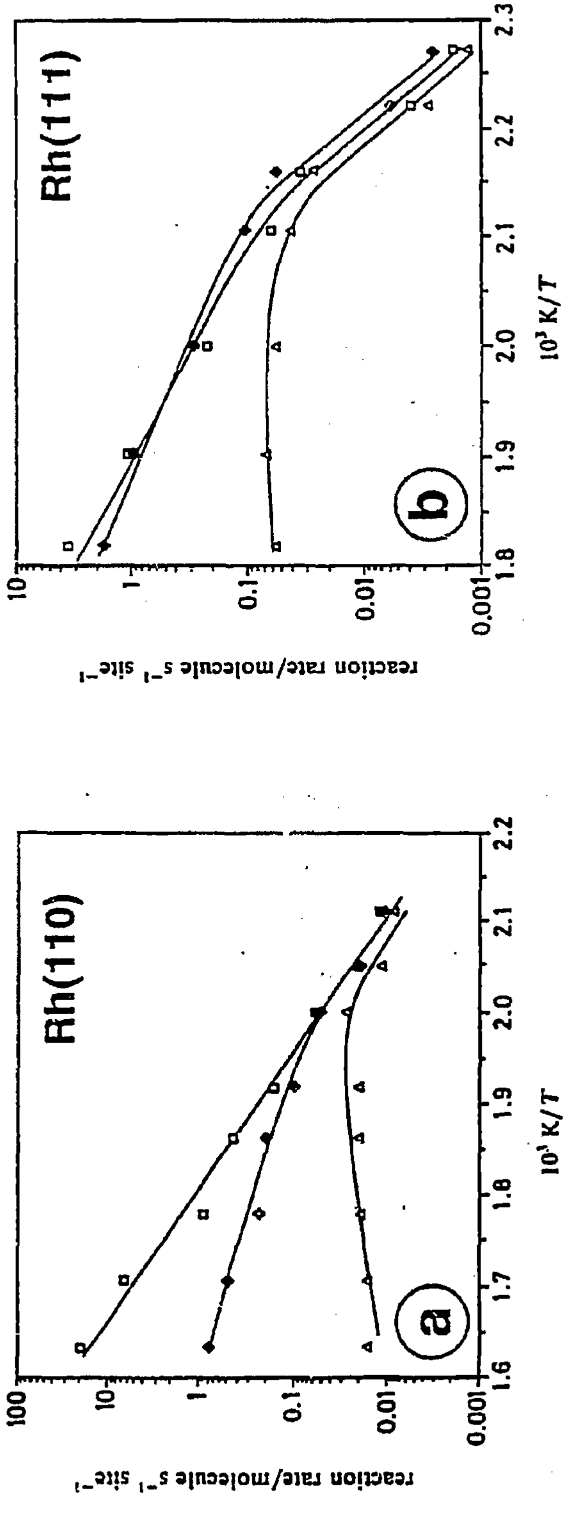
a
Rh(110)
reaction rate/molecule s⁻¹ site⁻¹
100
10
1
0.1
0.01
0.001
1.6
1.7
1.8
1.9
2.0
2.1
2.2
10³ K/T
b
Rh(111)
reaction rate/molecule s⁻¹ site⁻¹
10
1
0.1
0.01
0.001
1.8
1.9
2.0
2.1
2.2
2.3
10³ K/T

Fig. 44

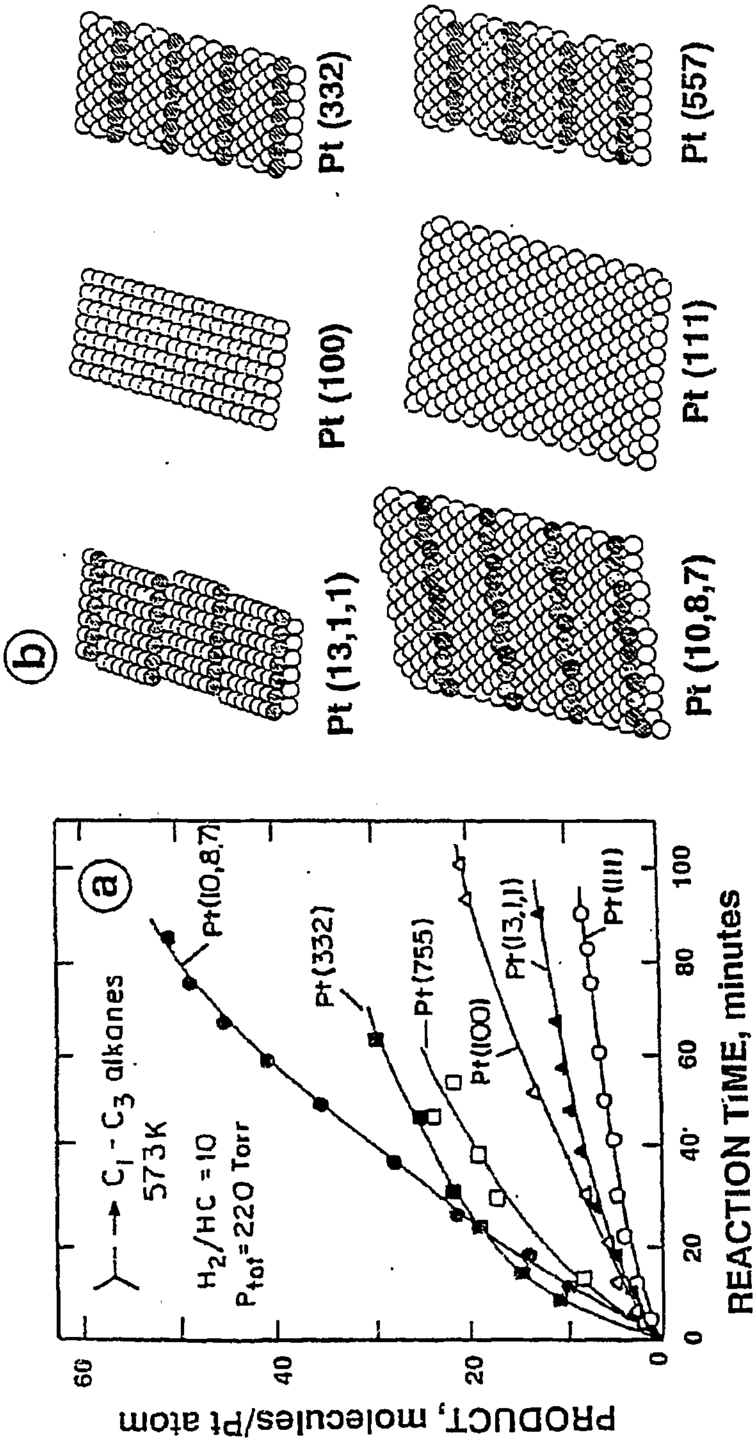
a
C1 - C3 alkanes
573K
H2/HC = 10
Ptot=220 Torr
Pt(10,8,7)
Pt(332)
Pt(755)
Pt(100)
Pt(13,1,1)
Pt(111)
PRODUCT, molecules/Pt atom
0
20
40
60
REACTION TIME, minutes
0
20
40
60
80
100
b
Pt (13,1,1)
Pt (100)
Pt (332)
Pt (10,8,7)
Pt (111)
Pt (557)

Fig. 45

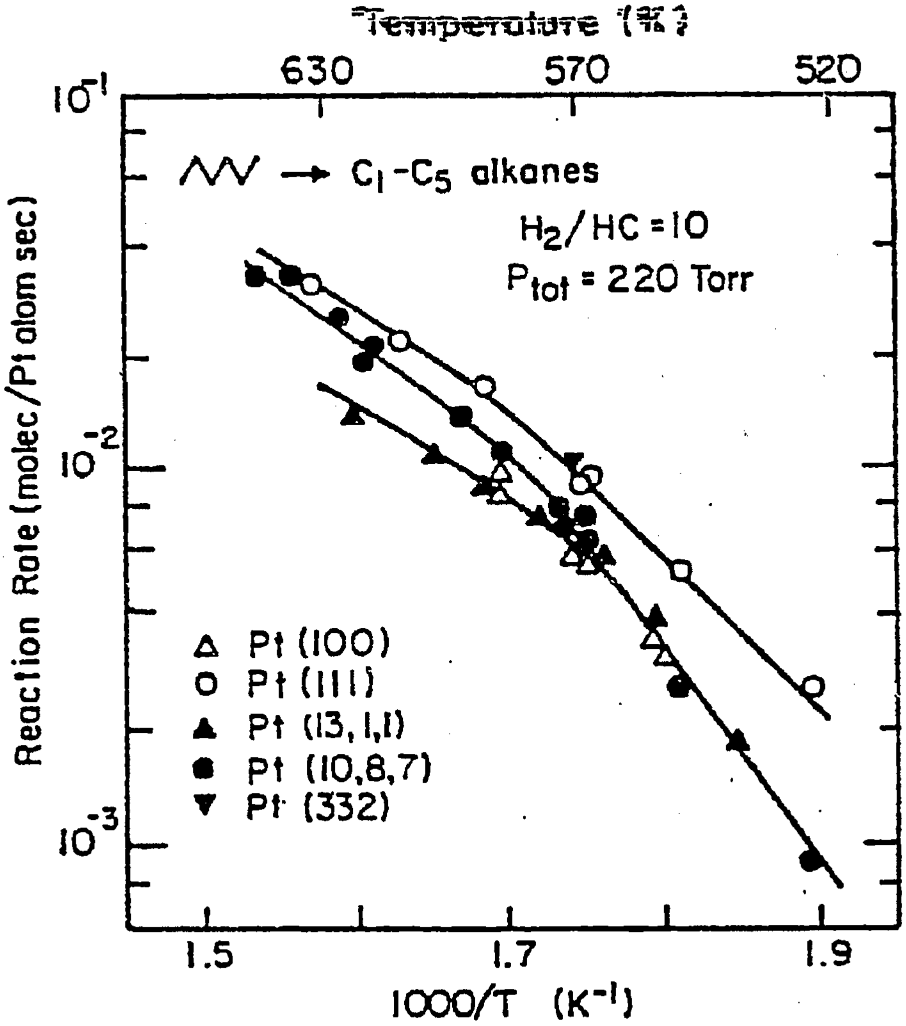
Temperature (K)
630
570
520
10^{-1}
10^{-2}
10^{-3}
→ C_1-C_5 alkanes
H_2/HC = 10
P_{tot} = 220 Torr
Reaction Rate (molec/Pt atom sec)
△ Pt (100)
○ Pt (111)
▲ Pt (13,1,1)
● Pt (10,8,7)
▼ Pt (332)
1.5
1.7
1.9
1000/T (K^{-1})

Fig. 46

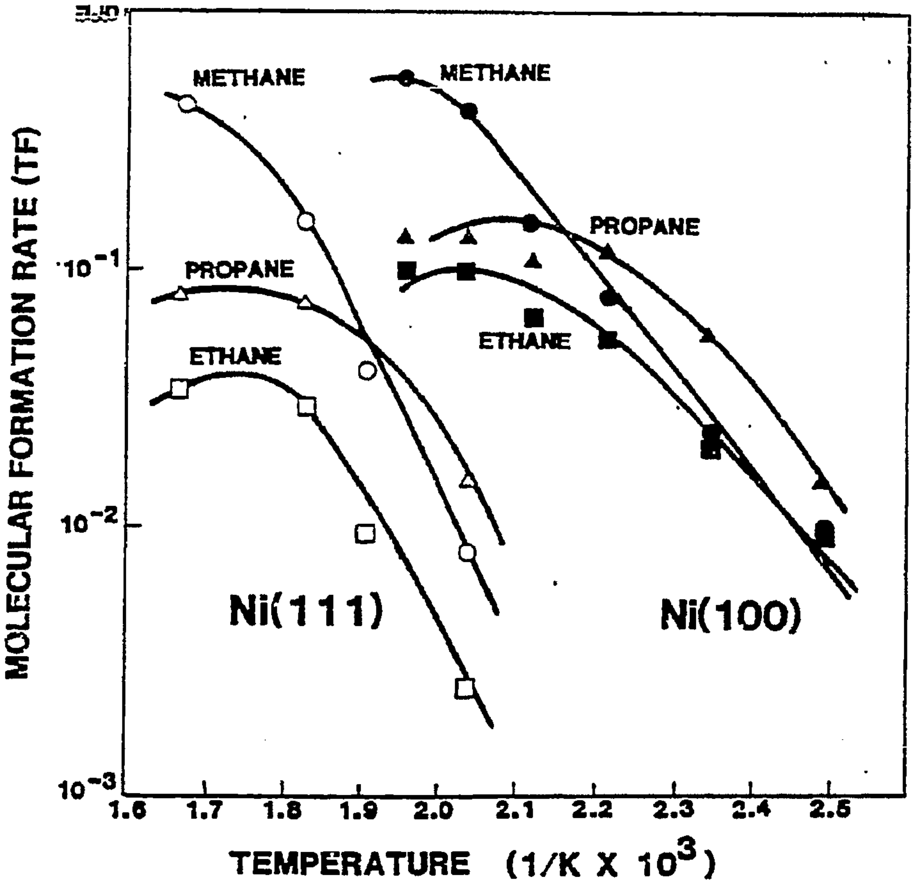METHANE
METHANE
PROPANE
PROPANE
ETHANE
ETHANE
Ni(111)
Ni(100)
MOLECULAR FORMATION RATE (TF)
10^-1
10^-2
10^-3
1.6
1.7
1.8
1.9
2.0
2.1
2.2
2.3
2.4
2.5
TEMPERATURE (1/K X 10^3)

Fig. 47

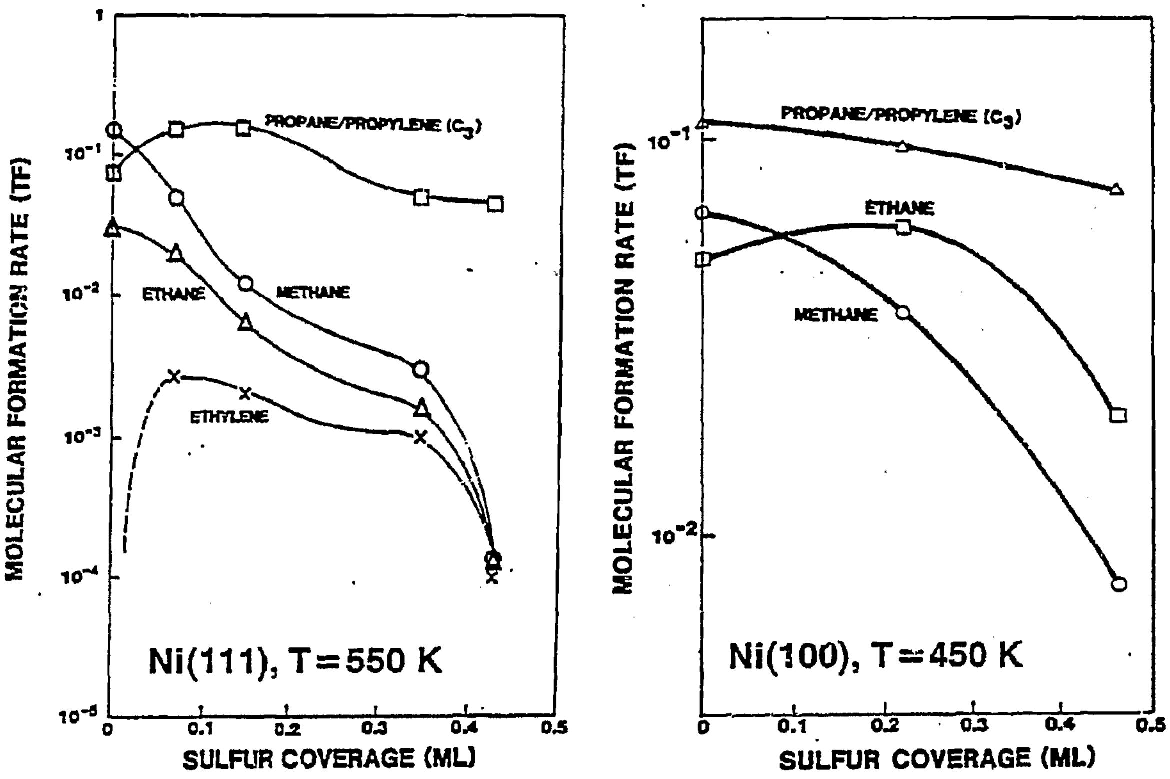

MOLECULAR FORMATION RATE (TF)
1
10⁻¹
10⁻²
10⁻³
10⁻⁴
10⁻⁵
PROPANE/PROPYLENE (C_3)
ETHANE
METHANE
ETHYLENE
Ni(111), T=550 K
0
0.1
0.2
0.3
0.4
0.5
SULFUR COVERAGE (ML)
MOLECULAR FORMATION RATE (TF)
10⁻¹
10⁻²
PROPANE/PROPYLENE (C_3)
ETHANE
METHANE
Ni(100), T=450 K
0
0.1
0.2
0.3
0.4
0.5
SULFUR COVERAGE (ML)

Fig. 48

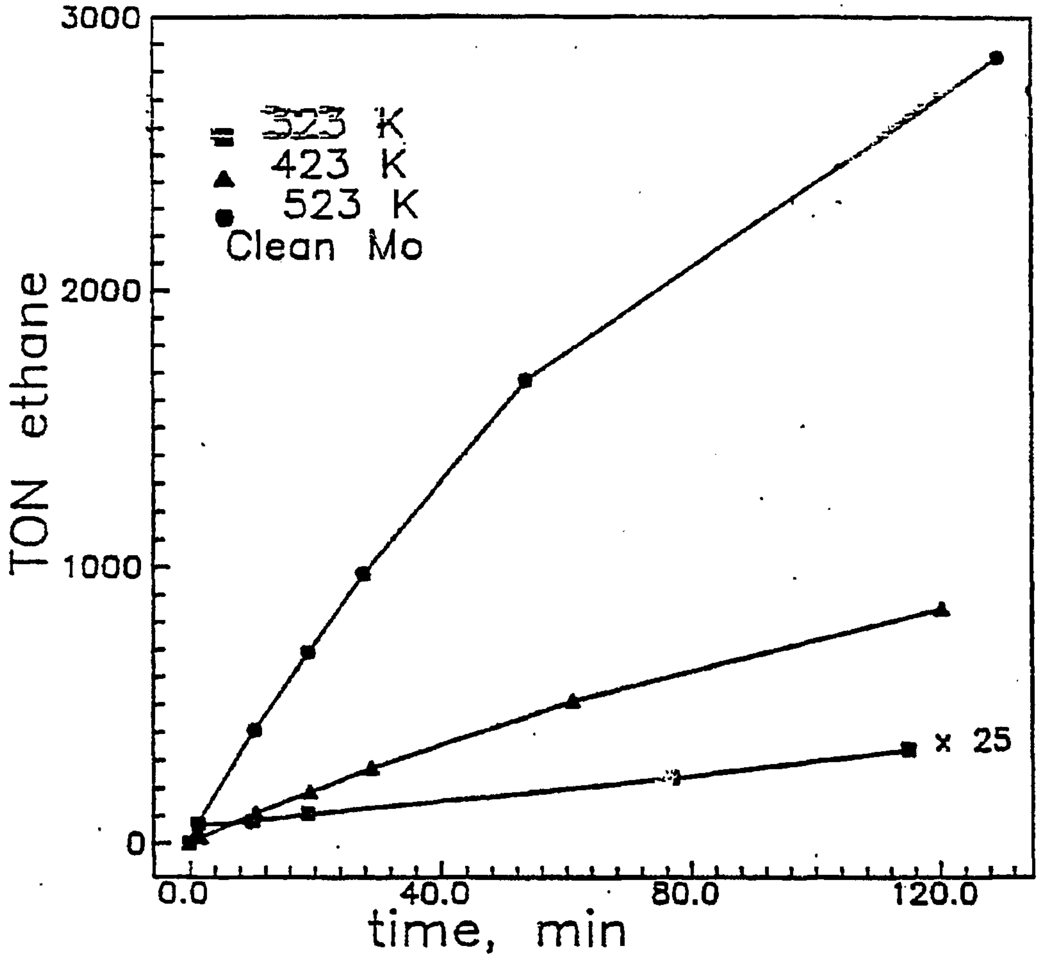
3000
2000
1000
0
0.0
40.0
80.0
120.0
TON ethane
time, min
■ 323 K
▲ 423 K
● 523 K
Clean Mo
x 25

Fig. 49

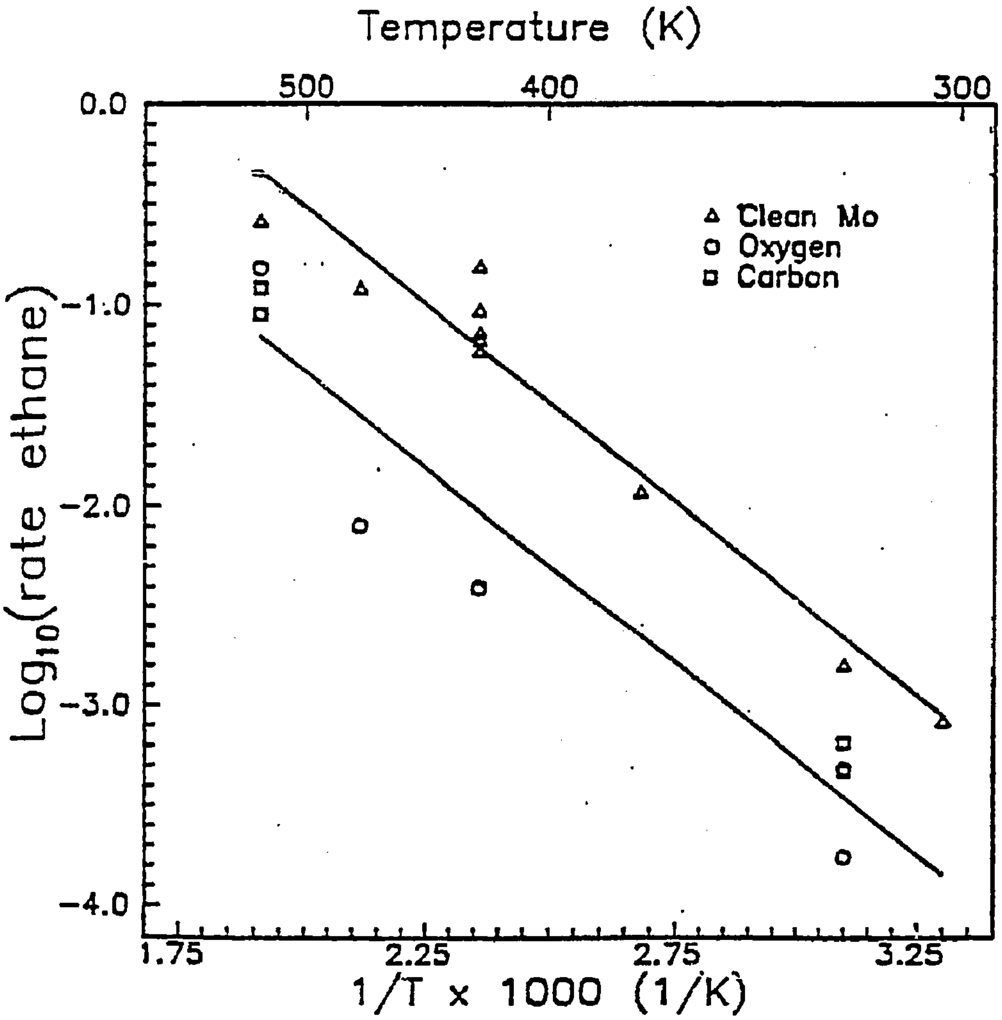
Temperature (K)
500
400
300
0.0
-1.0
-2.0
-3.0
-4.0
Log$_{10}$(rate ethane)
△ Clean Mo
○ Oxygen
□ Carbon
1.75
2.25
2.75
3.25
1/T x 1000 (1/K)

Fig. 50

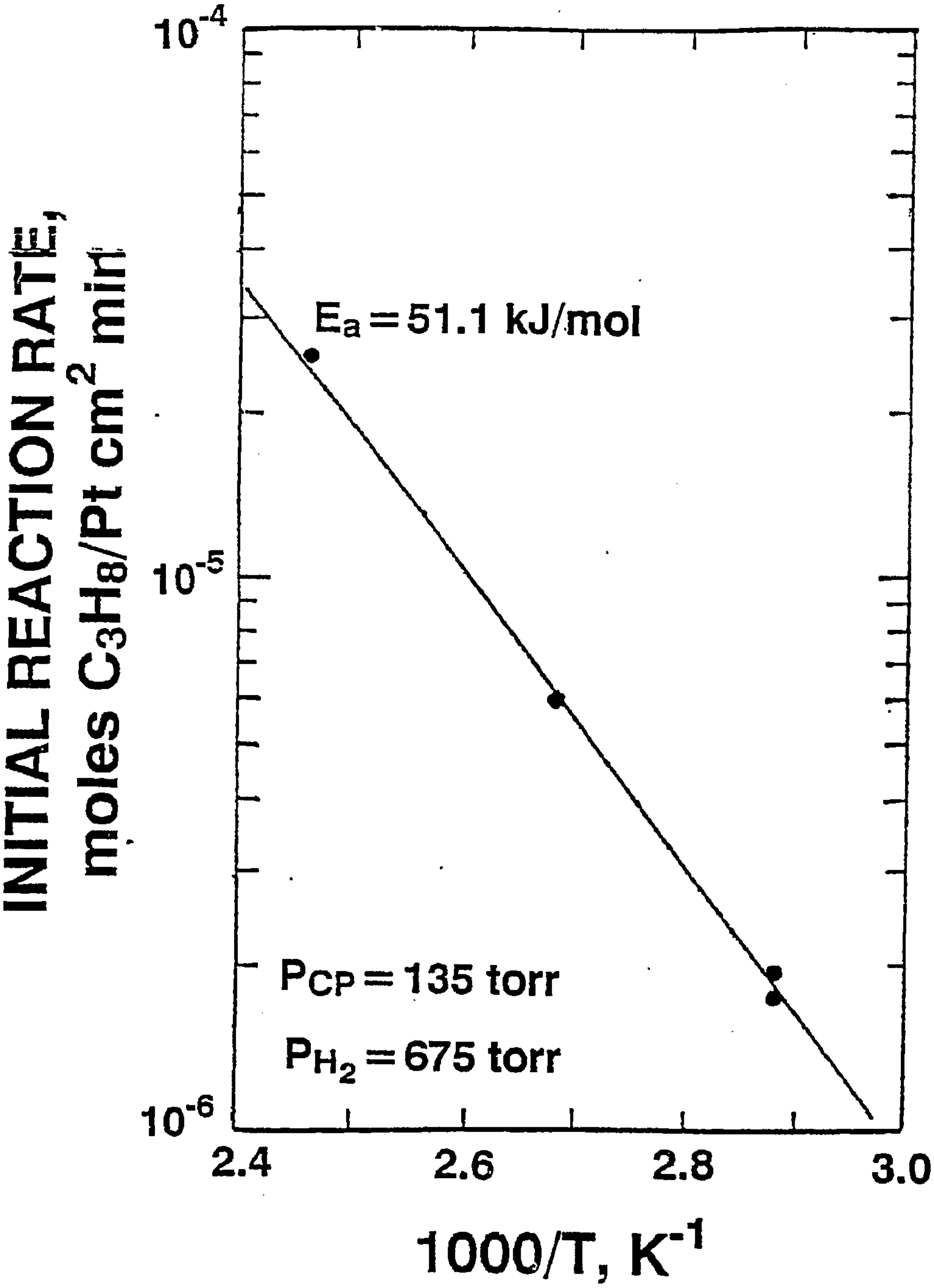

10^{-4}
10^{-5}
10^{-6}
INITIAL REACTION RATE, moles C_3H_8/Pt cm^2 min
$E_a = 51.1$ kJ/mol
$P_{CP} = 135$ torr
$P_{H_2} = 675$ torr
2.4
2.6
2.8
3.0
1000/T, K^{-1}

Fig. 51

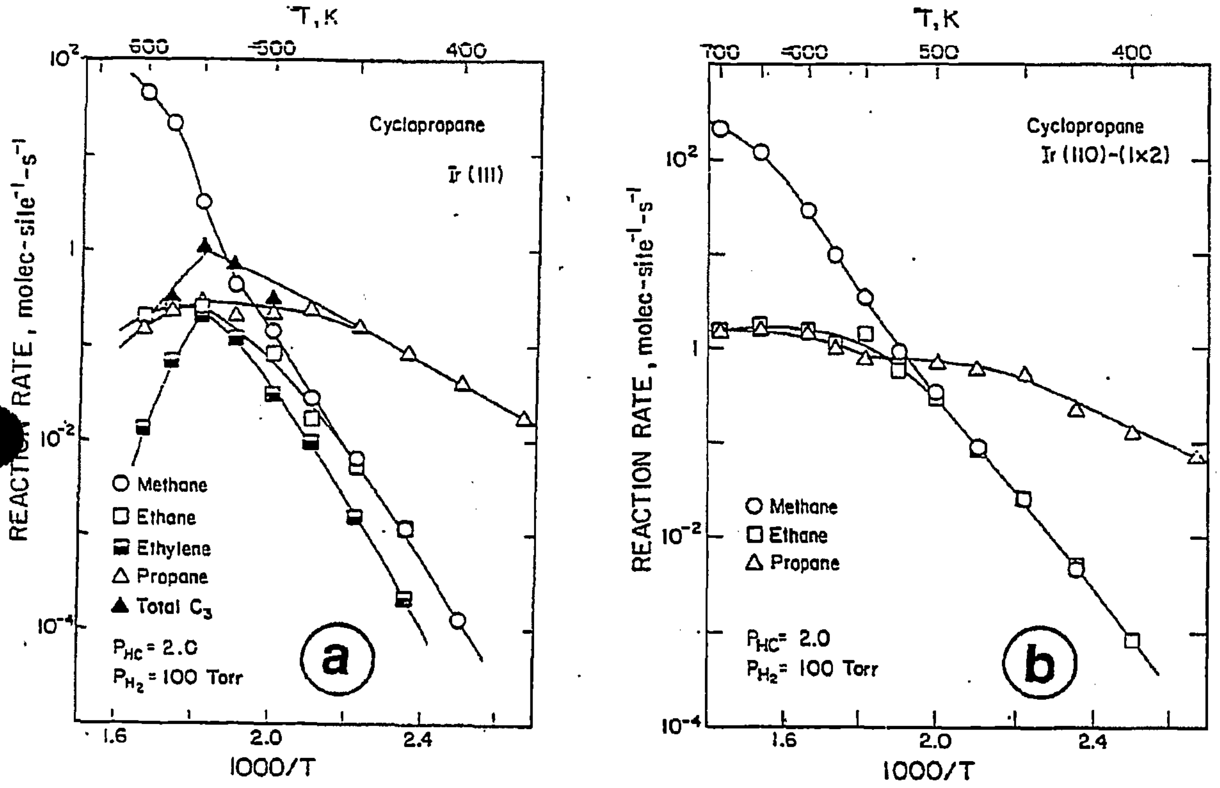
T, K
600
500
400
10²
1
10⁻²
10⁻⁴
REACTION RATE, molec-site⁻¹-s⁻¹
Cyclopropane
Ir (111)
○ Methane
□ Ethane
▣ Ethylene
△ Propane
▲ Total C₃
P_HC = 2.0
P_H₂ = 100 Torr
a
1.6
2.0
2.4
1000/T
T, K
700
600
500
400
10²
1
10⁻²
10⁻⁴
REACTION RATE, molec-site⁻¹-s⁻¹
Cyclopropane
Ir (110)-(1×2)
○ Methane
□ Ethane
△ Propane
P_HC = 2.0
P_H₂ = 100 Torr
b
1.6
2.0
2.4
1000/T

Fig. 52

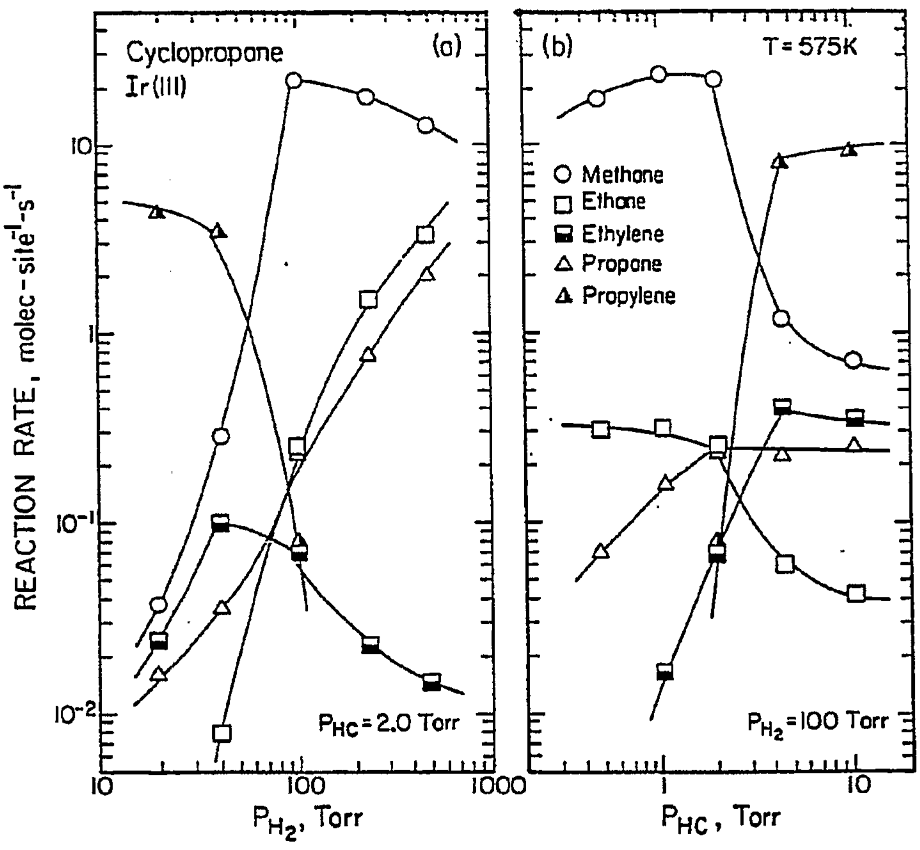

Cyclopropane
Ir(111)
(a)
(b)
T = 575K
○ Methane
□ Ethane
▣ Ethylene
△ Propane
▲ Propylene
REACTION RATE, molec-site^{-1}-s^{-1}
10
1
10^{-1}
10^{-2}
P_{HC} = 2.0 Torr
P_{H_2} = 100 Torr
10
100
1000
1
10
P_{H_2}, Torr
P_{HC}, Torr

Fig. 53

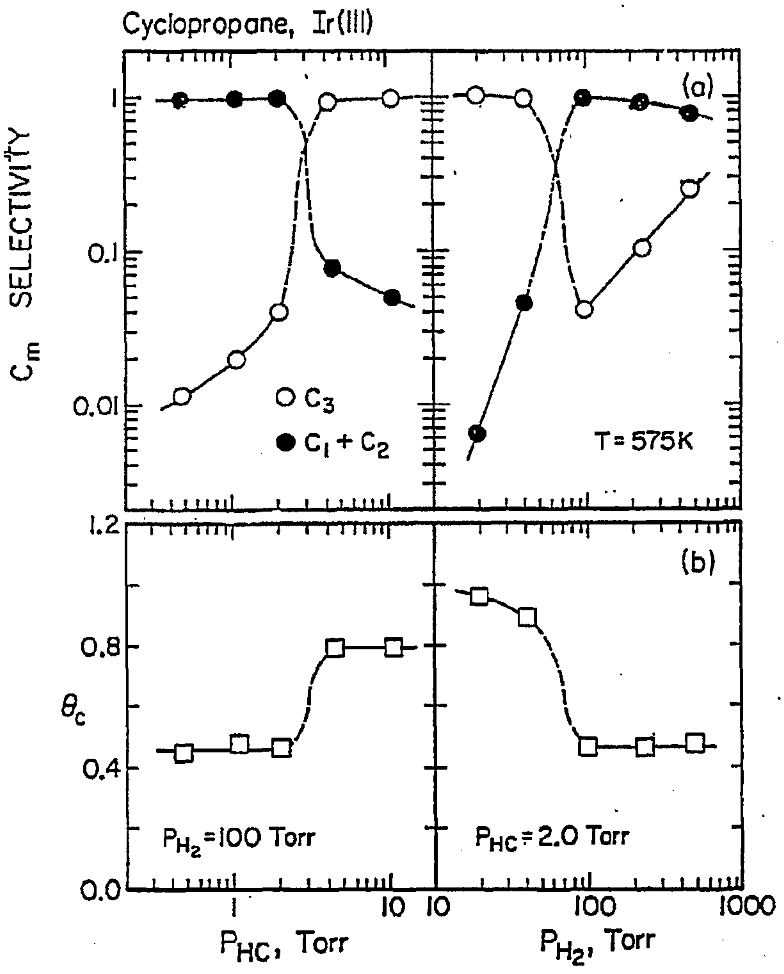Cyclopropane, Ir(111)
C_m SELECTIVITY
(a)
1
0.1
0.01
○ C_3
● $C_1 + C_2$
T = 575 K
(b)
1.2
0.8
0.4
0.0
θ_c
P_{H_2}=100 Torr
P_{HC}= 2.0 Torr
1
10
10
100
1000
P_{HC}, Torr
P_{H_2}, Torr

Fig. 54

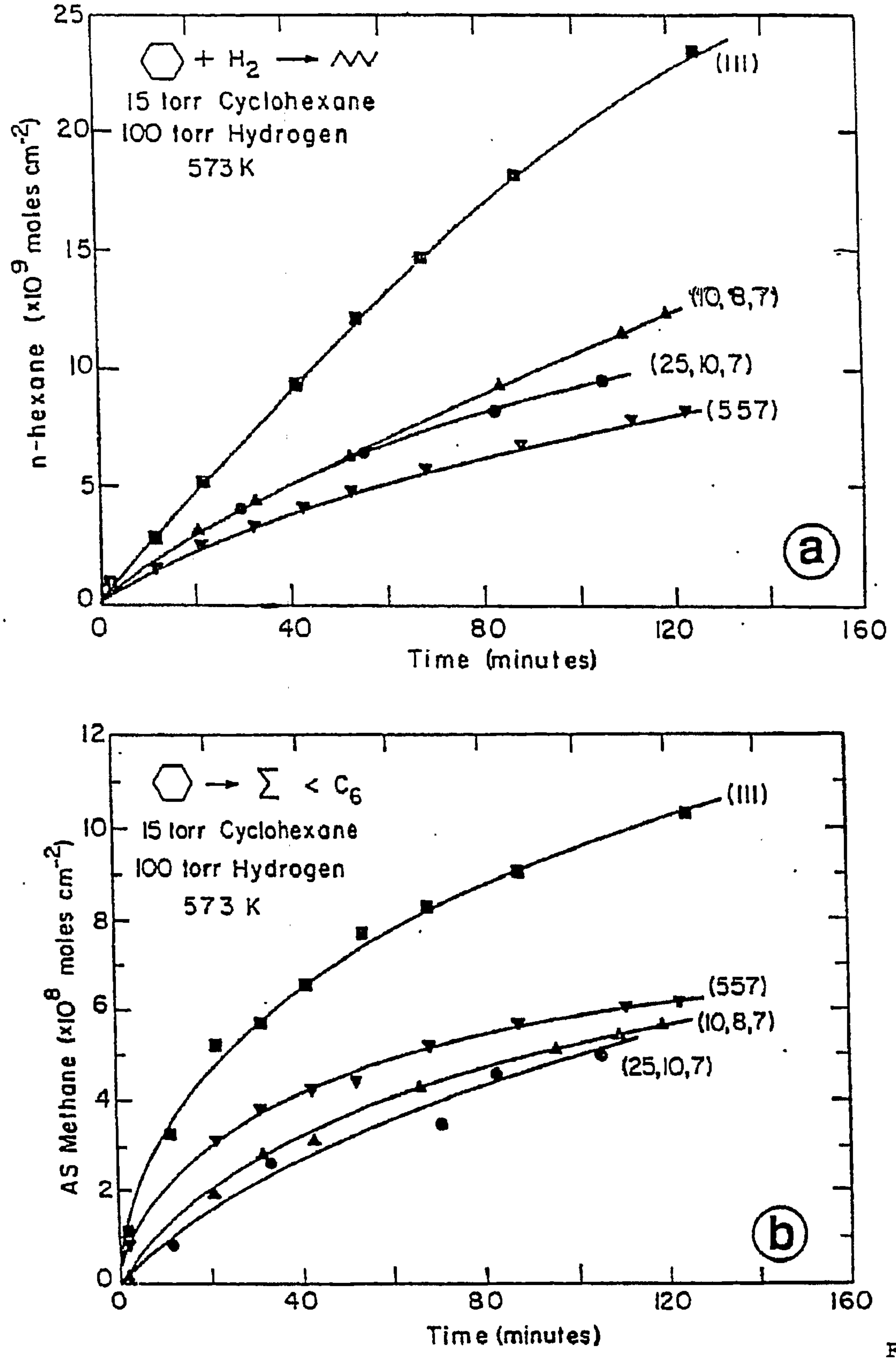

+ H2 →
15 torr Cyclohexane
100 torr Hydrogen
573 K
(111)
(10,8,7)
(25,10,7)
(557)
a
n-hexane (x10^9 moles cm^-2)
Time (minutes)
0
5
10
15
20
25
0
40
80
120
160
→ Σ < C6
15 torr Cyclohexane
100 torr Hydrogen
573 K
(111)
(557)
(10,8,7)
(25,10,7)
b
AS Methane (x10^8 moles cm^-2)
Time (minutes)
0
2
4
6
8
10
12
0
40
80
120
160

Fig. 55

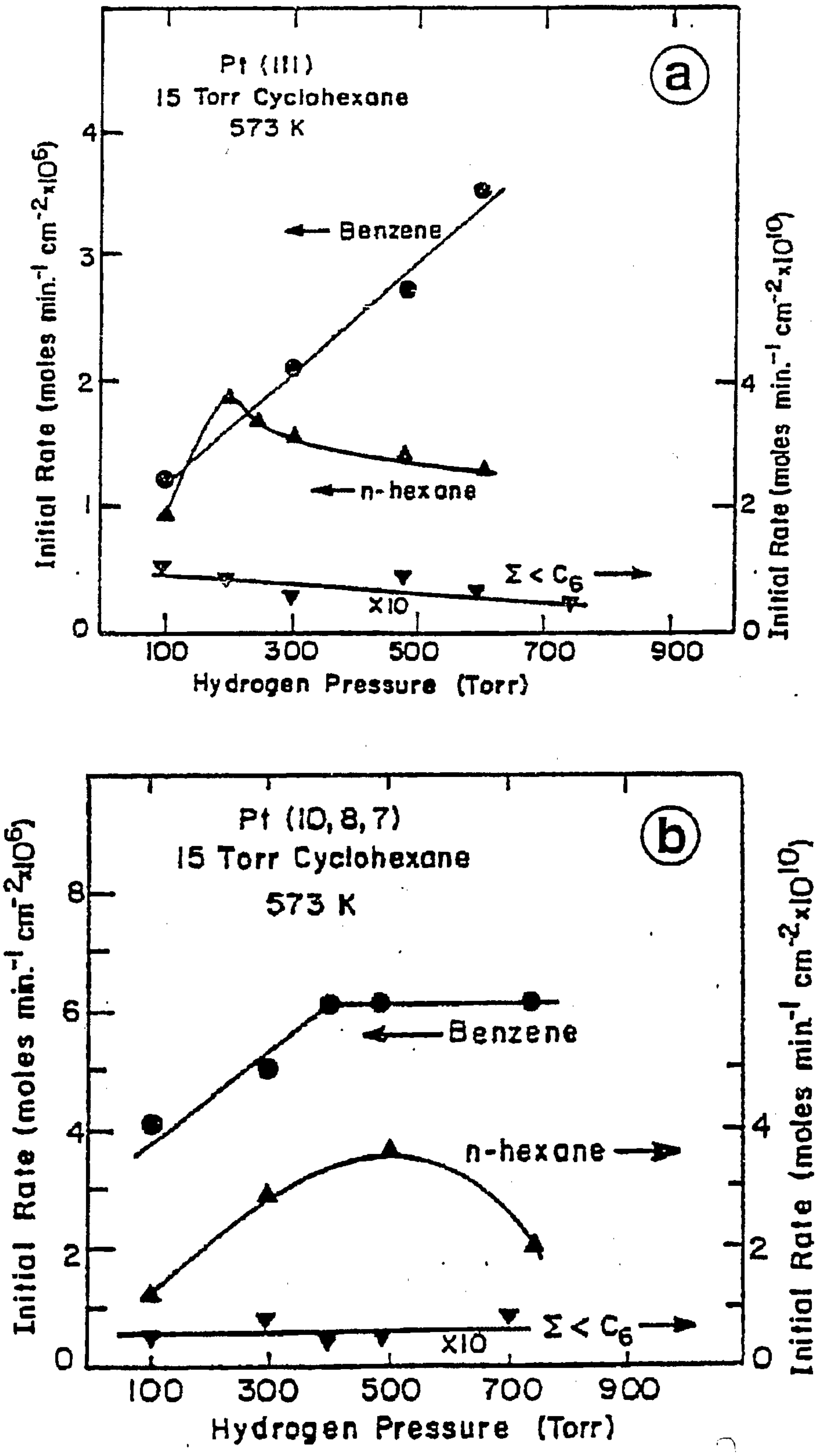
a
Pt (111)
15 Torr Cyclohexane
573 K
Benzene
n-hexane
Σ < C_6
x10
Initial Rate (moles min.$^{-1}$ cm^{-2} x10^{6})
Initial Rate (moles min.$^{-1}$ cm^{-2} x10^{10})
0
1
2
3
4
0
2
4
100
300
500
700
900
Hydrogen Pressure (Torr)
b
Pt (10, 8, 7)
15 Torr Cyclohexane
573 K
Benzene
n-hexane
Σ < C_6
x10
Initial Rate (moles min.$^{-1}$ cm^{-2} x10^{6})
Initial Rate (moles min.$^{-1}$ cm^{-2} x10^{10})
0
2
4
6
8
0
2
4
100
300
500
700
900
Hydrogen Pressure (Torr)

Fig. 56

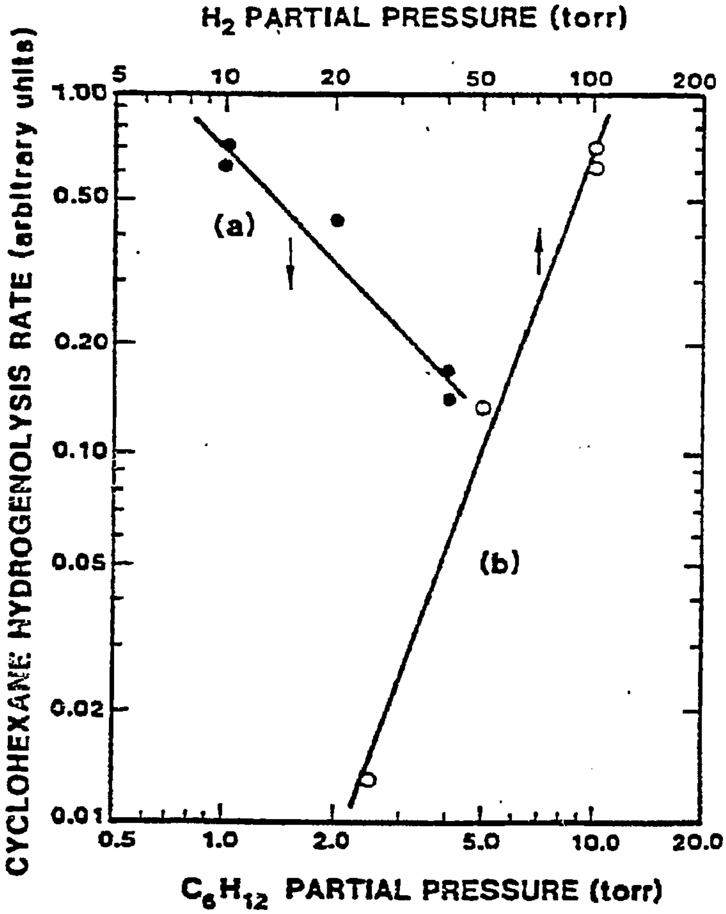

H_2 PARTIAL PRESSURE (torr)
5
10
20
50
100
200
CYCLOHEXANE HYDROGENOLYSIS RATE (arbitrary units)
1.00
0.50
0.20
0.10
0.05
0.02
0.01
(a)
(b)
0.5
1.0
2.0
5.0
10.0
20.0
C_6H_{12} PARTIAL PRESSURE (torr)

Fig. 57

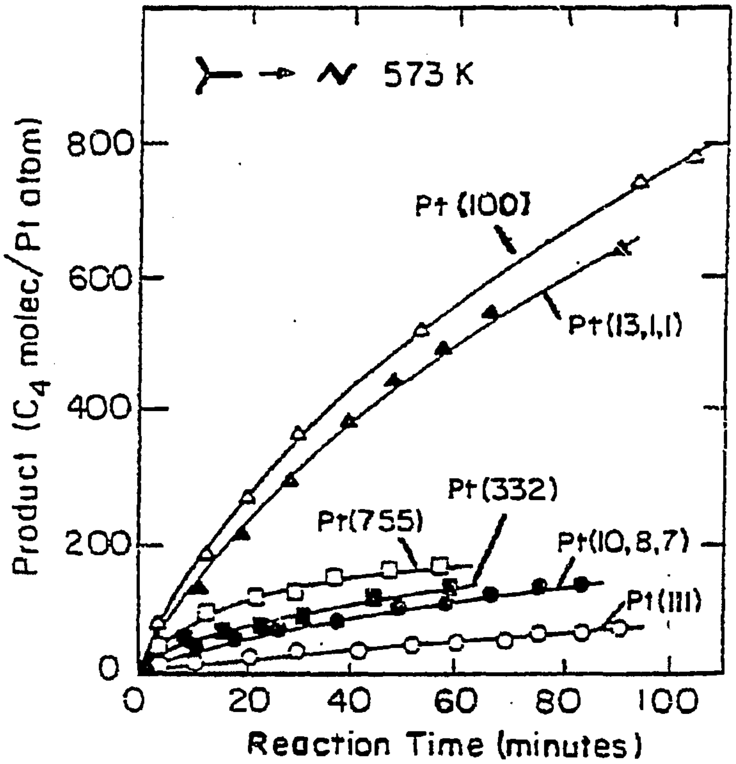

573 K
Pt (100)
Pt (13,1,1)
Pt (332)
Pt (755)
Pt (10,8,7)
Pt (111)
Product (C4 molec/Pt atom)
0
200
400
600
800
Reaction Time (minutes)
0
20
40
60
80
100

Fig. 58

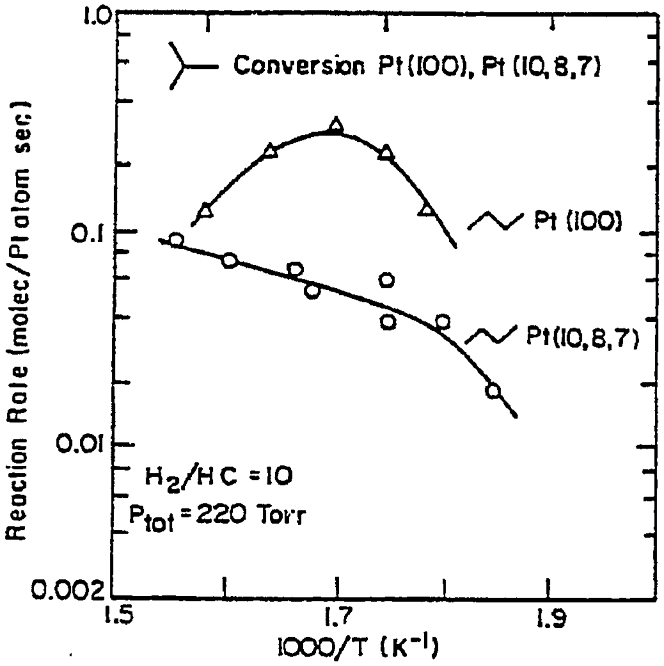

1.0
0.1
0.01
0.002
Reaction Rate (molec/Pt atom sec)
Conversion Pt(100), Pt (10,8,7)
Pt (100)
Pt(10,8,7)
H2/HC = 10
Ptot = 220 Torr
1.5
1.7
1.9
1000/T (K-1)

Fig. 59

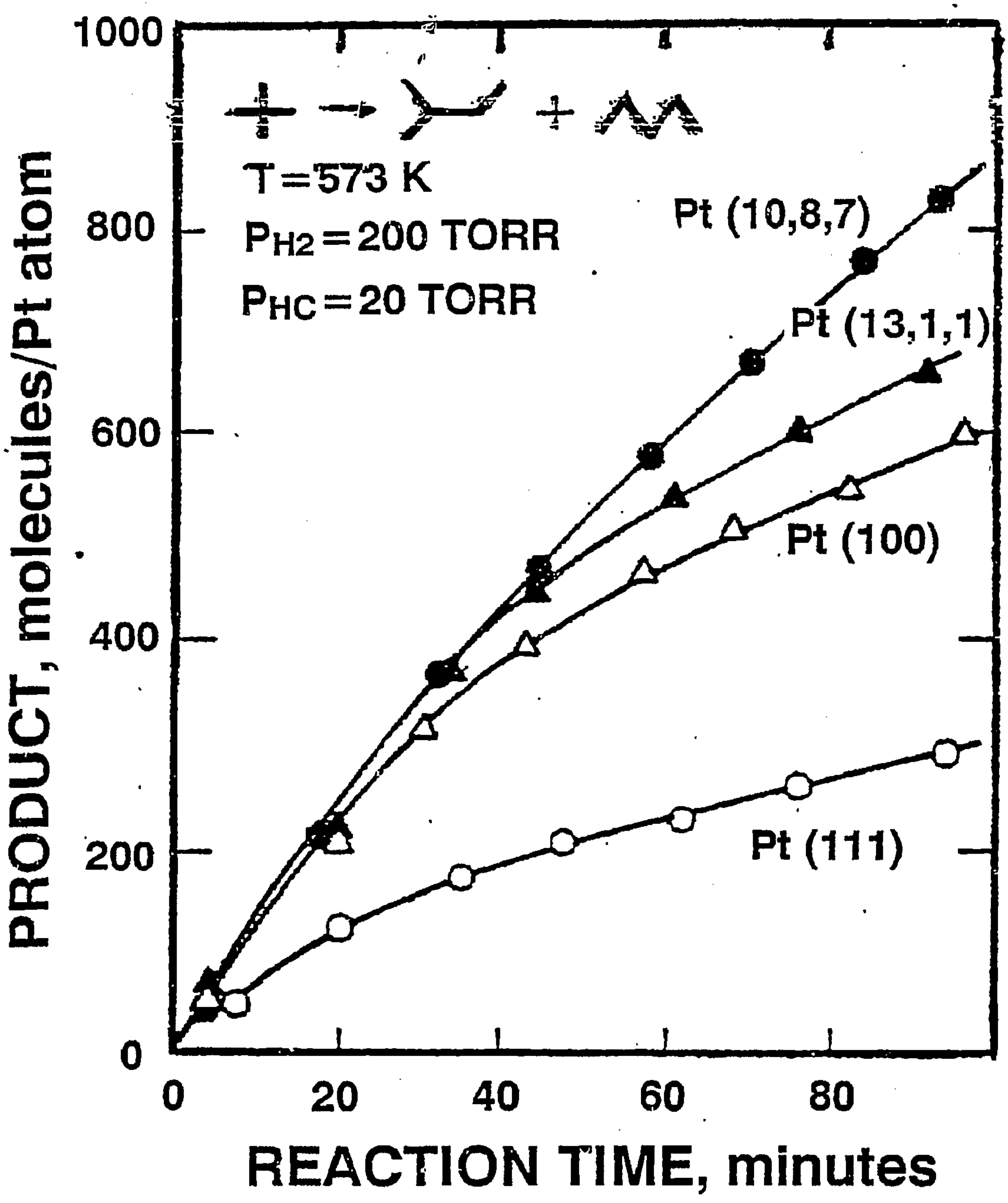
T=573 K
P_{H2}=200 TORR
P_{HC}=20 TORR
Pt (10,8,7)
Pt (13,1,1)
Pt (100)
Pt (111)
PRODUCT, molecules/Pt atom
REACTION TIME, minutes
1000
800
600
400
200
0
0
20
40
60
80

Fig. 60

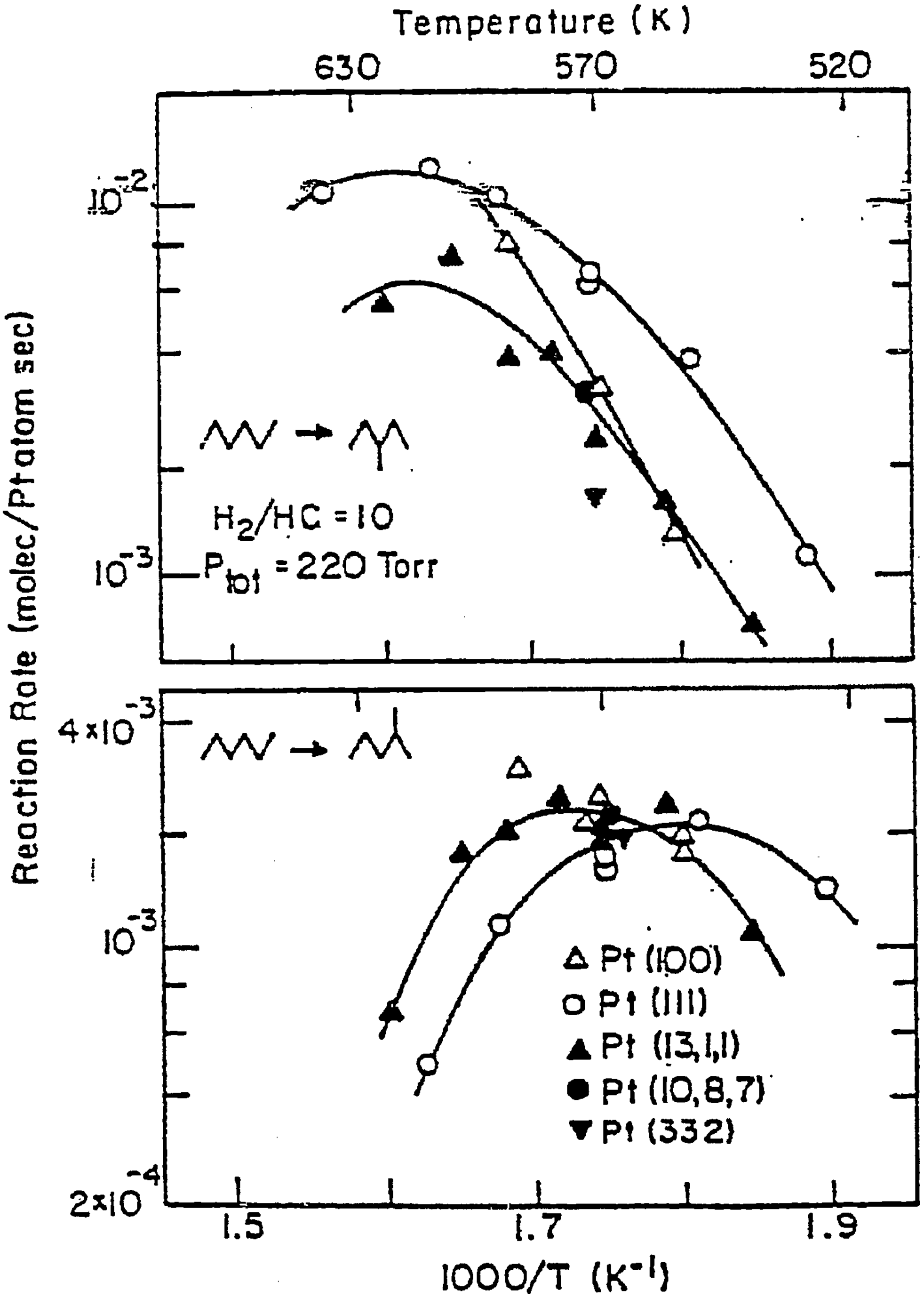
Temperature (K)
630
570
520
10^{-2}
10^{-3}
$H_2/HC = 10$
$P_{tot} = 220$ Torr
Reaction Rate (molec/Pt·atom sec)
4×10^{-3}
10^{-3}
2×10^{-4}
1.5
1.7
1.9
1000/T (K^{-1})
△ Pt (100)
○ Pt (111)
▲ Pt (13,1,1)
● Pt (10,8,7)
▼ Pt (332)

Fig. 61

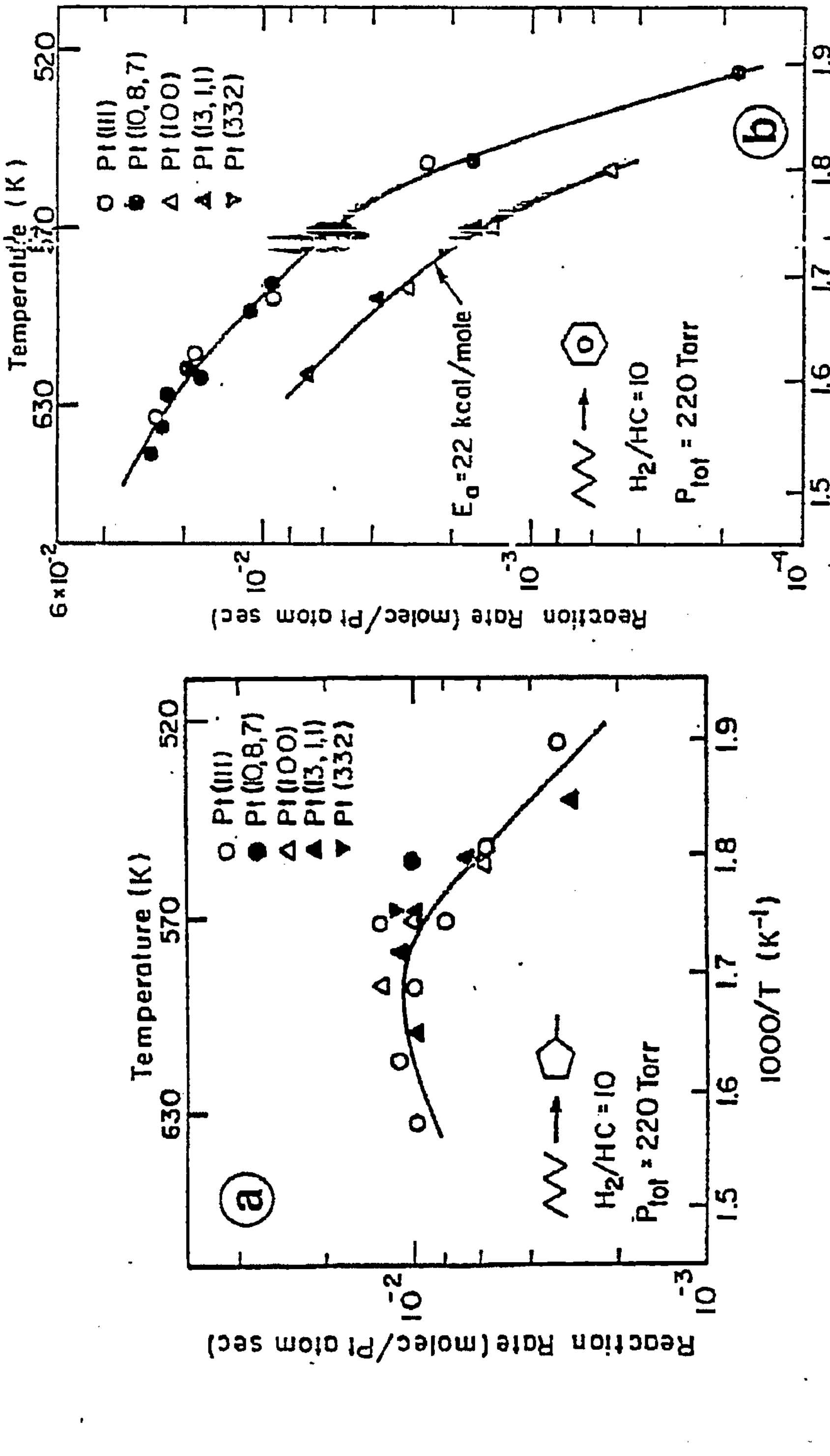
a
Temperature (K)
630
570
520
Pt(111)
Pt(10,8,7)
Pt(100)
Pt(13,1,1)
Pt(332)
$H_2/HC = 10$
$P_{tot} = 220$ Torr
1000/T (K^{-1})
1.5
1.6
1.7
1.8
1.9
Reaction Rate (molec/Pt atom sec)
10^{-2}
10^{-3}
b
Temperature (K)
630
570
520
Pt(111)
Pt(10,8,7)
Pt(100)
Pt(13,1,1)
Pt(332)
$E_a = 22$ kcal/mole
$H_2/HC = 10$
$P_{tot} = 220$ Torr
1000/T (K^{-1})
1.5
1.6
1.7
1.8
1.9
Reaction Rate (molec/Pt atom sec)
6×10^{-2}
10^{-2}
10^{-3}
10^{-4}

Fig. 62

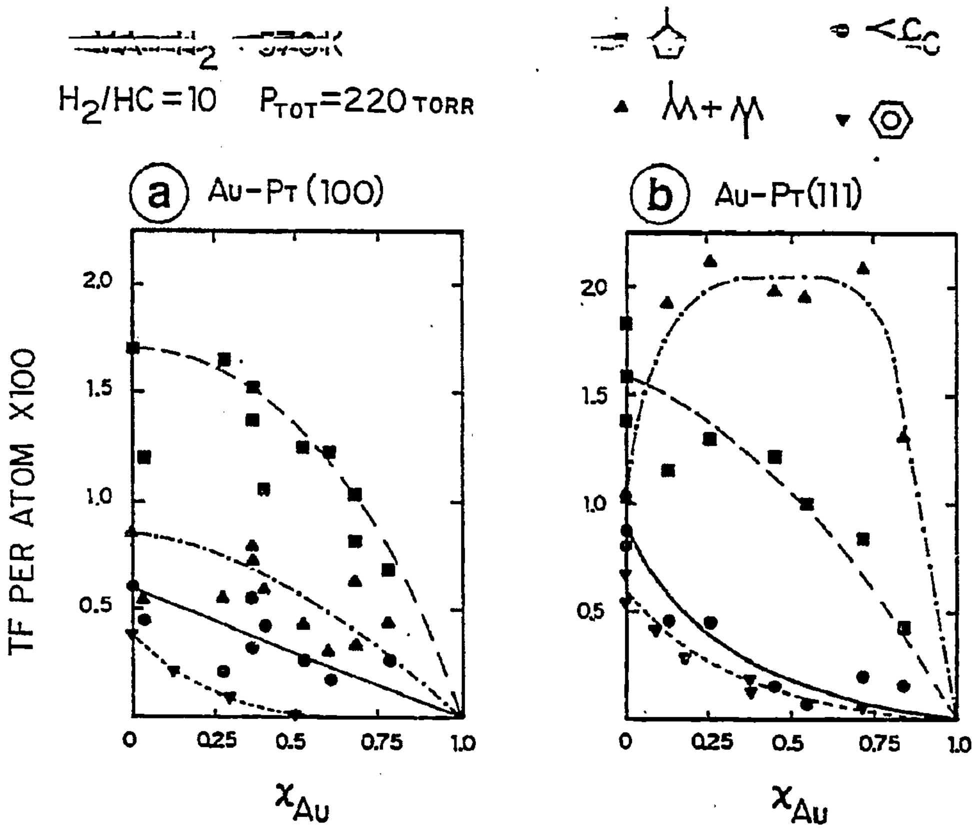H2/HC=10
PTOT=220 TORR
a
Au-Pt(100)
b
Au-Pt(111)
TF PER ATOM X100
2.0
1.5
1.0
0.5
0
0.25
0.5
0.75
1.0
χAu

Fig. 63

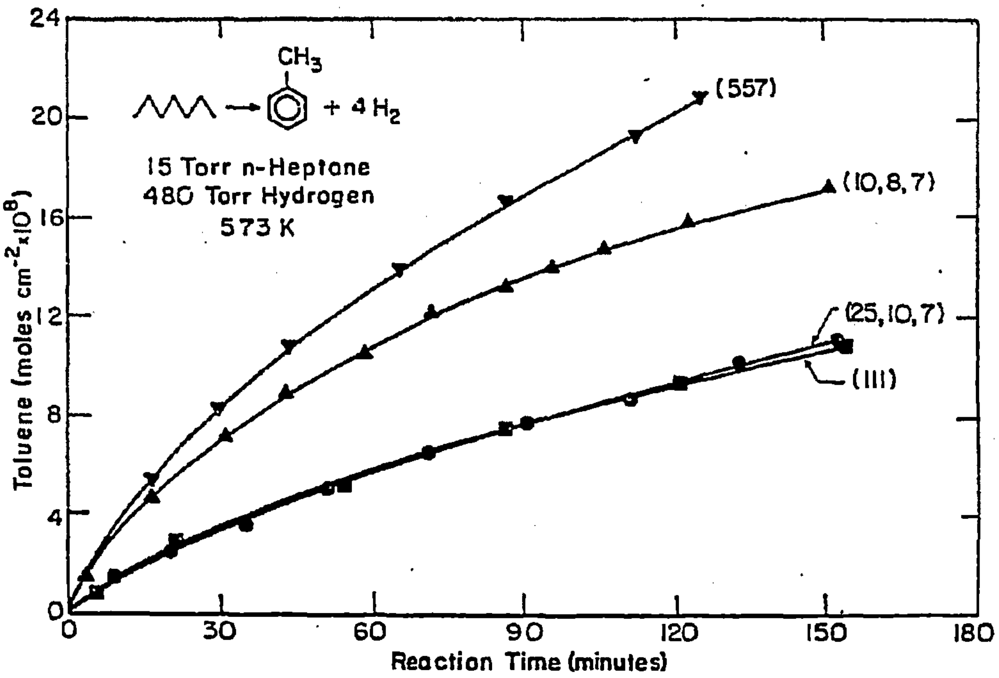
CH3
+ 4 H2
15 Torr n-Heptane
480 Torr Hydrogen
573 K
(557)
(10,8,7)
(25,10,7)
(111)
Toluene (moles cm-2x10^8)
0
4
8
12
16
20
24
0
30
60
90
120
150
180
Reaction Time (minutes)

Fig. 64

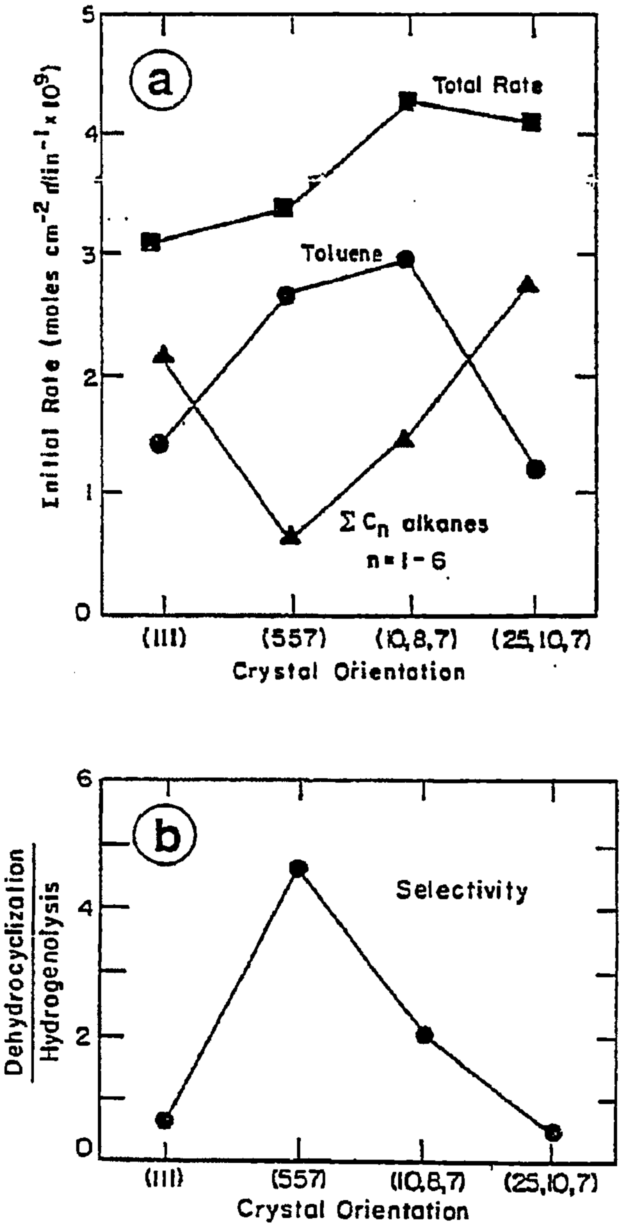
a
Total Rate
Toluene
ΣC_n alkanes
n = 1 - 6
Initial Rate (moles cm^{-2} min^{-1} x 10^9)
0
1
2
3
4
5
(111)
(557)
(10,8,7)
(25,10,7)
Crystal Orientation
b
Selectivity
Dehydrocyclization / Hydrogenolysis
0
2
4
6
(111)
(557)
(10,8,7)
(25,10,7)
Crystal Orientation

Fig. 65

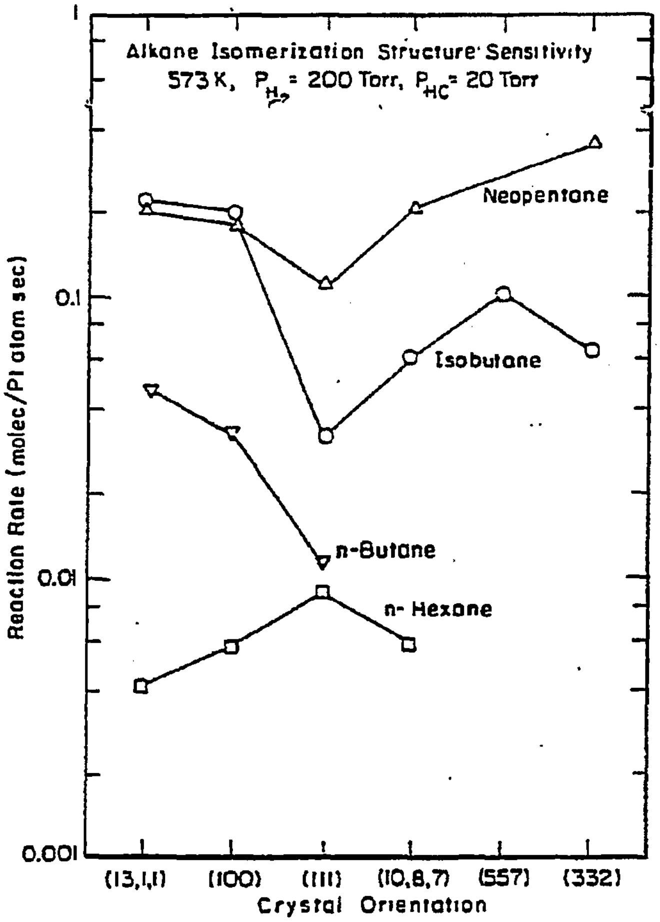
Alkane Isomerization Structure Sensitivity
573 K, P_{H_2} = 200 Torr, P_{HC} = 20 Torr
Neopentane
Isobutane
n-Butane
n- Hexane
Reaction Rate (molec/Pt atom sec)
1
0.1
0.01
0.001
(13,1,1)
(100)
(111)
(10,8,7)
(557)
(332)
Crystal Orientation

Fig. 66

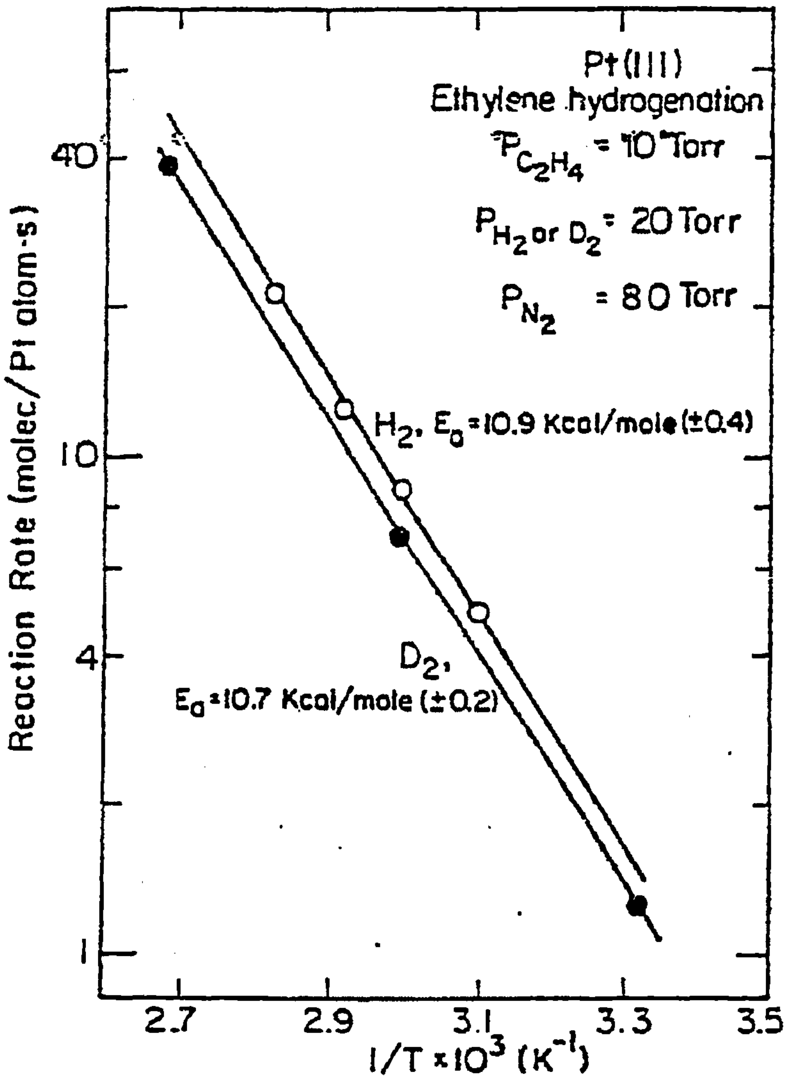
Pt(111)
Ethylene hydrogenation
P C2H4 = 10 Torr
P H2 or D2 = 20 Torr
P N2 = 80 Torr
H2, Ea=10.9 Kcal/mole (±0.4)
D2,
Ea=10.7 Kcal/mole (±0.2)
40
10
4
1
2.7
2.9
3.1
3.3
3.5
1/T ×10^3 (K^-1)
Reaction Rate (molec/Pt atom·s)

Fig. 67

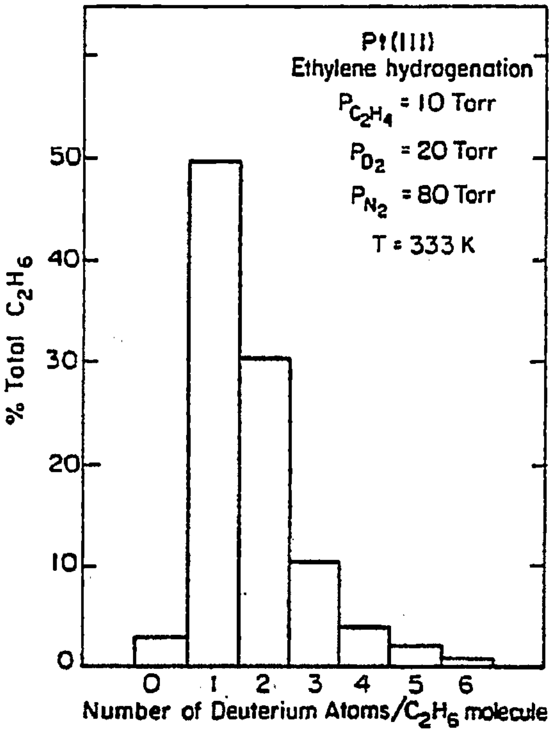

Pt(111)
Ethylene hydrogenation
$P_{C_2H_4}$ = 10 Torr
P_{D_2} = 20 Torr
P_{N_2} = 80 Torr
T = 333 K
% Total C_2H_6
0
10
20
30
40
50
0 1 2 3 4 5 6
Number of Deuterium Atoms/C_2H_6 molecule

Fig. 68

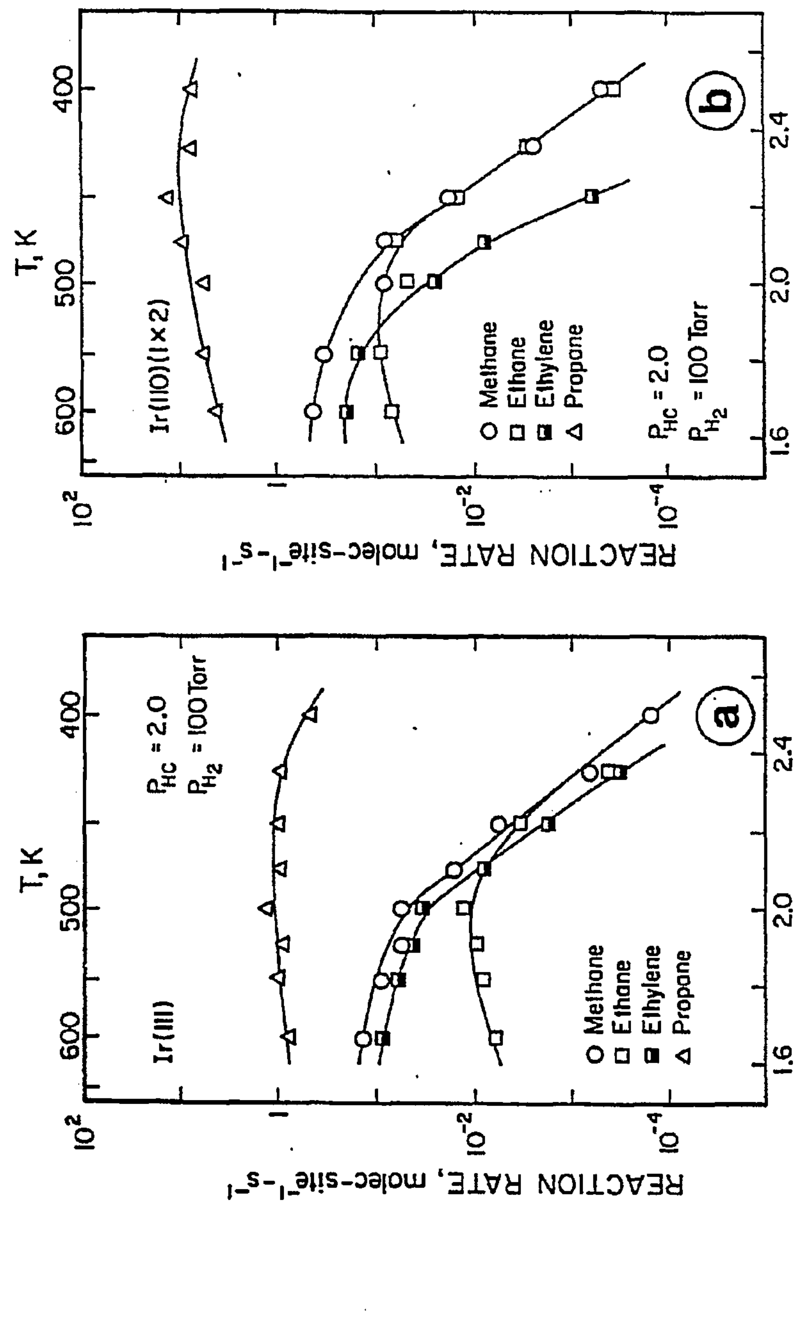
T, K
600
500
400
REACTION RATE, molec-site^{-1}-s^{-1}
10^2
1
10^{-2}
10^{-4}
1.6
2.0
2.4
1000/T
Ir(110)(1×2)
○ Methane
□ Ethane
■ Ethylene
△ Propane
P_{HC} = 2.0
P_{H_2} = 100 Torr
b
Ir(111)
P_{HC} = 2.0
P_{H_2} = 100 Torr
○ Methane
□ Ethane
■ Ethylene
△ Propane
a

Fig. 69

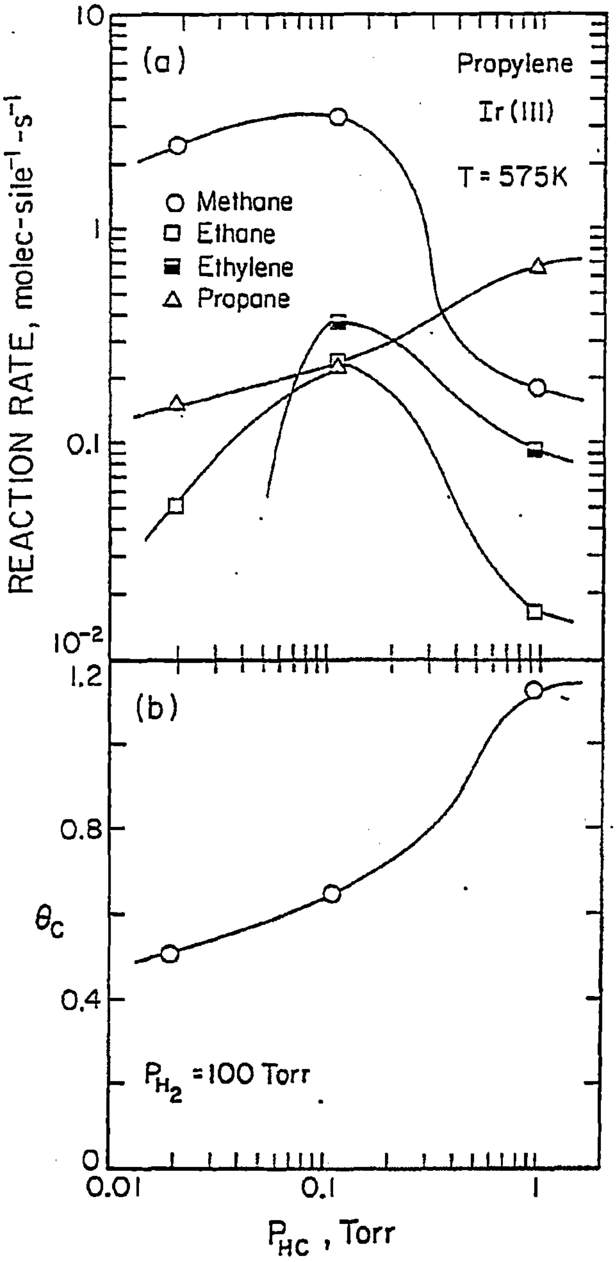
(a)
Propylene
Ir(III)
T = 575K
○ Methane
□ Ethane
■ Ethylene
△ Propane
REACTION RATE, molec-site⁻¹-s⁻¹
10
1
0.1
10⁻²
(b)
1.2
0.8
0.4
0
θc
PH2 = 100 Torr
0.01
0.1
1
PHC , Torr

Fig. 70

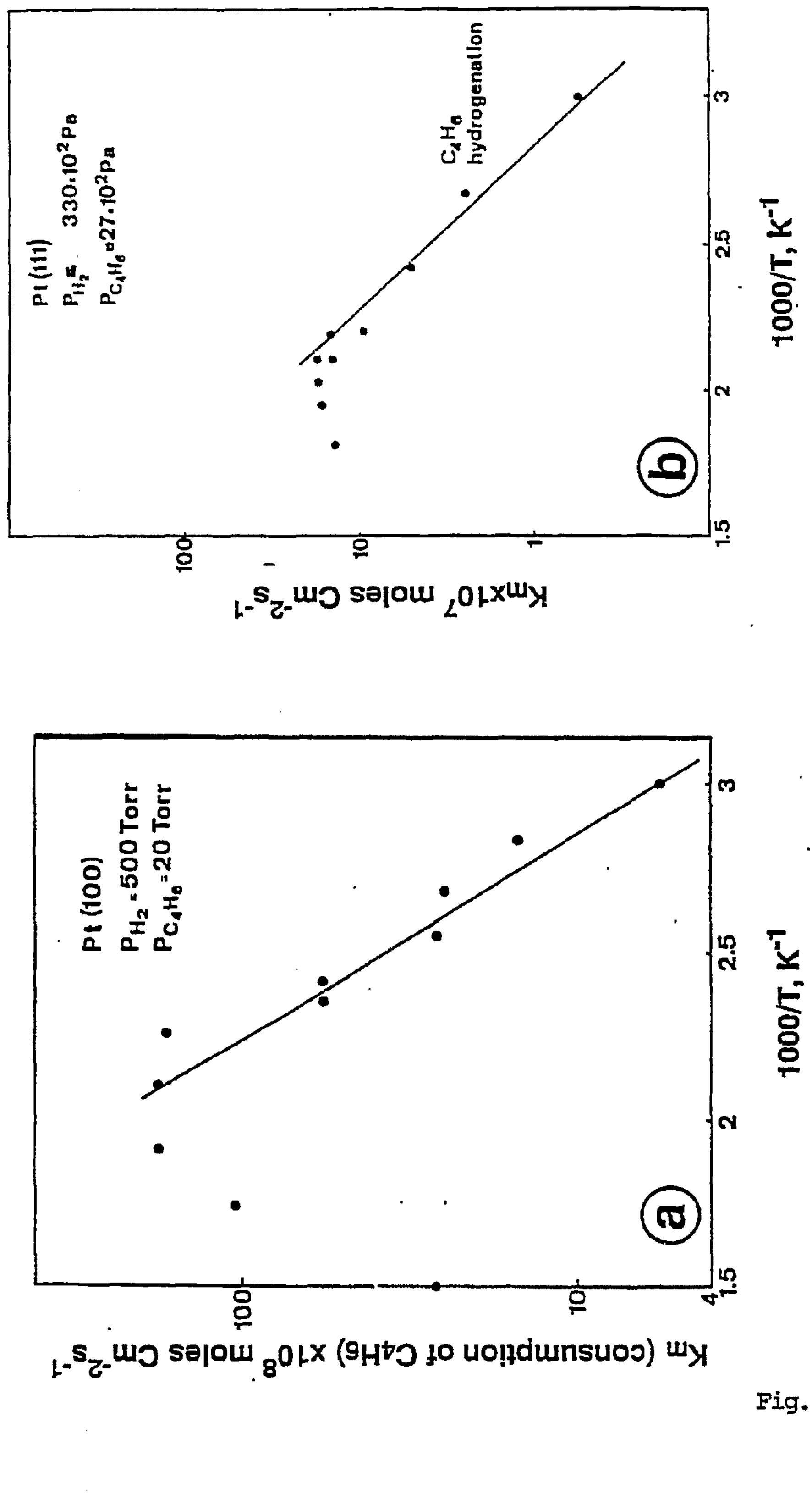

a
Pt (100)
P_{H_2} =500 Torr
$P_{C_4H_6}$ =20 Torr
Km (consumption of C4H6) x10^8 moles Cm^-2 s^-1
100
10
4
1.5
2
2.5
3
1000/T, K^-1
b
Pt (111)
P_{H_2} = 330·10^2 Pa
$P_{C_4H_6}$ =27·10^2 Pa
C_4H_6 hydrogenation
Km x10^7 moles Cm^-2 s^-1
100
10
1
1.5
2
2.5
3
1000/T, K^-1

Fig. 72

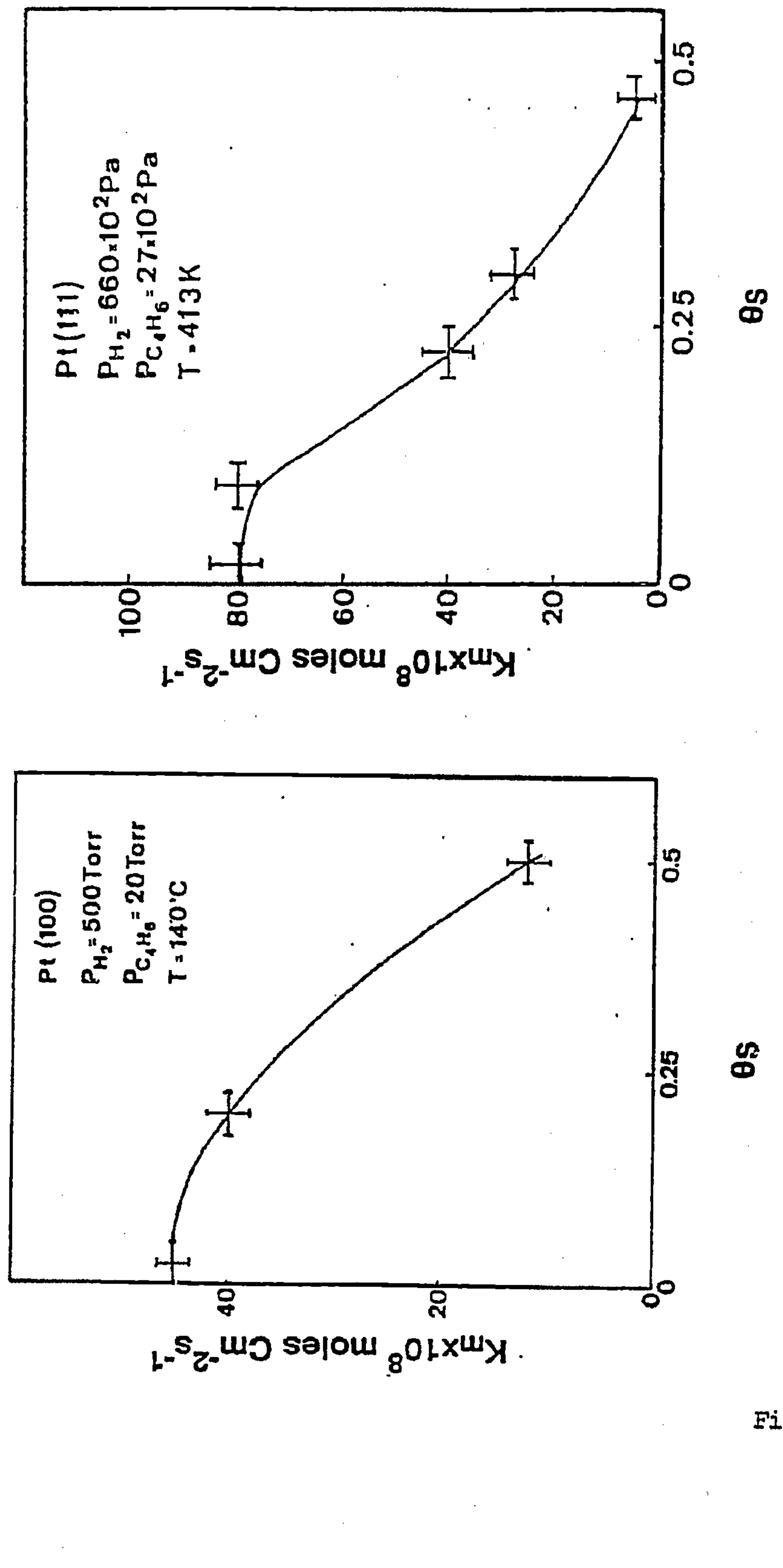
Pt (111)
P_{H_2} = 660×10²Pa
$P_{C_4H_6}$ = 27×10²Pa
T = 413K
Km×10⁸ moles Cm⁻²s⁻¹
100
80
60
40
20
0
0
0.25
0.5
θs
Pt (100)
P_{H_2} = 500 Torr
$P_{C_4H_6}$ = 20 Torr
T = 140°C
Km×10⁸ moles Cm⁻²s⁻¹
40
20
0
0
0.25
0.5
θs

Fig. 73

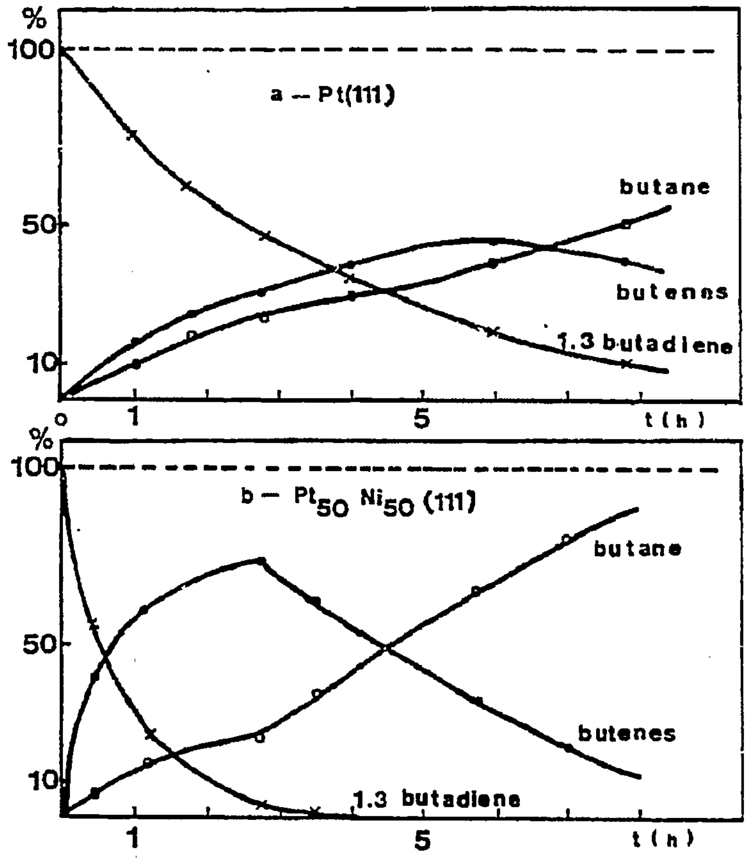
%
100
50
10
a — Pt(111)
butane
butenes
1.3 butadiene
0
1
5
t (h)
%
100
50
10
b — Pt_{50} Ni_{50} (111)
butane
butenes
1.3 butadiene
1
5
t (h)

Fig. 74

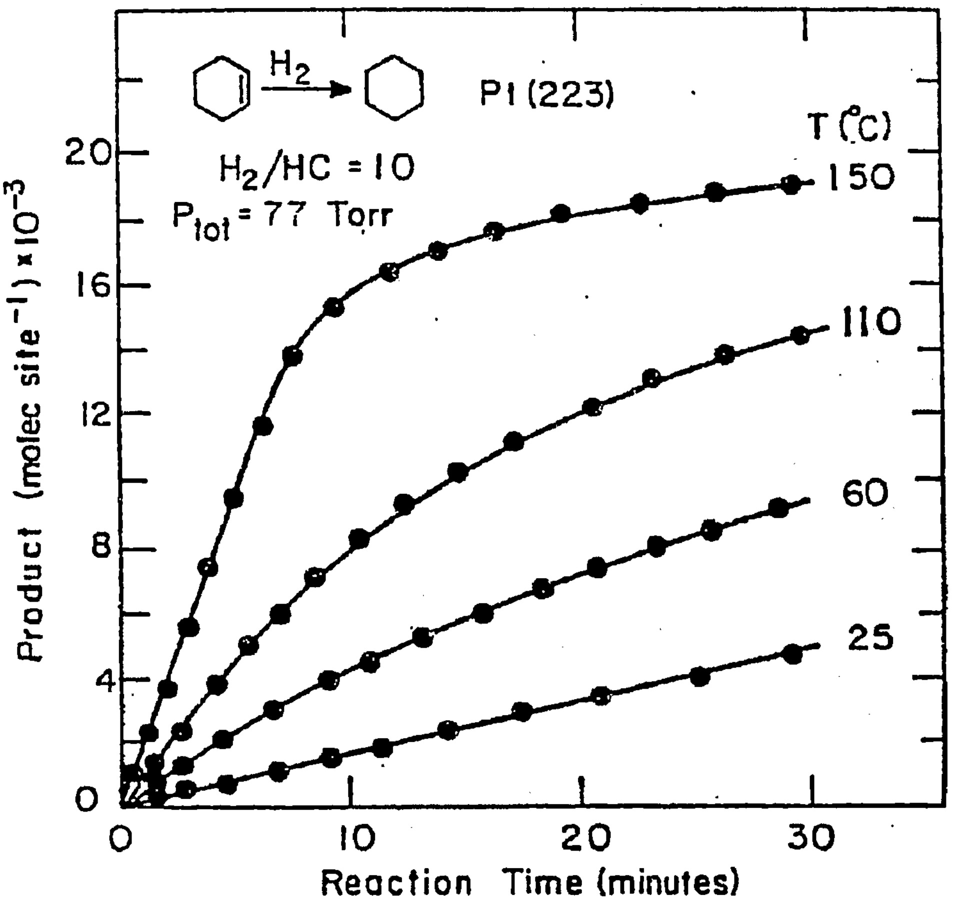

H_2
Pt (223)
$H_2/HC = 10$
$P_{tot} = 77$ Torr
T (°C)
150
110
60
25
Product (molec site^{-1}) ×10^{-3}
0
4
8
12
16
20
0
10
20
30
Reaction Time (minutes)

Fig. 75

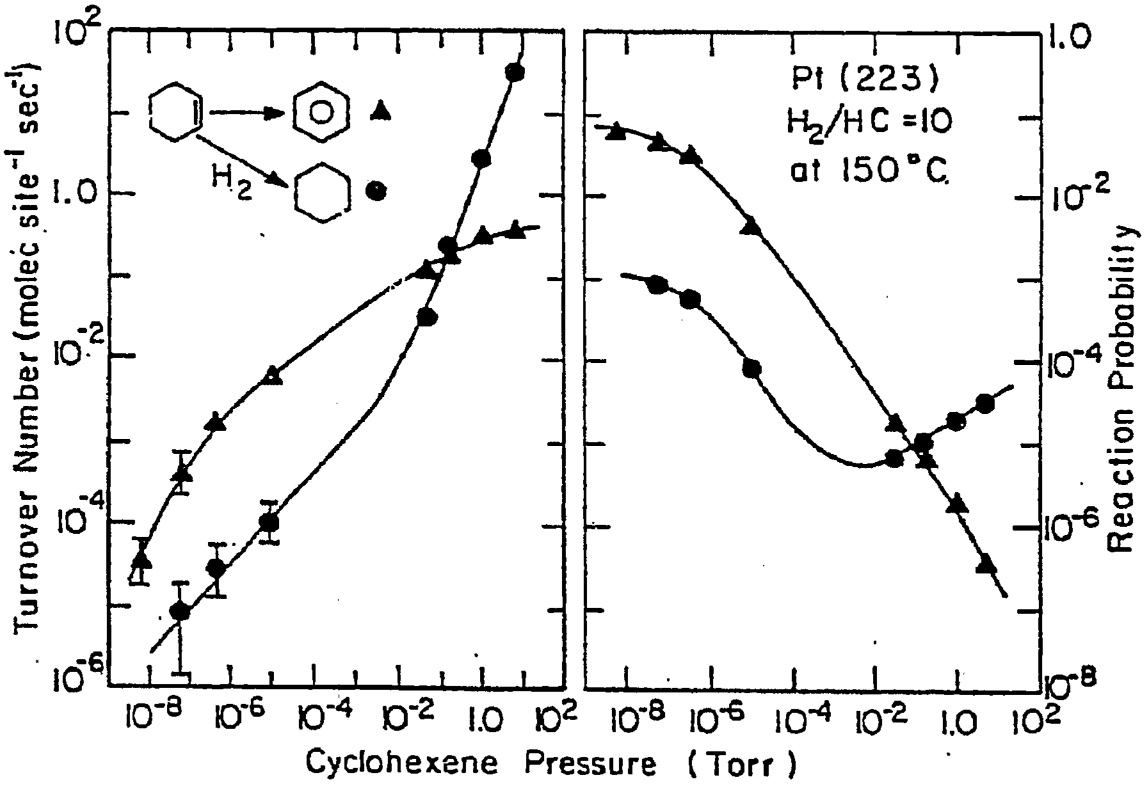

Turnover Number (molec site^{-1} sec^{-1})
10^2
1.0
10^{-2}
10^{-4}
10^{-6}
H_2
▲
●
Pt (223)
H_2/HC =10
at 150°C
1.0
10^{-2}
10^{-4}
10^{-6}
10^{-8}
Reaction Probability
10^{-8} 10^{-6} 10^{-4} 10^{-2} 1.0 10^2
10^{-8} 10^{-6} 10^{-4} 10^{-2} 1.0 10^2
Cyclohexene Pressure (Torr)

Fig. 76

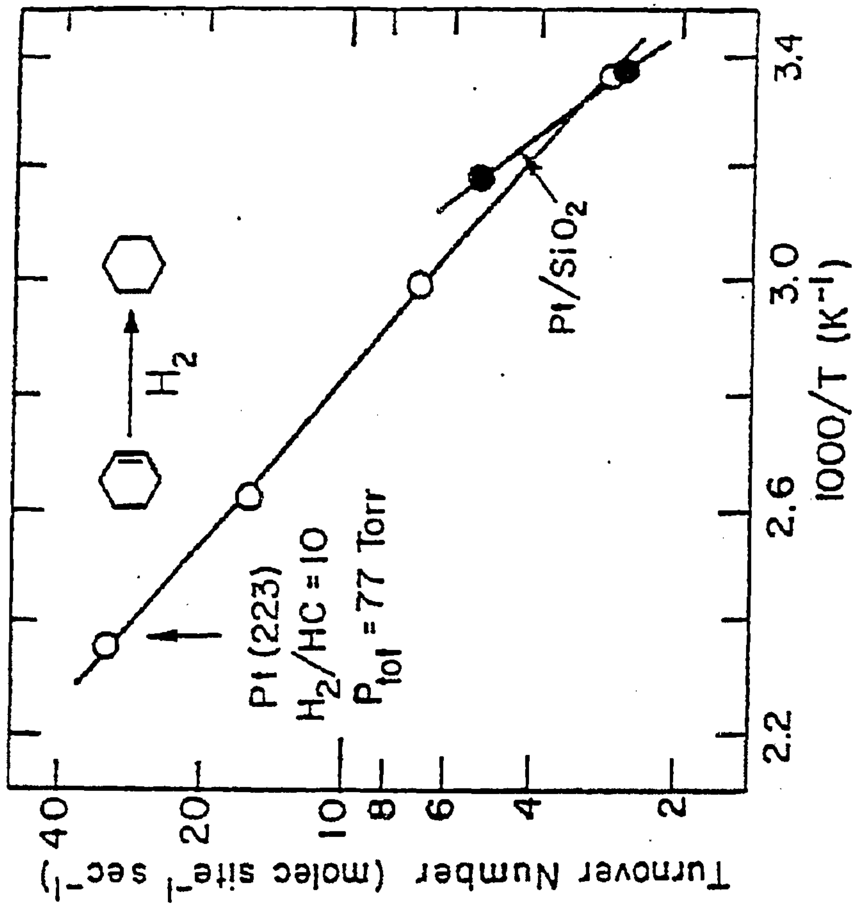
Turnover Number (molec site^{-1} sec^{-1})
40
20
10
8
6
4
2
2.2
2.6
3.0
3.4
1000/T (K^{-1})
H_2
Pt (223)
H_2/HC = 10
P_{tol} = 77 Torr
Pt/SiO$_2$

Fig. 77

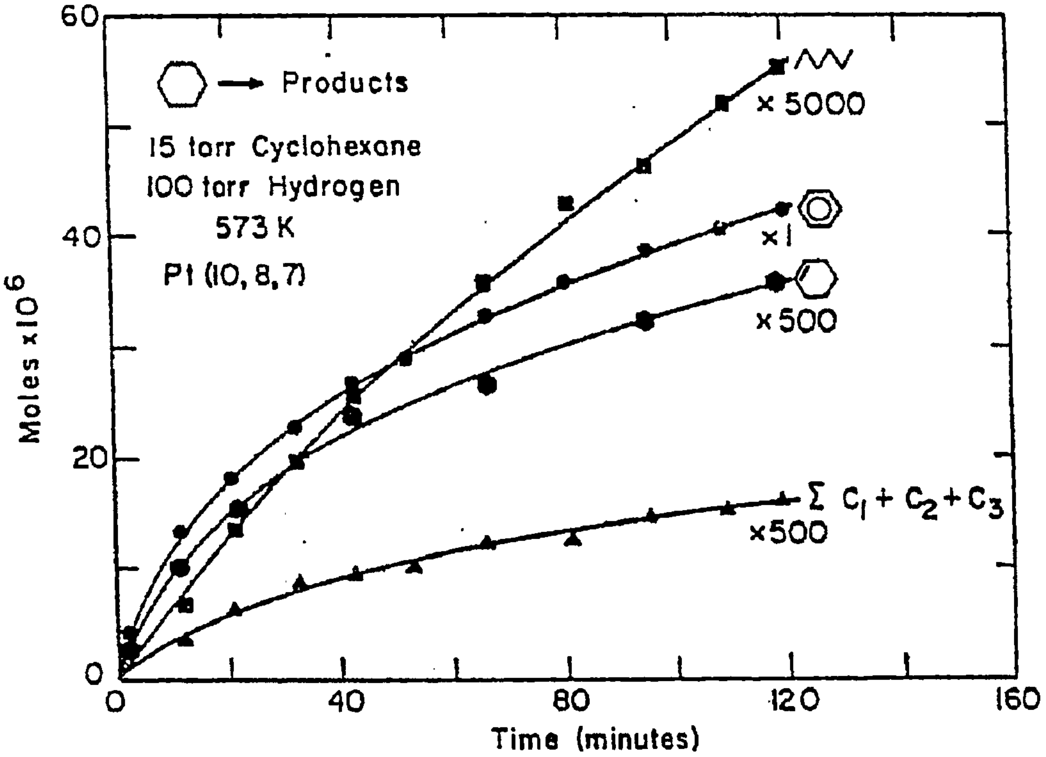
→ Products
15 torr Cyclohexane
100 torr Hydrogen
573 K
Pt (10, 8, 7)
× 5000
× 1
× 500
Σ C1 + C2 + C3
× 500
Moles × 10^6
Time (minutes)
0
20
40
60
0
40
80
120
160

Fig. 78

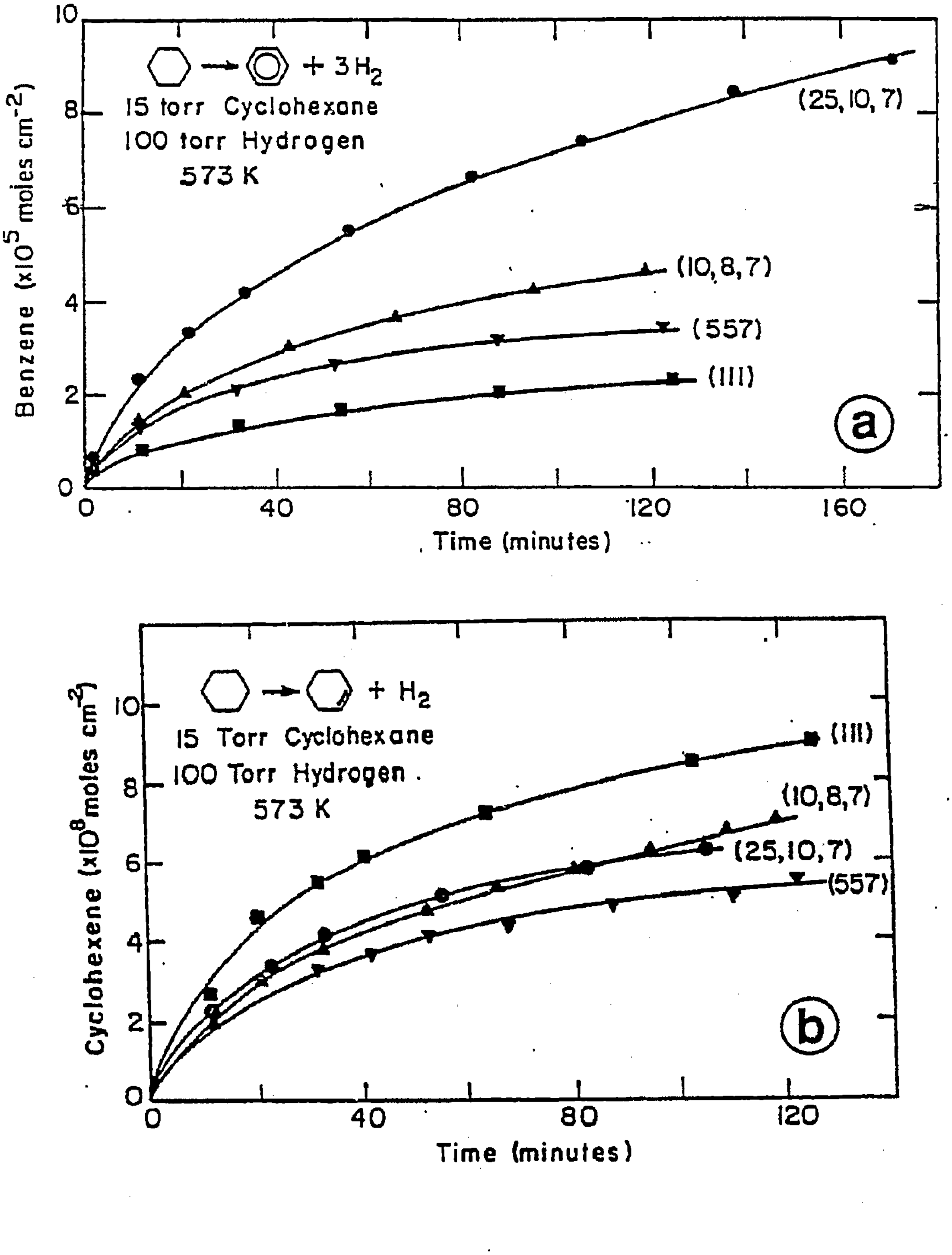
+ 3 H_2
15 torr Cyclohexane
100 torr Hydrogen
573 K
(25,10,7)
(10,8,7)
(557)
(111)
a
Benzene (x10^5 moles cm^{-2})
0
2
4
6
8
10
0
40
80
120
160
Time (minutes)
+ H_2
15 Torr Cyclohexane
100 Torr Hydrogen
573 K
(111)
(10,8,7)
(25,10,7)
(557)
b
Cyclohexene (x10^8 moles cm^{-2})
0
2
4
6
8
10
0
40
80
120
Time (minutes)

Fig. 79

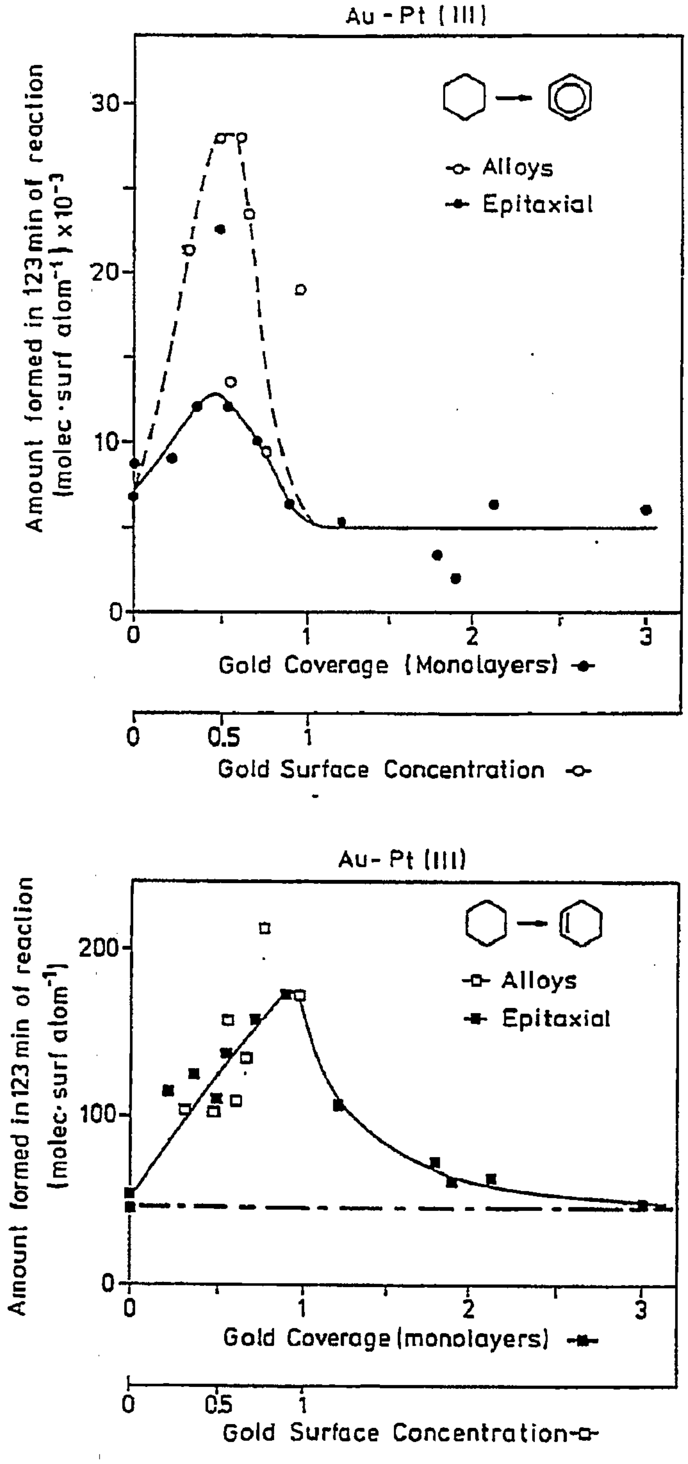
Au - Pt (111)
Amount formed in 123 min of reaction (molec · surf atom^{-1}) x10^{-3}
30
20
10
0
-o- Alloys
-•- Epitaxial
0
1
2
3
Gold Coverage (Monolayers) -•-
0
0.5
1
Gold Surface Concentration -o-
Au- Pt (111)
Amount formed in 123 min of reaction (molec· surf atom^{-1})
200
100
0
-□- Alloys
-■- Epitaxial
0
1
2
3
Gold Coverage (monolayers) -■-
0
0.5
1
Gold Surface Concentration-□-

Fig. 80

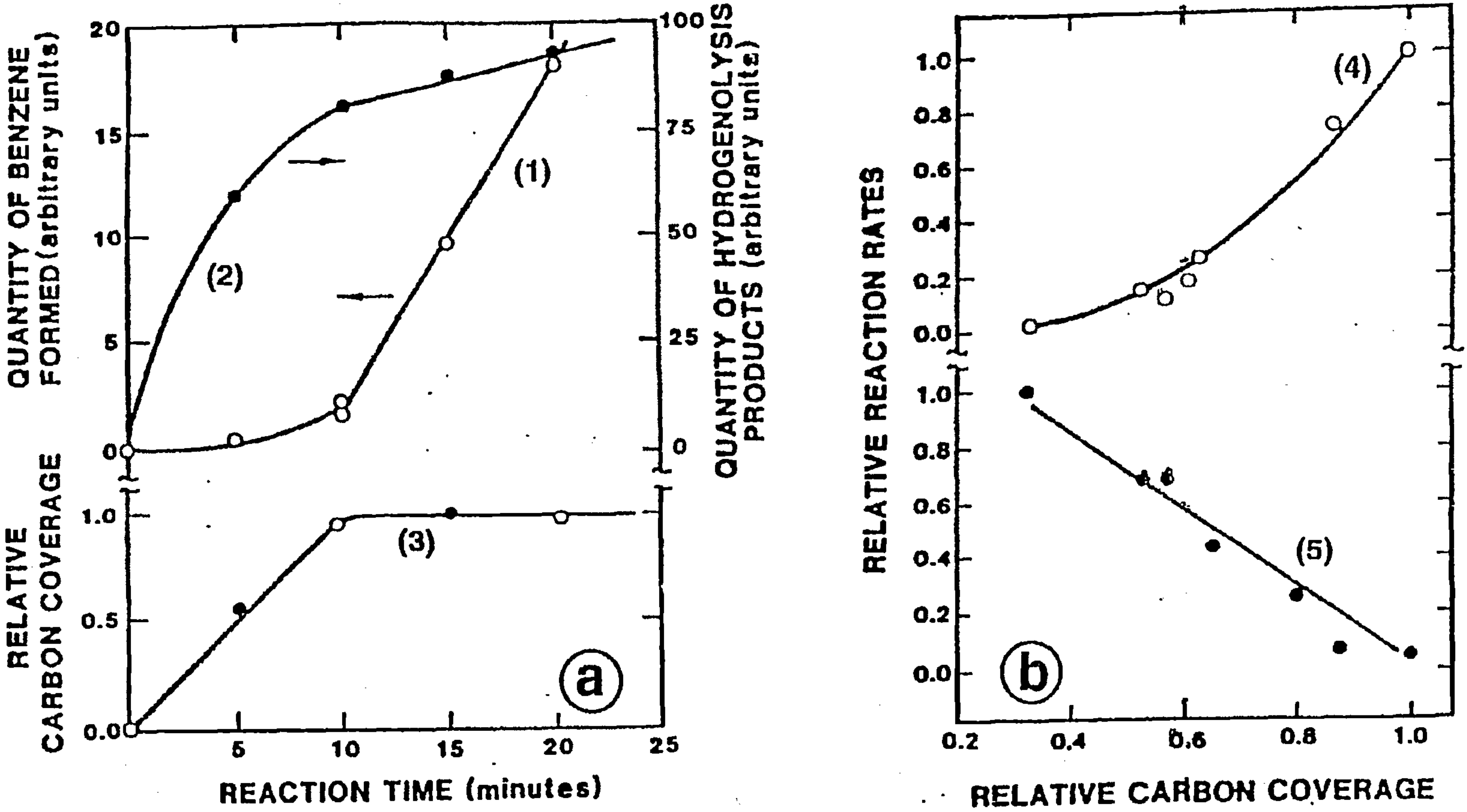
QUANTITY OF BENZENE FORMED (arbitrary units)
20
15
10
5
0
QUANTITY OF HYDROGENOLYSIS PRODUCTS (arbitrary units)
100
75
50
25
0
RELATIVE CARBON COVERAGE
1.0
0.5
0.0
(1)
(2)
(3)
a
5
10
15
20
25
REACTION TIME (minutes)
RELATIVE REACTION RATES
1.0
0.8
0.6
0.4
0.2
0.0
1.0
0.8
0.6
0.4
0.2
0.0
(4)
(5)
b
0.2
0.4
0.6
0.8
1.0
RELATIVE CARBON COVERAGE

Fig. 81

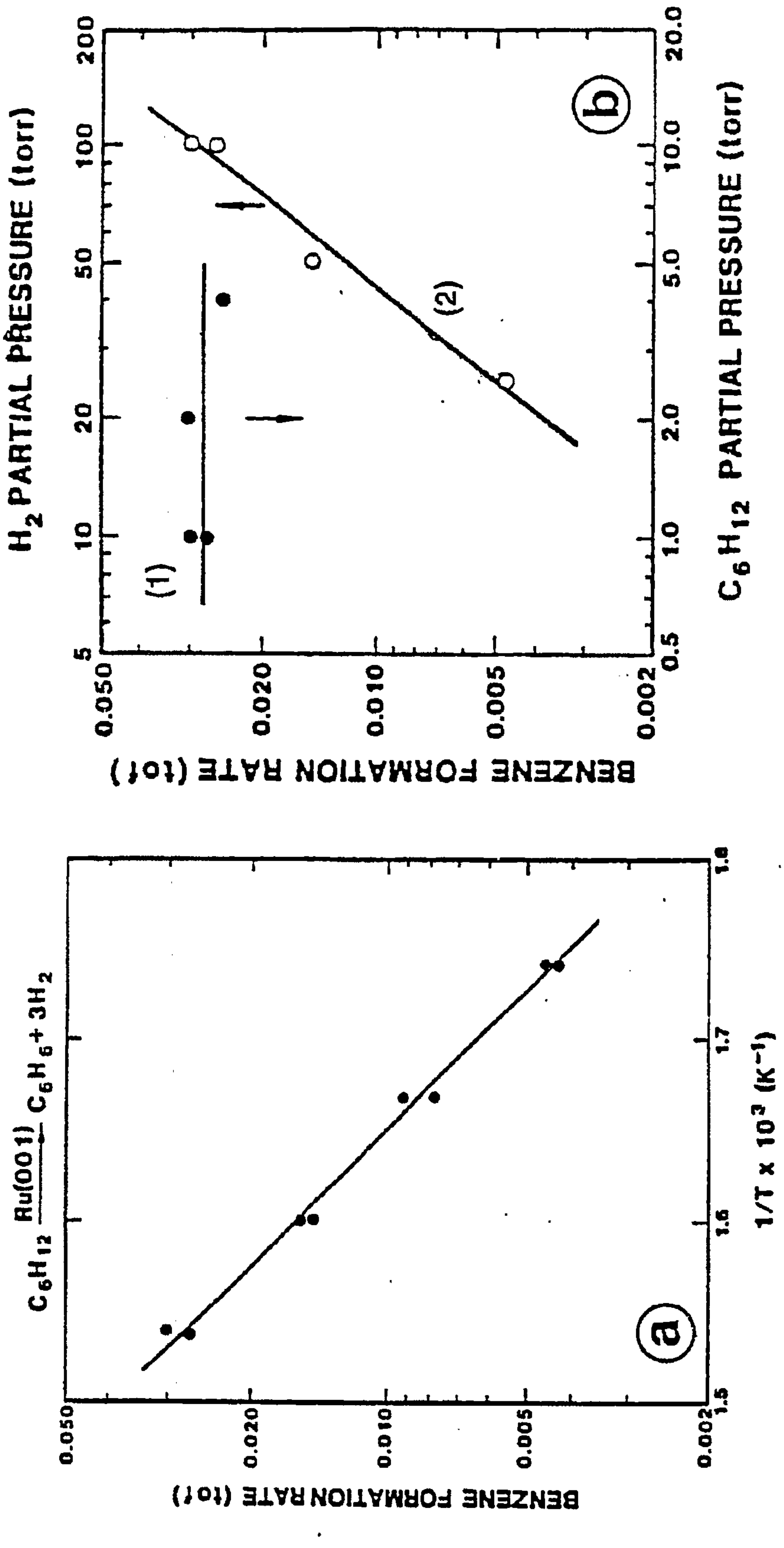

$C_6H_{12} \xrightarrow{Ru(001)} C_6H_6 + 3H_2$
BENZENE FORMATION RATE (tof)
0.050
0.020
0.010
0.005
0.002
1.5
1.6
1.7
1.8
1/T x 10^3 (K^{-1})
a
H_2 PARTIAL PRESSURE (torr)
5
10
20
50
100
200
(1)
(2)
b
BENZENE FORMATION RATE (tof)
0.050
0.020
0.010
0.005
0.002
C_6H_{12} PARTIAL PRESSURE (torr)
0.5
1.0
2.0
5.0
10.0
20.0

Fig. 82

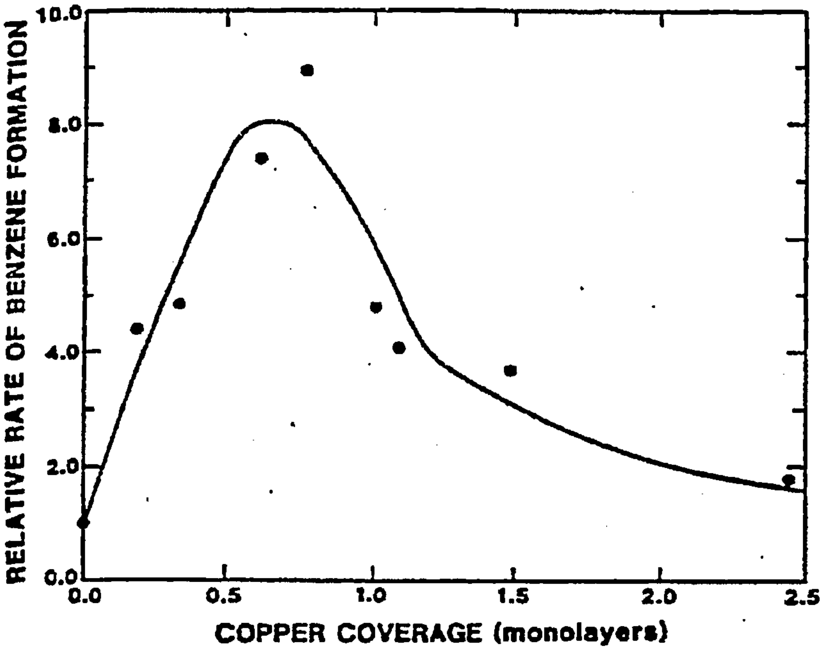
RELATIVE RATE OF BENZENE FORMATION
10.0
8.0
6.0
4.0
2.0
0.0
0.0
0.5
1.0
1.5
2.0
2.5
COPPER COVERAGE (monolayers)

Fig. 83

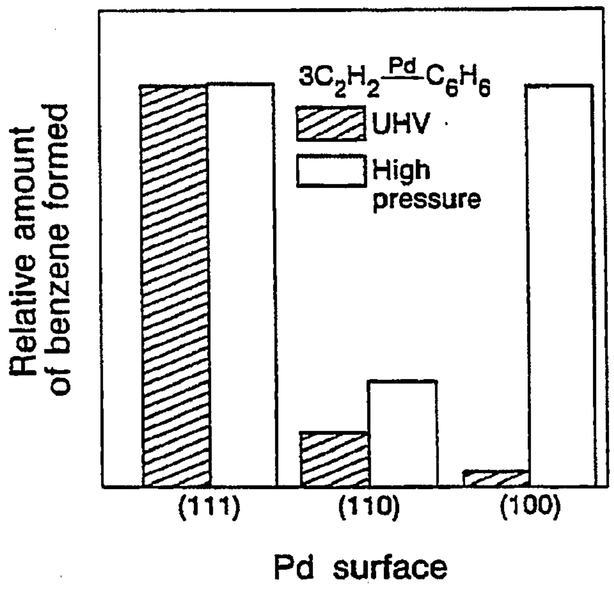
$3C_2H_2 \xrightarrow{Pd} C_6H_6$
▨ UHV
☐ High pressure
Relative amount of benzene formed
(111)
(110)
(100)
Pd surface

Fig. 84

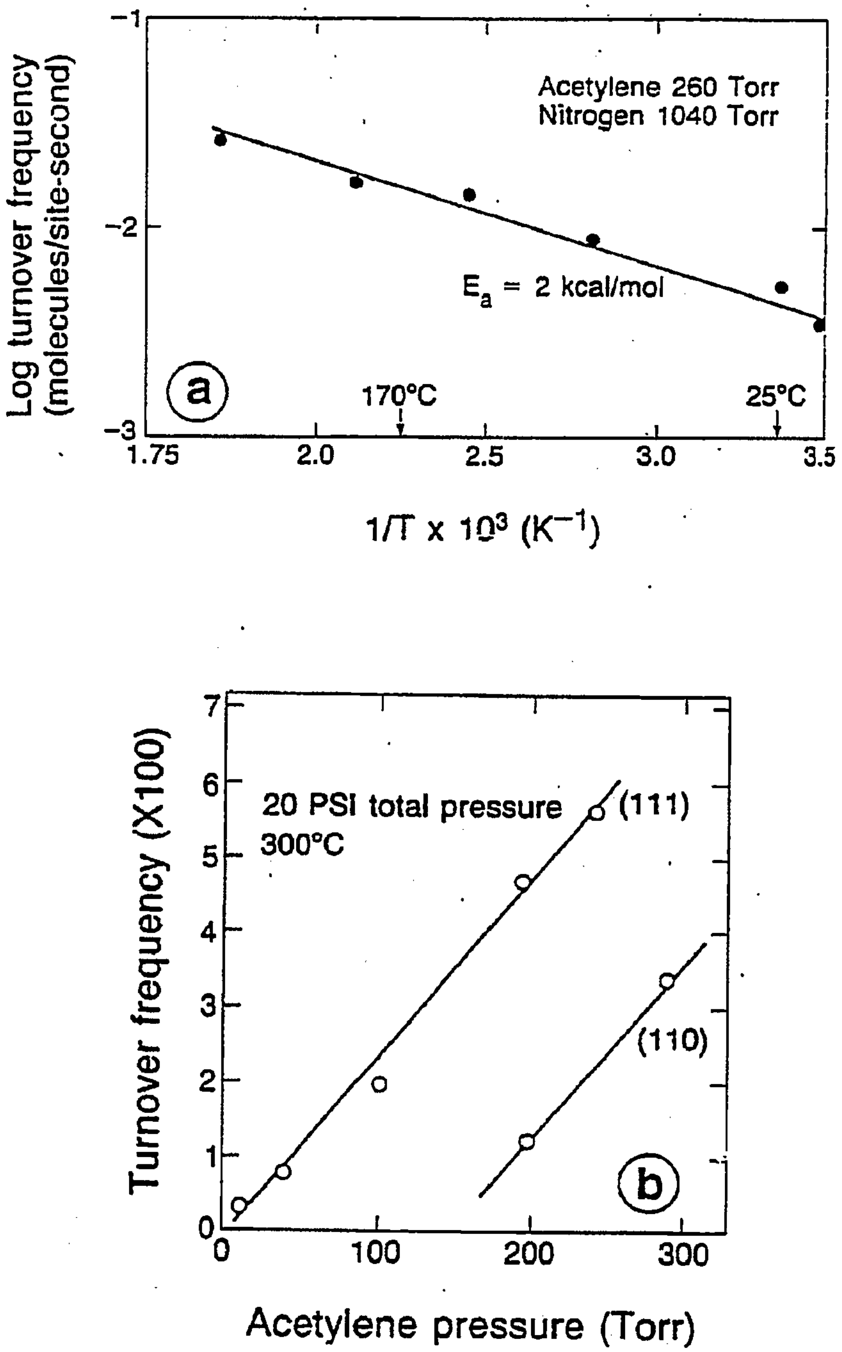
Log turnover frequency (molecules/site-second)
−1
−2
−3
1.75
2.0
2.5
3.0
3.5
1/T x 10³ (K⁻¹)
Acetylene 260 Torr
Nitrogen 1040 Torr
Ea = 2 kcal/mol
a
170°C
25°C
Turnover frequency (X100)
0
1
2
3
4
5
6
7
0
100
200
300
Acetylene pressure (Torr)
20 PSI total pressure
300°C
(111)
(110)
b

Fig. 85

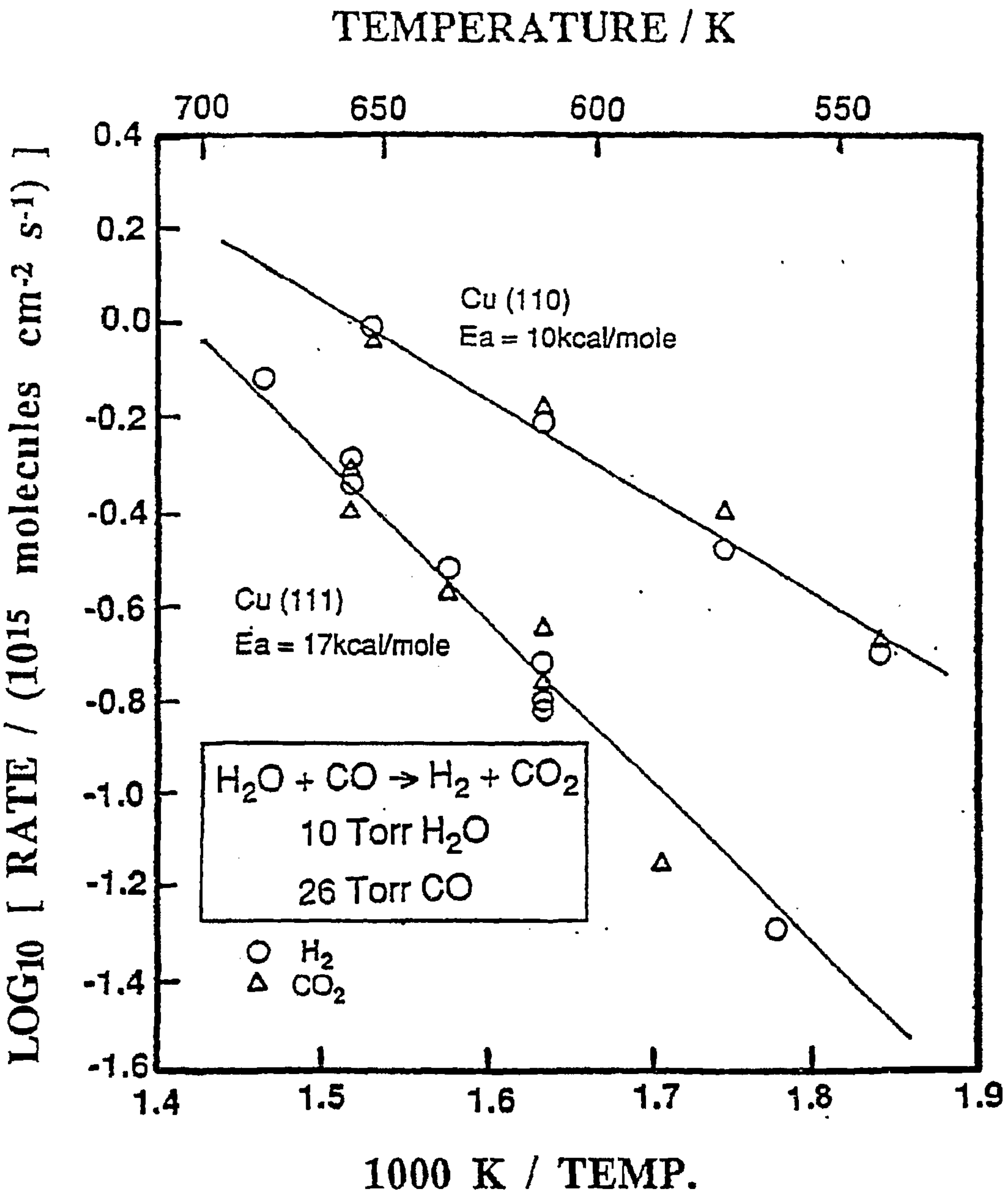
TEMPERATURE / K
700
650
600
550
0.4
0.2
0.0
-0.2
-0.4
-0.6
-0.8
-1.0
-1.2
-1.4
-1.6
1.4
1.5
1.6
1.7
1.8
1.9
LOG10 [RATE / (1015 molecules cm-2 s-1)]
1000 K / TEMP.
Cu (110)
Ea = 10kcal/mole
Cu (111)
Ea = 17kcal/mole
H2O + CO -> H2 + CO2
10 Torr H2O
26 Torr CO
○ H2
Δ CO2

Fig. 86

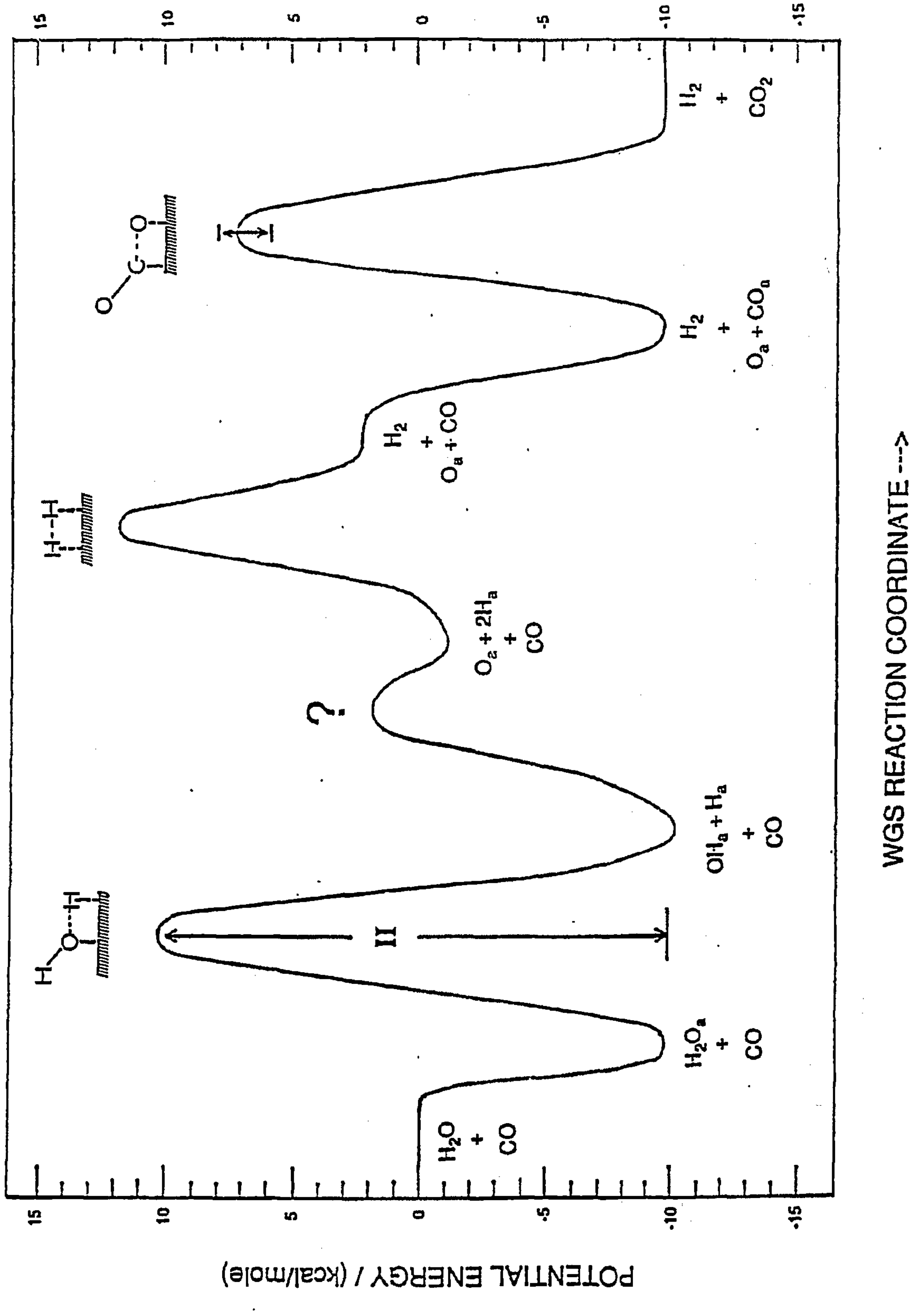
POTENTIAL ENERGY / (kcal/mole)
15
10
5
0
-5
-10
-15
H_2O + CO
H_2O_a + CO
H–O---H
II
$OH_a + H_a$ + CO
?
$O_a + 2H_a$ + CO
H--H
H_2 + O_a + CO
H_2 + $O_a + CO_a$
O–C--O
H_2 + CO_2
WGS REACTION COORDINATE --->

Fig. 87

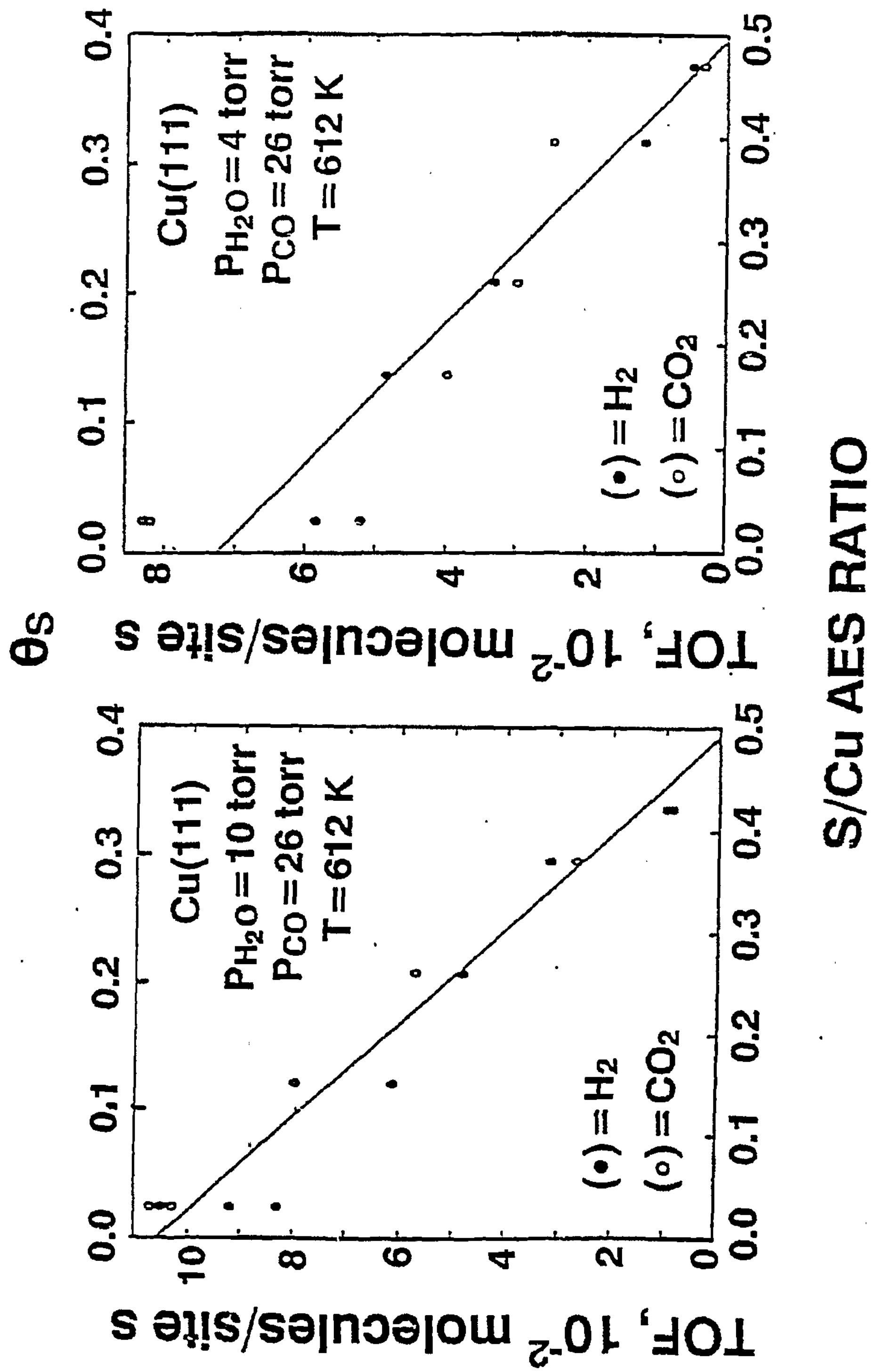
θS
0.0
0.1
0.2
0.3
0.4
TOF, 10-2 molecules/site s
0
2
4
6
8
10
Cu(111)
PH2O = 10 torr
PCO = 26 torr
T = 612 K
(•) = H2
(∘) = CO2
Cu(111)
PH2O = 4 torr
PCO = 26 torr
T = 612 K
(•) = H2
(∘) = CO2
0.5
S/Cu AES RATIO

Fig. 88

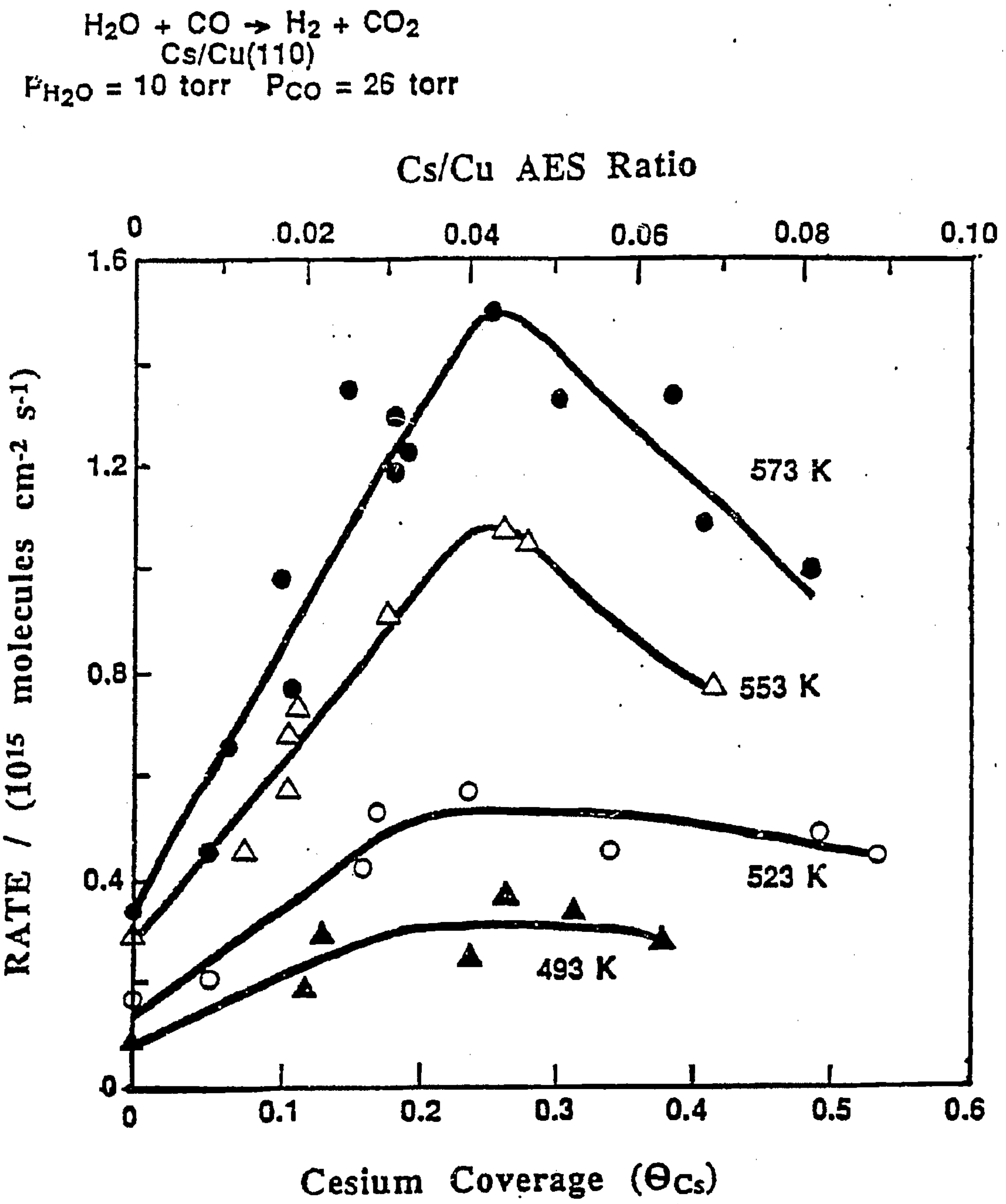
$H_2O + CO \rightarrow H_2 + CO_2$
Cs/Cu(110)
P_{H_2O} = 10 torr P_{CO} = 26 torr
Cs/Cu AES Ratio
0
0.02
0.04
0.06
0.08
0.10
1.6
1.2
0.8
0.4
0
RATE / (1015 molecules cm^{-2} s^{-1})
573 K
553 K
523 K
493 K
0
0.1
0.2
0.3
0.4
0.5
0.6
Cesium Coverage (Θ_{Cs})

Fig. 89

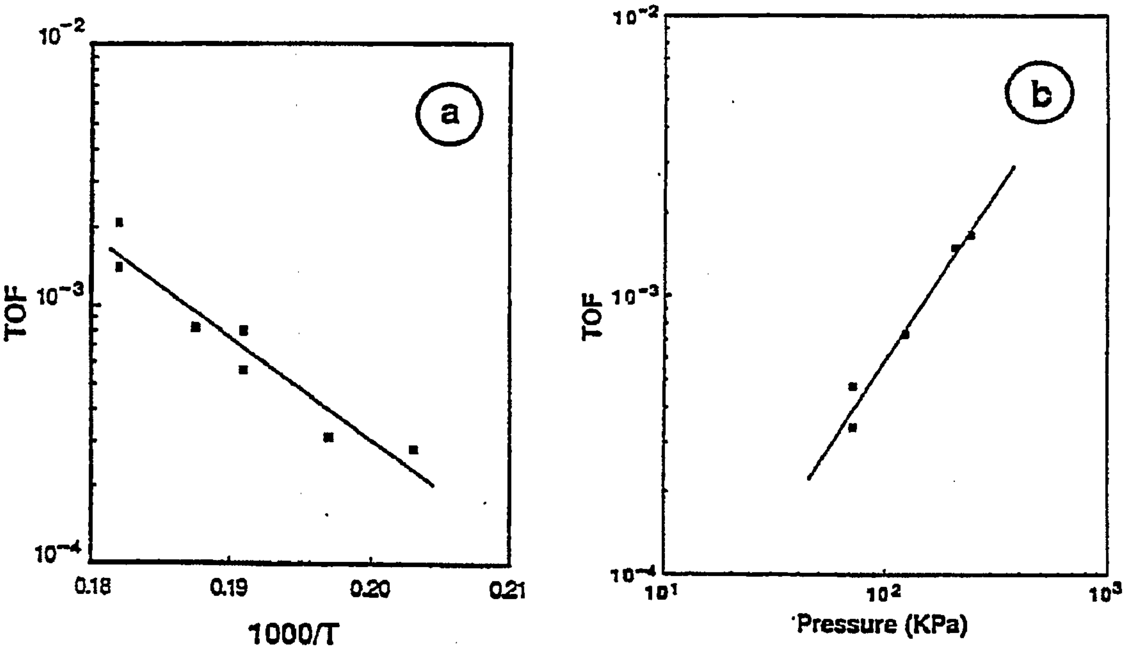
10^-2
10^-3
10^-4
TOF
a
0.18
0.19
0.20
0.21
1000/T
10^-2
10^-3
10^-4
TOF
b
10^1
10^2
10^3
Pressure (KPa)

Fig. 90

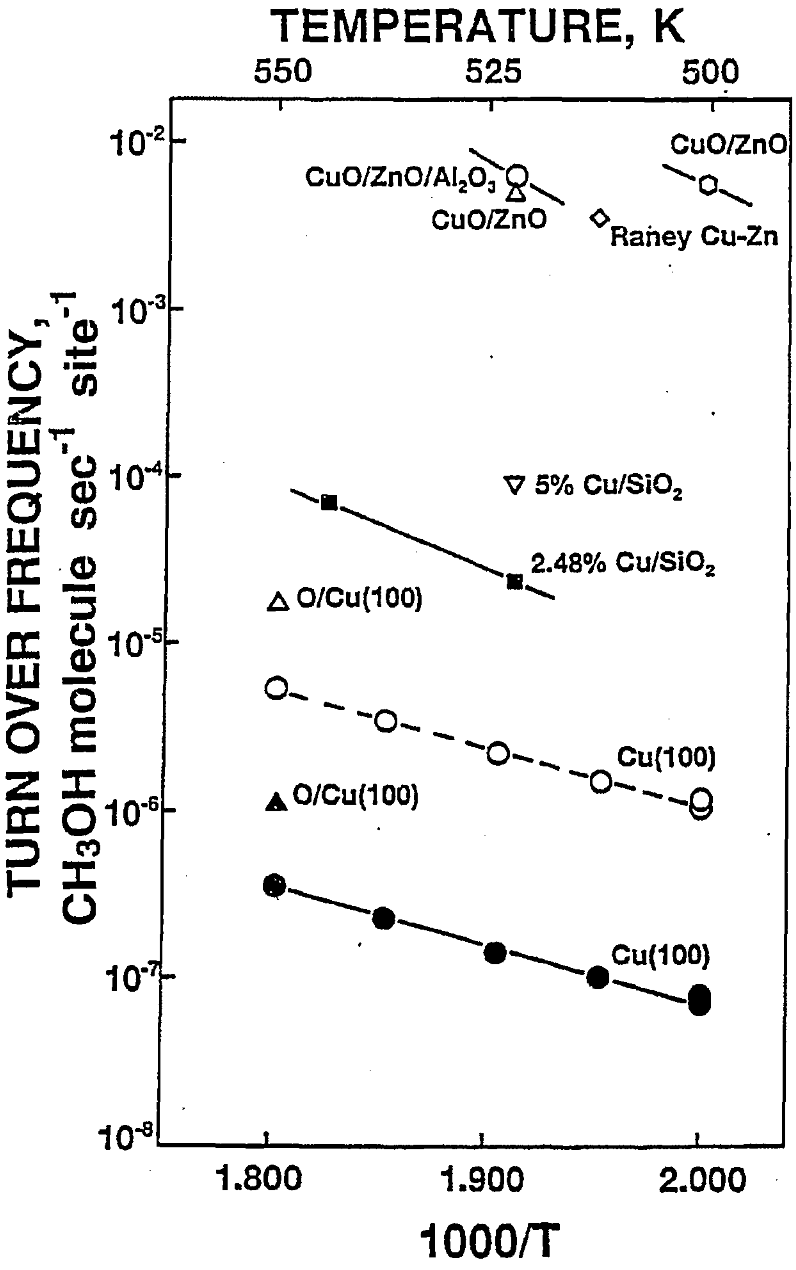
TEMPERATURE, K
550
525
500
TURN OVER FREQUENCY, CH₃OH molecule sec⁻¹ site⁻¹
10⁻²
10⁻³
10⁻⁴
10⁻⁵
10⁻⁶
10⁻⁷
10⁻⁸
CuO/ZnO/Al₂O₃
CuO/ZnO
CuO/ZnO
Raney Cu-Zn
5% Cu/SiO₂
2.48% Cu/SiO₂
O/Cu(100)
Cu(100)
O/Cu(100)
Cu(100)
1.800
1.900
2.000
1000/T

Fig. 91